Spring August 2014

FUNCTIONAL PHOSPHORYLCHOLINE POLYMERS: PRODRUGS AND BIOMATERIALS

Samantha B.M. Page
University of Massachusetts - Amherst

FUNCTIONAL PHOSPHORYLCHOLINE POLYMERS: PRODRUGS AND BIOMATERIALS

A Dissertation Presented

By

SAMANTHA B.M. PAGE

Submitted to the Graduate School of the
University of Massachusetts Amherst in partial fulfillment
of the requirements for the degree of

DOCTOR OF PHILOSOPHY

May 2014

Polymer Science and Engineering

FUNCTIONAL PHOSPHORYLCHOLINE POLYMERS:
PRODRUGS AND BIOMATERIALS

A Dissertation Presented

By

SAMANTHA B.M. PAGE

Approved as to style and content by:

_____
Todd Emrick, Chair

_____
Ryan Hayward, Member

_____
James Chambers, Member

                        _____
                        David Hoagland, Department Head
                        Polymer Science and Engineering

ACKNOWLEDGEMENTS

I would like to thank my parents, Tom and Sandy McRae, and my sister, Courtney McRae, for their love and encouragement though all my academic endeavors. Finally, I especially want to acknowledge Zak Page, my husband, for his love and support over the past five years. Thank you for the chemistry conversations, making these years some of the best yet, and for your continued support as we explore the next chapter of our lives together.

ABSTRACT

FUNCTIONAL PHOSPHORYLCHOLINE POLYMERS:
PRODRUGS AND BIOMATERIALS

MAY 2014

SAMANTHA B.M. PAGE, B.A., MOUNT HOLYOKE COLLEGE

M.S., UNIVERSITY OF MASSACHUSETTS AMHERST

PH.D., UNIVERSITY OF MASSACHUSETTS AMHERST

Directed by: Professor Todd Emrick

This thesis describes the synthesis and applications of multifunctional, hydrophilic polymers consisting of a methacrylate backbone and zwitterionic phosphorylcholine (PC) pendent groups, prepared by free radical polymerization of the zwitterionic monomer, 2-methacryloyloxyethyl phosphorylcholine (MPC). Advances in polymer chemistry, applied to PC polymers, allowed for the preparation of well-defined structures with controlled molecular weight, narrow polydispersity, and facile incorporation of functional comonomers, giving breadth to the range of materials accessible for different applications. Built-in functionality included fluorophores and reactive groups for post-polymerization transformations, such as drug conjugation or cross-linking. The ability to form well-defined structures based on the polyMPC backbone is attractive to the fields of polymer therapeutics and biomaterials, due to the high level of biocompatibility associated with PC polymers. The work presented here examines methacrylate-based PC polymers as (1) polymer-protein conjugates, (2) polymer prodrugs, and (3) polymeric hydrogels.

In Chapter 2, synthetic advances center on tailoring chain-end functionality and utilizing such structures as polymer-protein conjugates. The design of new ATRP initiators containing specific functionality allowed for polymer conjugation to lysozyme as a model protein. PolyMPC-lysozyme conjugates retained their native enzymatic activity, and pharmacokinetic profiles of the conjugates in mice revealed increased circulation half-life compared to lysozyme alone.

Chapter 3 describes PC-polymers that enhance intravenous drug delivery of potent chemotherapeutic agents. Functionalized methacrylates for copolymerization with MPC were designed, such that multiple copies of a drug can be loaded onto the polymer backbone, affording highly water soluble polymer prodrugs with unprecedented drug loading (>30 wt %). PolyMPC prodrugs of camptothecin (CPT) and doxorubicin (DOX) demonstrated cytotoxicity against several human cancer cell lines *in vitro*. PolyMPC-DOX prodrugs displayed prolonged circulation half-lives, and reduced uptake in healthy tissue, enhanced accumulation in tumors, and superior treatment efficacy in 4T1-tumor bearing mice.

Chapter 4 highlights multifunctional polyMPC as a precursor to new phosphorylcholine hydrogels. Two cell lines, live mouse skeletal muscle myoblasts (C_2C_{12}) and human ovarian cancer (SKOV3) cells, were observed to specifically attach, spread, and proliferate on PC-hydrogels containing the GRGDS peptide sequence, with a notable dependence on peptide concentration. The remarkable hydrophilicity and biocompatibility attributed to polyMPC combined with facile gelation conditions affords a platform of new bio-cooperative materials suitable for cell studies.

TABLE OF CONTENTS

Page

LIST OF TABLES

LIST OF FIGURES

LIST OF SCHEMES

CHAPTER 1

HYDROPHILIC POLYMERS FOR BIOMEDICAL APPLICATIONS

1.1 Introduction

Polymers have transformed society in many areas of science and technology, including breakthroughs in biomedical applications. Synthetic polymers now offer unique and versatile platforms for drug delivery, as they can be chemically "bio-tailored" for use as implants, medical devices, and injectable polymer-drug conjugates.[1,2] While several currently-used therapeutic proteins and small molecule drugs have benefited from synthetic polymers, the full potential of polymer-based drug delivery platforms has not yet been realized. For injectable therapeutics, fundamental problems that can be addressed with synthetic polymer delivery platforms include poor drug solubility in aqueous media, short *in vivo* circulation time, fast clearance, and undesirable (even life-threatening) side-effects. The first notion of improving drug behavior *in vivo* with a polymer-drug conjugate came in the 1950's,[3] with the concept gaining momentum in the 1970's when Ringsdorf and coworkers presented a model for polymer-drug conjugates. The model is composed of three major components: a water-soluble polymer scaffold, a therapeutic moiety covalently bound to the polymer, and a degradable (either hydrolytically or enzymatically) linkage between the drug and the polymer backbone.[4]

Advances in polymer chemistry provided alternatives to standard linear polymers, and architectures began to evolve, as well as drug-incorporation strategies, including covalent conjugation and encapsulation techniques, and novel release mechanisms.[5] Commonly used polymer architectures for biomedical and therapeutic systems are shown in Figure 1.1. Typical linear polymers (Figure 1.1A) tend to suffer from limited drug

loading, where conjugation is generally restricted to chain-ends. Alterations to the hydrophilic/lipophilic balance through, for example, block copolymers, lead to novel self-assembled structures such as micelles and polymersomes, amenable to drug encapsulation (Figure 1.1B and Figure 1.1C). In addition to drug delivery applications, synthetic polymers also find use in other biomedical applications, including coatings for medical implant devices[6] (Figure 1.1D and Figure 1.1E) and water-swollen hydrogel networks for regenerative medicine (Figure 1.1F).[7-10] While these and other systems are interesting for use in various applications, this thesis focuses on a new synthetic polymer platform technology and demonstrates the breadth of applications accessible by simply manipulating the chemistry.
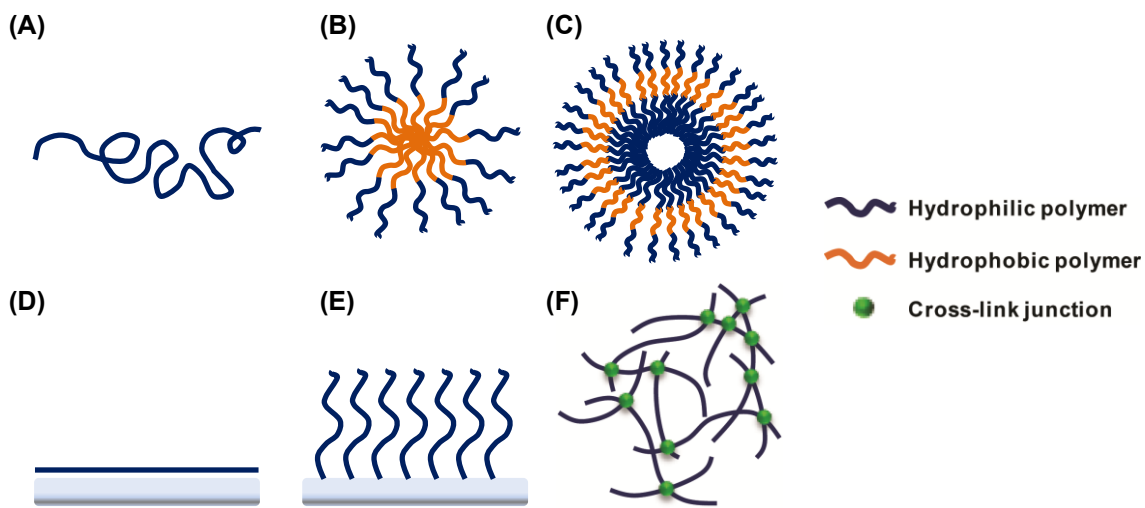
Figure 1.1 Polymer architectures for biomedical applications: (A) linear polymers, (B) micellar assemblies, (C) polymersomes, (D) thin film coatings, (E) surface-grafted coatings, (F) cross-linked networks (hydrogel).

1.2 PEGylated polymers for medicine

Improving the efficacy and efficiency of therapeutics by focusing on the mode of delivery, rather than the drug itself, is an emerging yet challenging area of interest in

medicine, where improved delivery vehicles present an opportunity to maximize the therapeutic benefit of existing drugs. Synthetic polymers have long been established as plastics, adhesives, foams, and rubbers, and more recently have emerged as key components of drug delivery platforms.[1,2] The notion of polymers for medicine has expanded significantly in recent years, yet the potential for synthetic polymers in drug delivery was identified early on. In 1955, polymer-drug conjugates composed of poly(vinyl pyrrolidinone)-*co*-poly(acrylic acid) random copolymers containing oligopeptide pendent groups were reported to prolong the circulation half-life relative to the drug alone,[3] suggesting the potential impact of synthetic polymers on drug delivery.

Poly(ethylene glycol) (PEG) has proven a "workhorse" polymer for medicine, useful for both protein therapeutics as well as small molecule drugs. Conjugation of PEG to therapeutics imparts the critically important characteristics of increased water solubility and *in vivo* residence, and decreased enzymatic degradation and immunogenicity.[11] PEGylated therapeutic agents also are capable of passive tumor targeting by the enhanced permeability and retention (EPR) effect.[12-15] The EPR effect refers to the preferential uptake of larger moieties (i.e., polymer conjugates) into the "leaky" vasculature of cancer tissue relative to healthy tissue, and subsequent retention due to poor lymphatic drainage.

Most commonly, PEGylation of therapeutic moieties is performed by coupling a reactive chain end of PEG to a functional handle on the drug or protein, and the number of reactive PEG derivatives available has undoubtedly contributed to its wide-spread use in this field. Some of the more widely used chemistries for PEG attachment include PEG-NHS ester or PEG-aldehyde for coupling to amines, and PEG-maleimide for thiol

coupling.[5] Recent efforts geared towards expanding the scope of conjugation chemistry include "click" chemistry; "click" reactions generally give high yields, produce by-products which are easily removed, require mild conditions, and products are isolated by facile methods.[16]

The PEGylated protein Adagen® was the first successful application of PEGylation chemistry to a therapeutic protein, gaining FDA approval for the treatment of severe combined immunodeficiency disease (SCID), and serving as an alternative to bone marrow transplants.[4,17] PEG Intron®, a PEGylated version of Intron A® (interferon-α-2b) developed by Schering-Plough, is another example of a PEGylated protein exhibiting advantages over the native protein *in vivo*. Interferon-α-2b is a cytokine that inhibits tumor growth and angiogenesis, and is therapeutically relevant for treatment of hepatitis B and C, malignant melanoma, and leukemia.[18,19] To prepare PEG Intron®, a succinimidyl carbonate functionalized PEG is conjugated to interferon-α-2b at histidine-34, giving monoPEGylated protein.[20] *In vivo* degradation of the carbamate releases the protein during circulation in the bloodstream. Other PEGylated proteins include PEGylated erythropoietin (PEG-EPO) for the treatment of anemia resulting from chemotherapy,[21] and PEGylated granulocyte-colony stimulating factor (PEG-G-CSF), used in chemotherapy treatment (marketed as Neulasta®), the success of which is attributed to the greater solubilization provided by PEG, as well as the prevention of aggregation.[22]

Synthetic polymers are also of current interest for enhancing delivery of small-molecule cancer therapeutics. The use of polymers offers several advantages over the drug alone, as well as small-molecule derivatives, for reasons relating to solubility,

reduction of toxic side effects, long circulation times due to slow renal clearance, and passive tumor targeting by the EPR effect. Exploiting the EPR effect renders polymeric materials a viable drug delivery platform, however actively targeted polymer-drug conjugates are also desirable to increase the specificity of prodrug uptake to cancerous tissues, while eliminating or reducing uptake (and potential damage) to healthy cells that occurs despite the EPR effect.

One prominent example of a PEGylated small-molecule drug is camptothecin (CPT), a topoisomerase I inhibitor, active against several types of cancer.[23] CPT, however, suffers from extremely poor water solubility, as well as physiological instability of the E-ring lactone. Several synthetic derivatives have been synthesized to provide better solubility, including the piperidinyl-functionalized Camptosar®. These derivatives exhibit poor efficacy and life-threatening dehydration, among other side effects.[5] Prothecan®, developed by Enzon, is one of the earliest examples of PEGylated CPT, where two CPT molecules are covalently bound at the chain ends of a 40,000 g/mole linear PEG through ester linkages at the 20-OH position of the drug.[24] Modification at this position inhibits lactone ring opening, a critically important factor in preserving the therapeutic activity of the drug. Prothecan® displayed significantly improved circulation time, with a half-life of more than 75 hours in patients with advanced solid malignancies.[25] Other examples of PEGylated CPT prodrugs include IT-101, a PEGylated cyclodextrin containing polymer,[26] PEG-SN38, a four-arm PEG star containing four drugs per conjugate,[27] as well as degradable PEGylated polyesters grafted with pendent CPT molecules prepared by click chemistry.[28] These camptothecin derivatives are shown in Figure 1.2.
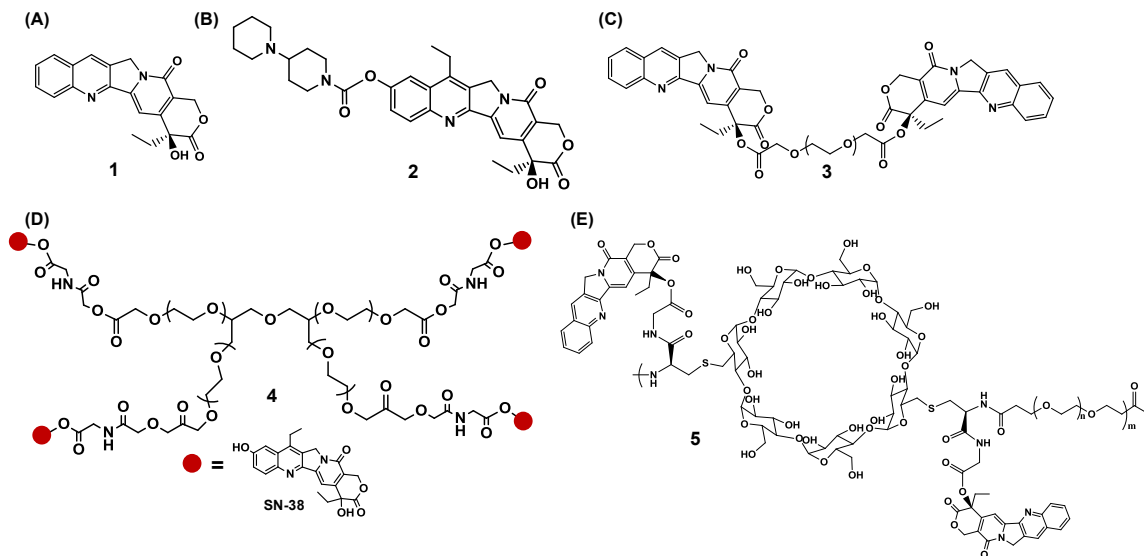
Figure 1.2 (A) Camptothecin, (B) Camptosar® (irinotecan), (C) Prothecan®, (D) multi-arm PEG star with four glycine-linked SN38 molecules, and (E) a PEGylated linear cyclodextrin polymer bearing 2 glycine-linked CPT drugs per repeat unit.

Polymer micelles stemming from PEGylated block copolymer structures have also proven useful in the delivery of hydrophobic drugs. Polymer micelles assemble spontaneously following placement of amphiphilic polymers into selective solvents. Hydrophobic-hydrophilic diblock copolymers in aqueous media are especially effective, producing core-shell type structures in which the hydrophobic block collapses to generate the core, leaving the hydrophilic block as the surrounding corona. The core-shell morphology of polymer micelles makes them ideally suited for drug delivery; the core can function as an encapsulating matrix, while the shell, in addition to providing aqueous solubility, presents unique opportunities for chemical functionality useful, for example, for providing cellular recognition or targeting ligands. Polymer micelles bear some resemblance to liposomal structures in that hydrophobic drugs can be sequestered into a hydrophobic region and the structures are of appropriate size to exploit the EPR effect. Polymer micelles represent a viable alternative to polymer-based drug delivery as the

polymer structure is chemically tunable, where, for example, stimuli responsive linkages or cross-links can be incorporated and the size and shape can be controlled.

PEGylated block copolymer micelles have emerged as systems with great potential in drug delivery, as they combine biocompatibility with synthetic versatility. Relevant examples include poloxamers, also known by their trade name Pluronics®. Pluronics® are composed of triblock copolymers of poly(ethylene oxide)-*block*-poly(propylene oxide)-*block*-poly(ethylene oxide) (PEO-*b*-PPO-*b*-PEO) that form core-shell micelles in aqueous media, imparting the advantages of micellar platforms and also contributing unique *in vivo* properties.[29]   Studies on doxorubicin (DOX)-loaded SP1049C, a mixed micelle system of Pluronic® L61 and Pluronic® F127,[30] indicated activity against multiple DOX-sensitive cancer cell lines, with a 2-5 fold greater *in vitro* sensitivity (IC_{50} values) relative to free DOX. Interestingly, these drug-loaded micelles also showed orders-of-magnitude higher activity compared to free DOX against cancer cell lines not normally sensitive to DOX. SP1049C is able to bind with DNA ten times more efficiently than unmodified DOX, due to a combination of factors including an increase in drug influx and tissue accumulation by the EPR effect, inhibition of efflux, and changes in intracellular trafficking (*i.e.,* is able to enter the cell by endocytosis rather than relying solely on DOX diffusion).

Another DOX-encapsulated polymer micelle delivery system, reported in 2001 by Kataoka and coworkers, used PEG-*b*-poly(aspartic acid) diblock copolymers, with DOX attached covalently to the aspartic acid block.[31] When taken up in water, the diblock copolymer formed micelles, in which the DOX-conjugated hydrophobic block facilitates additional physical sequestration of DOX into the hydrophobic core (the amide-linked

drug is stable under physiological conditions). These DOX-loaded micelles proved very effective, resulting in cures against C-26 colon carcinomas (a model cancer cell line); administration of free DOX did not result in any cures. Kataoka and coworkers added sophistication to this polymer-DOX delivery system by attaching the drug to the hydrophobic segment of the micelle through a hydrazine linkage,[32] which releases the drug in a pH dependent manner, by covalent bond cleavage at pH ~5. These polymer micelles were constructed from PEG-*block*-poly(β-benzyl-L-aspartate) (PEG-*b*-PBLA) chains functionalized with hydrazide moieties, following removal of the benzyl protecting groups from the aspartate repeat units. Conjugation of DOX with pendent hydrazine moieties gives PEG-*block*-poly(ASP)$_{37}$-*co*-poly(Asp-Hyd-DOX)$_{28}$. These polymer-drug micelles were characterized by dynamic light scattering to be ~65 nm average diameter, and displayed the desired pH dependent DOX release. Incubation of these micelles with human small lung cancer SBC-3 cells revealed an effective inhibition of cell growth, approaching that found in experiments using unmodified DOX.

Camptothecin may also benefit from delivery using PEGylated micelles. The uptake and release of camptothecin was studied *in vitro* with poly(ethylene glycol)-*b*-poly(benzyl L-aspartate) (PEG-*b*-PBLA) micelles, in which the hydrophobicity of the core was varied by controlling the percentage of benzyl ester protecting groups.[33] Micelles richer in benzyl ester groups (~two-thirds benzylated) were seen to more effectively sequester the drug (~90 %). The same micelle also showed the slowest camptothecin release (100 hours were needed to release ~80 % of the sequestered drug).

Synthetic polymers provide many varieties of opportunities for optimization of drug delivery, including tools to alter solubility and biodistribution, reduce side effects,

and increase the overall efficacy of the treatment. Chemical composition has clear importance for biocompatibility and, in some cases, degradability, however polymer architecture is also known to be of considerable importance. Novel synthetic polymers will continue to benefit the medical community as new synthetic methodologies lead to more efficient conjugation, encapsulation, and release chemistries.

1.3 Polyzwitterions

The growing interest in polymers for medicine has created a need for superior polymer platform technologies that can be tailored to suit multiple chemical, physical, and biological requirements. While the benefits of PEGylation for increasing the therapeutic efficacy of proteins and small molecule drugs have shown preliminary success, other polymer structures present intriguing alternatives. The phospholipid bilayer of a cell membrane is considered optimal for interacting with biologics, thus polymeric materials composed of synthetic phospholipid analogues have received much effort and attention. These biomimetic analogues constitute a class of hydrophilic polymers aside from the more conventional hydroxyl- and ether-rich structures (PEG), known as polyzwitterions. Polyzwitterions are net-neutral, hydrophilic polymers, with different architectures compared to conventional linear PEG prepared from ethylene oxide ring-opening polymerization. The difference in backbone structure also renders them amenable to different chemistries. Due to the presence of the zwitterion on each repeat unit, polyzwitterions are well established as biocompatible and anti-fouling.[34] Examples of these polymers are shown in Scheme 1.1, including poly(sulfobetaine methacrylate) (polySBMA), poly(carboxybetaine methacrylate) (polyCBMA), and poly(methacryloyloxyethyl phosphorylcholine) (polyMPC). This thesis will focus on

new syntheses of functional phosphorylcholine methacrylates designed for applications in prodrugs and biomaterials.
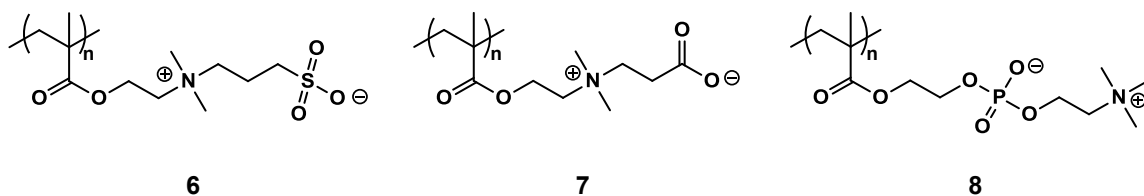
Scheme 1.1 Structure of polySBMA (**6**), polyCBMA (**7**), and polyMPC (**8**).

Phosphorylcholine (PC)-based polymers resemble naturally occurring phospholipids, and are hydrophilic due to the close association of water molecules with the zwitterion (about 15-25 molecules per repeat unit).[35] Perhaps most prominent among PC-based polymers are those prepared from the methacrylic derivative 2-methacryloyloxyethyl phosphorylcholine (MPC). PolyMPC is quickly becoming recognized as perhaps the most biocompatible synthetic polymer, lending itself to applications in contact lenses, stents, and coatings for various medical devices and implants.[36-38]

MPC monomer is polymerized using either conventional or controlled free radical polymerization techniques.[39] For the biomedical applications described in this thesis, predictable molecular weights with narrow polydispersity indices were desirable, requiring controlled "living" polymerization techniques, including atom transfer radical polymerization (ATRP) and reversible addition-fragmentation transfer (RAFT) polymerization.

ATRP is a versatile, copper-catalyzed radical polymerization technique which is easily extended to MPC. This process relies on an equilibrium between an activated and deactivated propagating species, mediated by a transition metal catalyst (usually copper

(I) bromide or copper(I)chloride) which reversibly deactivates the propagating chain with a terminal halogen.[40] The ATRP mechanism is shown in Figure 1.3A. Typically a halide-containing initiator is used, and the MPC polymerization is performed in dimethylsulfoxide/methanol solvent mixtures to fully solubilize all components of the reaction. The resulting MPC polymers are highly water-soluble (>100 mg/mL), with close-to-targeted molecular weights and narrow polydispersity indices (PDI) (~1.1-1.3). The polymers possess two well-defined end groups: one from the ATRP initiator, and the halide that exchanges with the propagating chain.

RAFT polymerization is similar to ATRP in that it also is a form of living radical polymerization. RAFT is based on the conventional free radical polymerization of an alkene-bearing monomer, but is carried out in the presence of a chain transfer agent (CTA).[41] Common RAFT CTAs include dithioesters, dithiocarbamates, trithiocarbonates, and xanthates, and are responsible for mediating the polymerization through a reversible chain transfer process. The mechanism for RAFT is shown in Figure 1.3B. RAFT represents an alternative approach to living polymerizations, where no metal catalyst is required, as in the case of ATRP.
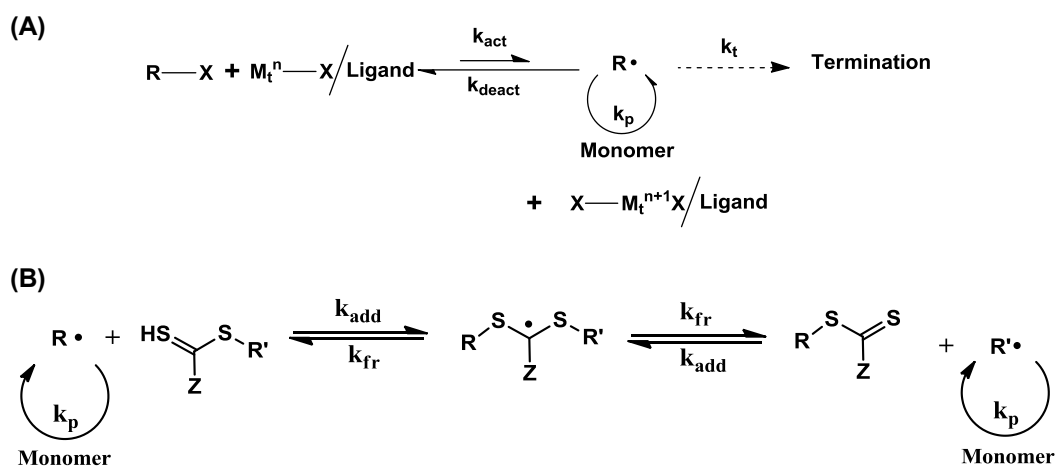
Figure 1.3 Mechanism of (A) ATRP and (B) RAFT polymerization.

Additional benefits of extending controlled polymerization techniques such as ATRP and RAFT to MPC include the high degree of functional group tolerance. This allows, for example, chain-end functionality to be easily installed on polyMPC by using an initiator (ATRP) or CTA (RAFT) containing the desired functional group at the outset of polymerization. End-functional polymers represent important precursor materials for post-polymerization conjugation to proteins, ligands, fluorophores, or other therapeutic, diagnostic, or targeting moieties. Furthermore, copolymers (random or block) can be synthesized with ease by both ATRP and RAFT. This allows for functional monomers to be incorporated, resulting in reactive sites along the polymer backbone for subsequent drug conjugation, or for the addition of hydrophobic blocks to drive self-assembly into nanoscale structures such as micelles or capsules.

1.4 Thesis Outline

The use of PC-polymers has largely been restricted to applications such as anti-fouling coatings due to the uncontrolled molecular weight and polydisperse nature of polymers prepared by conventional free radical polymerization techniques. With the advent of controlled polymerization techniques such as ATRP and RAFT, the synthesis of well-defined PC-polymers with predictable molecular weights, end-group fidelity, and functionality achieved through careful design of initiators or comonomers is now possible. The purpose of this thesis was to investigate the synthesis of PC-methacrylates and the incorporation of new functional groups. Reactive groups were installed at the chain-end or as pendent groups along the backbone, giving novel random and diblock copolymer structures.

Chapter 2 describes the synthesis of MPC monomer and polymerization using ATRP. Polymers were synthesized in a range of molecular weights with narrow dispersity and include specific chain-end functionality. End-functional polyMPC is explored for conjugation to proteins using lysozyme as a model (Biomacromolecules, 2008; Macromolecules, 2010; Biomacromolecules, 2012).[42-44] Two conjugation strategies were explored: 1) amine-reactive polyMPC was conjugated non-specifically to surface available lysine residues and 2) ketone/aldehyde-reactive polyMPC was synthesized in order to prepare polymer-protein conjugates with some degree of site-selectivity.

Chapter 3 describes PC-polymers that enhance the intravenous drug delivery of the potent chemotherapeutic agents camptothecin (CPT)[45,46] and doxorubicin (DOX) (Bioconjugate Chemistry, 2009; Molecular Pharmaceutics, 2013; Molecular Pharmaceutics, 2014).[45-48] Functionalized methacrylates for copolymerization with MPC were designed such that multiple copies of a drug can be loaded onto the polymer backbone, affording highly water soluble polymer prodrugs with high drug loading (>30 wt %). PolyMPC prodrugs demonstrated cytotoxicity against several human cancer cell lines *in vitro*. PolyMPC-DOX prodrugs displayed prolonged circulation half lives, preferential tumor accumulation, and superior treatment efficacy in 4T1 tumor-bearing mice.

Lastly, Chapter 4 highlights multifunctional polyMPC as a precursor to new phosphorylcholine hydrogels (Journal of Materials Chemistry B, 2014). The remarkable hydrophilicity and biocompatibility of polyMPC combined with facile gelation conditions affords a platform of new bio-cooperative materials suitable for cell studies.[49]

1.5 References

1. Jatzkewitz, H. Peptamin (glycyl-L-leucyl-mescaline) bound to blood plasma expander (polyvinylpyrrolidone) as a new depot form of a biologically active primary amine (mescaline). *Z. Naturforsch* **1955**, *10b*, 27-31.

2. Ringsdorf, H. Structure and properties of pharmacologically active polymers. *Journal of Polymer Science: Symposium* **1975**, *51*, 135-53.

3. Duncan, R.; Ringsdorf, H.; Satchi-Fainaro, R. Polymer Therapeutics - Polymers as Drugs, Conjugates and Gene Delivery Systems: Past, present and future opportunities. *Advances in Polymer Science* **2006**, *192*, 1-8.

4. Greenwald, R.; Choe, Y.; McGuire, J.; Conover, C. Effective drug delivery by PEGylated drug conjugates. *Advanced Drug Delivery Reviews* **2003**, *55*, 217–50.

5. Joralemon, M.J.; McRae, S.; Emrick, T. PEGylated Polymers for Medicine: From conjugatin to self-assembled systems. *Chemical Communications*, **2010**, *46*, 1377-93.

6. Bridges, A.; García, A. Anti-inflammatory polymeric coatings for implantable biomaterials and devices. *Journal of Diabetes Science and Technology* **2008**, *2*, 984–94.

7. Lee, K.; Mooney, D. Hydrogels for tissue engineering. *Chemical Reviews* **2001**, *101*, 1869–79.

8. Burdick, J.; Anseth, K. Photoencapsulation of osteoblasts in injectable RGD-modified PEG hydrogels for bone tissue engineering. *Biomaterials* **2002**, *23*, 4315–23.

9. Lutolf, M.; Hubbell, J. Synthetic biomaterials as instructive extracellular microenvironments for morphogenesis in tissue engineering. *Nature Biotechnology* **2004**, *23*, 47–55.

10. Zhu, J. Bioactive modification of poly(ethylene glycol) hydrogels for tissue engineering. *Biomaterials* **2010**, *31*, 4639–56.

11. Abuchowski, A.; van Es, T.; Palczuk, N.C.; Davis, F.F. Alteration of immunological properties of bovine serum albumin by covalent attachment of polyethylene glycol. *Journal of Biological Chemistry* **1977**, *252,* 3578-3581.

12. Maeda, H.; Greish, K.; Fang, J. The EPR effect and polymeric drugs: a paradigm shift for cancer chemotherapy in the 21st century. *Advances in Polymer Science* **2006**, *193*, 103–121.

13.　　Maeda, H.; Wu, J.; Sawa, T.; Matsumura, Y.; Hori, K. Tumor vascular permeability and the EPR effect in macromolecular therapeutics: a review. *Journal of Controlled Release* **2000**, *65*, 271-84.

14.　　Matsumura,Y.; Maeda, H. A new concept for macromolecular therapeutics in cancer chemotherapy: mechanism of tumoritropic accumulation of proteins and the antitumor agent smancs. *Cancer Research* **1986,** *46,* 6387-92.

15.　　Peer, D.; Karp, J.M.; Hong, S.; Farokhzad, O.C.; Margalit, R.; Langer, R. Nanocarriers as an emerging platform for cancer therapy. *Nature Nanotechnology* **2007**, *2*, 751-60.

16.　　Yigit, S.; Sanyal, R.; Sanyal, A. Fabrication and functionalization of hydrogels through "click" chemistry. *Chemistry, an Asian Journal* **2011**, *6,* 2648–59.

17.　　Davis, S.; Abuchowski, A.; Park, Y.K.; Davis, F.F. Alteration of the circulating life and antigenic properties of bovine adenosine deaminase in mice by attachment of polyethylene glycol. *Clinical and Experimental Immunology* **1981**, *46*, 649-52.

18.　　Satchi-Fainaro, R.; Duncan, R.; Barnes, C. M. Polymer therapeutics for cancer: current status and future challenges. *Advances in Polymer Science* **2006**, *193*, 1–65.

19.　　Bhadra, D.; Bhadra, S.; Jain, S.; Jain, N.K. Pegnology: a review of PEG-ylated systems. *International Journal of Pharmaceutics* **2003**, *257*, 111-24.

20.　　Wang, Y.-S.; Youngster, S.; Grace, M.; Bausch, J.; Bordens, R.; Wyss, D. Structural and biological characterization of pegylated recombinant interferon alpha-2b and its therapeutic implications. *Advanced Drug Delivery Reviews* **2002**, *54*, 547–70.

21.　　Tillman, H.; Kuhn, B.; Kranzlin, B.; Sadick, M.; Gross, J.; Gretz, N.; Pill, J. Efficacy and immunogenicity of novel erythropoietic agents and conventional rhEPO in rats with renal insufficiency. *Kidney International* **2006**, *69*, 60-67.

22.　　Rajan, R.; Li, T.; Aras, M.; Sloey, C.; Sutherland, W.; Arai, H.; Briddell, R.; Kinstler, O.; Lueras, A.; Zhang, Y.; Yeghnazar, H.; Treuheit, M.; Brems, D. Modulation of protein aggregation by polyethylene glycol conjugation: GCSF as a case study. *Protein science : a publication of the Protein Society* **2006**, *15*, 1063–75.

23.　　Slichenmyer, W.J.; Rowinsky, E.K.; Donehower, R.C.; Kaufman, S.H. The current status of camptothecin analogues as antitumor agents. *Journal of the National Cancer Institute* **1993**, *85*, 271-91.

24.   Greenwald, R.B.; Pendri, A.; Conover, C.; Gilbert, C.; Yang, R.; Xia, J. Drug delivery systems. 2. Camptothecin 20-O-poly(ethylene glycol) ester transport forms. *Journal of Medicinal Chemistry*, **1996**, *39*, 1938-40.

25.   Rowinsky, E.K.; Rizzo, J.; Ochoa, L.; Takimoto, C.H.; Forouzesh, B.; Schwartz, G.; Hammond, L.A.; Patnaik, A.; Kwiatek, J.; Goetz, A.; Denis, L.; McGuire, J.; Tolcher, A. A phase I and pharmacokinetic study of PEGylated camptothecin as a 1-hour infusion every 3 weeks in patients with advanced solid malignancies. *Journal of Clinical Oncology* **2003**, *21*, 148-157.

26.   Schluep, T.; Cheng, J.; Khin, K.; Davis, M. Pharmacokinetics and biodistribution of the camptothecin-polymer conjugate IT-101 in rats and tumor-bearing mice. *Cancer Chemotherapy and Pharmacology* **2006**, *57*, 654–62.

27.   Zhao, H.; Rubio, B.; Sapra, P.; Wu, D.; Reddy, P.; Sai, P.; Martinez, A.; Gao, Y.; Lozanguiez, Y.; Longley, C.; Greenberger, L.; Horak, I. Novel prodrugs of SN38 using multiarm poly(ethylene glycol) linkers. *Bioconjugate Chemistry* **2008**, *19*, 849–59.

28.   Parrish, B.; Emrick, T. Soluble camptothecin derivatives prepared by click cycloaddition chemistry on functional aliphatic polyesters. *Bioconjugate Chemistry* **2006**, *18*, 263–7.

29.   Kabanov, A.; Batrakova, E.; Alakhov, V. Pluronic block copolymers as novel polymer therapeutics for drug and gene delivery. *Journal of Controlled Release* **2002**, *82*, 189–212.

30.   Alakhov, V.; Klinski, E.; Li, S.; Pietrzynski, G.; Venne, A.; Batrakova, E.; Bronitch, T.; Kabanov, A. Block copolymer-based formulation of doxorubicin. From cell screen to clinical trials. *Colloids and Surfaces B: Biointerfaces* **1999**, *16*, 113-134.

31.   Nakanishi, T.; Fukushima, S.; Okamoto, K.; Suzuki, M.; Matsumura, Y.; Yokoyama, M.; Okano, T.; Sakurai, Y.; Kataoka, K. Development of the polymer micelle carrier system for doxorubicin *Journal of Controlled. Release* **2001**, *74*, 295-302

32.   Bae, Y.; Fukushima, S.; Harada, A.; Kataoka, K. Design of environment-sensitive supramolecular assemblies for intracellular drug delivery: polymeric micelles that are responsive to intracellular pH change. *Angewandte Chemie (International ed. in English)* **2003**, *42*, 4640–3.

33.   Opanasopit, P.; Yokoyama, M.; Watanabe, M.; Kawano, K.; Maitani, Y.; Okano, T. Block copolymer design for camptothecin incorporation into polymeric micelles for passive tumor targeting. *Pharmaceutical Research* **2004**, *21*, 2001–8.

34. Lowe, A.B.; McCormick, C.L. Synthesis and solution properties of zwitterionic polymers. *Chemical Reviews* **2002**, *102*, 4177-89.

35. Chen, M.; Briscoe, W.; Armes, S.; Klein, J. Lubrication at physiological pressures by polyzwitterionic brushes. *Science* **2009**, *323*, 1698–701.

36. Ishihara, K. New polymeric biomaterials - phospholipid polymers with a biocompatible surface. *Frontiers of Medical and Biological Engineering* **2000**, *10*, 83-95.

37. Ishihara, K.; Takai, M. Bioinspired interface for nanobiodevices based on phospholipid polymer chemistry. *Journal of the Royal Society Interface* **2009**, *6*, S279-91.

38. Ishihara, K.; Ueda, T.; Nakabayashi, N. Preparation of phospholipid polymers and their properties as polymer hydrogel membranes. *Polymer Journal* **1990**, *22*, 355-60.

39. Lobb, E.; Ma, I.; Billingham, N.; Armes, S.; Lewis, A. Facile synthesis of well-defined, biocompatible phosphorylcholine-based methacrylate copolymers via atom transfer radical polymerization at 20 degrees C. *Journal of the American Chemical Society* **2001**, *123*, 7913–4.

40. Wang, J.-S.; Matyjaszewski, K. Controlled/"Living" Radical Polymerization. Halogen Atom Transfer Radical Polymerization Promoted by a Cu(I)/Cu(II) Redox Process. *Macromolecules* **1995**, *28*, 7901-10.

41. Moad, G.; Chiefari, J.; Chong, (Bill) Y.; Krstina, J.; Mayadunne, R. T.; Postma, A.; Rizzardo, E.; Thang, S. H. Living free radical polymerization with reversible addition - fragmentation chain transfer (the life of RAFT). *Polymer International* **2000**, *49*, 993-1001.

42. Samanta, D.; McRae, S.; Cooper, B.; Hu, Y.; Emrick, T.; Pratt, J.; Charles, S. End-functionalized phosphorylcholine methacrylates and their use in protein conjugation. *Biomacromolecules* **2008**, *9*, 2891–7.

43. Chen, X.; McRae, S.; Samanta, D.; Emrick, T. Polymer−Protein Conjugation in Ionic Liquids. *Macromolecules* **2010**, *43*, 6261-3.

44. McRae, S.; Chen, X.; Kratz, K.; Samanta, D.; Henchey, E.; Schneider, S.; Emrick, T. Pentafluorophenyl ester-functionalized phosphorylcholine polymers: preparation of linear, two-arm, and grafted polymer-protein conjugates. *Biomacromolecules* **2012**, *13*, 2099–109.

45. Chen, X.; McRae, S.; Parelkar, S.; Emrick, T. Polymeric phosphorylcholine-camptothecin conjugates prepared by controlled free radical polymerization and click chemistry. *Bioconjugate Chemistry* **2009**, *20*, 2331–41.

46. Page, S.M.; Martorella, M.; Parelkar, S., Kosif, I.; Emrick, T. Disulfide Cross-Linked Phosphorylcholine Micelles for Triggered Release of Camptothecin. *Molecular Pharmaceutics* **2013**, *10*, 2684-92.

47. Chen, X.; Parelkar, S.; Henchey, E.; Schneider, S.; Emrick, T. PolyMPC-Doxorubicin Prodrugs. *Bioconjugate Chemistry* **2012**, *23*, 1753-1763.

48. Page, S.M.; Henchey, E.; Chen, X.; Schneider, S.; Emrick T. Efficacy of polyMPC-DOX prodrugs in 4T1 tumor-bearing mice. *Molecular Pharmaceutics* **2014**, Accepted.

49. Page, S.M.; Parelkar, S.; Gerasimenko, A.; Shin, D.Y.; Peyton, S.; Emrick, T. Promoting Cell Adhesion on Slippery Phosphorylcholine Hydrogel Surfaces. *Journal of Materials Chemistry B* **2014**, *2*, 620-624.

CHAPTER 2

PHOSPHORYLCHOLINE METHACRYLATES FOR PROTEIN CONJUGATION

2.1 Introduction

Covalent conjugation of synthetic polymers, such as poly(ethylene glycol) (PEG), to therapeutic proteins is a clinically relevant example of polymer therapeutics.[1-3] Such PEGylated proteins exhibit improved therapeutic efficacy over the native proteins, with prolonged *in vivo* circulation time resulting from enhanced protein stability in the bloodstream, increased size, and an associated reduction in immunogenicity.[4] A major therapeutic benefit stemming from these characteristics is a decreased dosing frequency required for effective therapy, enabled by the enhanced *in vivo* pharmacokinetics of the PEGylated proteins.

Early pioneering studies of PEGylated proteins showed their therapeutic benefit, using for example, PEGylated bovine serum albumin (BSA)[5] and insulin.[6] Numerous proteins have since been PEGylated, including uricase,[7] collagen,[8] trypsin,[9] alkaline phosphatase,[10] granulocyte colony stimulating factor (G-CSF),[11] and interferon.[12] The commercial availability of PEG derivatives containing terminal functionality suitable for protein conjugation, such as maleimides and N-hydroxysuccinimidyl (NHS)-esters, contributed to the rapid advances in this field.

The aqueous solubility and protein resistant characteristics of PEG are attributed to the association of water with the polyether backbone. The hydrophilic environment extending from the polymer shields indiscriminant protein adsorption, as described for PEGylated surfaces.[13] Several other synthetic polymers have also been studied in protein

conjugation, including poly(N-hydroxypropyl methacrylamide) (polyHPMA)[14-17] and poly(N-isopropylacrylamide) (polyNIPAAm).[18-20]

Methacryloyloxyethyl phosphorylcholine (MPC) polymers, despite their extensive track record of biocompatibility in coatings, contact lenses, and blood-contacting devices such as stents, have been under-exploited for polymer therapeutics.[21] Like PEG, polyMPC is hydrophilic due to an extensive association of water molecules with the backbone (15-25 per repeat unit).[21-22] Unlike PEG, which is an amphiphile, polyMPC is strictly hydrophilic, exhibiting insolubility in nearly all organic solvents. The absence of commercially available polyMPC derivatives has limited its use in protein conjugation to only a few recent studies, including our published work presenting the first report of end-functional polyMPC for protein conjugation.[23-28] This thesis also discusses subsequent efforts to expand the scope of conjugation chemistries available for use with polyMPC.

2.2 NHS- and benzaldehyde-polyMPC for protein conjugation

Traditionally, non-specific conjugation to proteins is achieved by reaction of surface available amine groups of lysine residues. Common functionalities employed to achieve this type of conjugation include 1) activated esters, such as N-hydroxysuccinimidyl (NHS), forming stable amide bonds, and 2) aldehydes for reductive amination chemistry where the initially-formed imine can be reduced irreversibly to an amine linkage. Early efforts towards polyMPC for protein conjugation focused on these two functional groups, incorporated at the polymer chain-end with an appropriately functionalized ATRP initiator (Biomacromolecules, 2008).

Until recently, MPC monomer was not readily commercially available, and was prepared according to literature procedures.[29]   MPC was synthesized from reaction of 2-hydroxyethyl methacrylate **9** (HEMA) and ethylene chlorophosphate, followed by ring-opening with trimethylamine (Scheme 2.1).
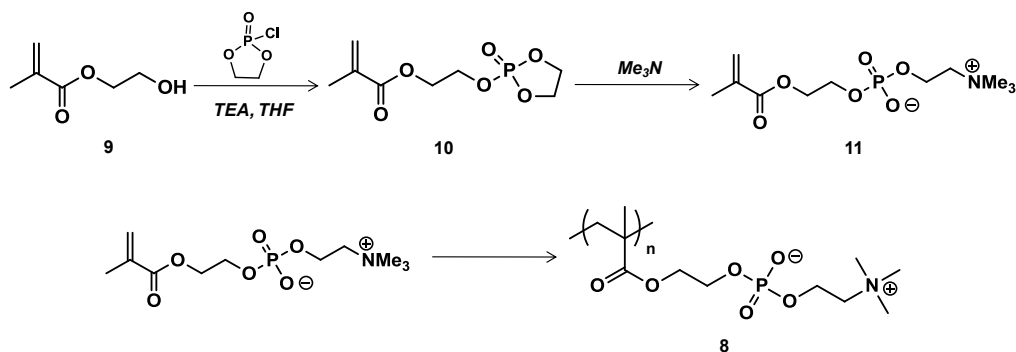
Scheme 2.1 Synthesis of MPC (**11**) and polymerization to give polyMPC.

Compound **11** is isolated by filtration and lyophilization, giving the desired MPC monomer as a white, hygroscopic powder in 50-60 % yield.   NMR spectroscopy confirmed formation of the monomer, showing the characteristic methacrylate alkene resonances (^{1}H at 5.5 and 6.0 ppm), as well as the expected ring-opened phospholane signal at 0 ppm in the ^{31}P NMR spectrum.   This process was found to be scalable, ultimately producing ~60 grams per batch.

NHS- and benzaldehyde- functionalized initiators were prepared according to Scheme 2.2 and subsequently used to polymerize MPC by ATRP in methanol/dimethylsulfoxide solvent mixtures with Cu(I)Br and bipyridine as the catalyst and ligand, respectively.   These conditions give nearly quantitative monomer conversion in 12 hours as judged by disappearance of monomeric olefins at 5.7 and 6.1 ppm, and the appearance of broad signals centered at 1.0 and 2.0 ppm for the methyl and methylene groups of the polymer backbone, respectively.   The polymer products were purified by

elution through a short plug of silica gel to give white solids. Signals at 2.8 ppm arising from the NHS methylenes, or at 9.7 ppm from the aldehyde resonance are useful for molecular weight estimation by end-group analysis. Polymers bearing the NHS or aldehyde functionality demonstrated predictable molecular weights up to 10 kDa with reasonably narrow polydispersities, determined by aqueous gel permeation chromatography (GPC) against linear poly(ethylene oxide) (PEO) standards (0.1 M $NaNO_3$ + 0.01 wt % NaN_3). Molecular weights determined by GPC were in good agreement with the results of end-group analysis from ^{1}H NMR. A summary of polymerization results is provided in Table 2.1.
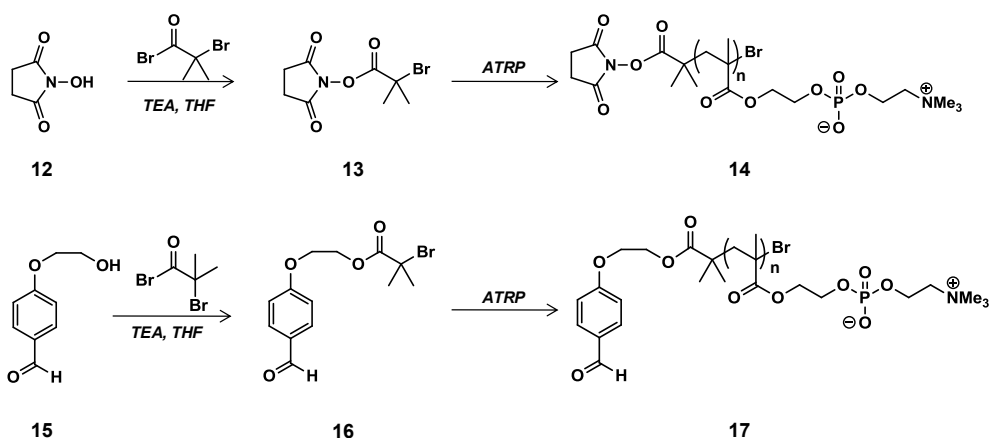
Scheme 2.2 Synthetic route to NHS- and benzaldehyde-functionalized polyMPC using ATRP.

Table 2.1 Summary of polymerization results for polymers **14** and **17**.

Sample	Initiator	Target Molecular Weight (g/mole)	Conversion by ^{1}H NMR Spectroscopy	Molecular Weight by ^{1}H NMR (g/mole)	Aq. GPC M_n (g/mole)	Aq. GPC PDI (M_w/M_n)
14 A	13	3,200	Quantitative	2,300	3,500	1.5
14 B	13	4,500	Quantitative	4,000	5,200	1.2
14 C	13	7,500	Quantitative	5,900	7,700	1.5
14 D	13	11,000	Quantitative	8,200	9,600	1.3
17 A	16	4,000	Quantitative	4,200	4,500	1.1
17 B	16	6,000	Quantitative	6,000	7,000	1.1
17 C	16	8,000	Quantitative	9,000	9,700	1.1

NHS- and benzaldehyde-terminated polyMPC were tested for protein conjugation using lysozyme as a model. Lysozyme is a 14.4 kDa protein isolated from chicken egg white, and contains seven surface-available amine groups (6 from lysine residues, 1 from the N-terminus of the protein) as possible reactive sites. PolyMPC samples **14** and **17** were conjugated to lysozyme under aqueous buffer conditions (from pH 6 to 9), and at different functional group stoichiometry and concentration (Figure 2.1A). The conjugation reactions were monitored by high performance liquid chromatography (HPLC) fitted with a size exclusion column, as well as by polyacrylamide gel electrophoresis (SDS-PAGE). Successful conjugation relied on working within an appropriate concentration range; dilute conditions, using, for example, a 1 mg/mL protein solution at pH 9.0 gave only ~25 % protein conjugation in 24 hours (conversion estimated from the relative areas of protein and conjugate in the HPLC trace). However, at ten-fold higher concentration, 80 % conversion was seen in 24 hours, with nearly quantitative conversion achieved following a second addition of polymer. Clearly the higher concentration is preferred, with the dual benefit of increasing the reaction rate and reducing the impact of competitive hydrolysis of the NHS end-group. Further evidence in support of lysozyme conjugation with polymer **14** was obtained by SDS-PAGE, which separates the PC-protein conjugate (Figure 2.1C, lane 3) from unreacted lysozyme (Figure 2.1C, lane 2). The conjugates smear on the gel (as seen also for PEGylated proteins[30,31]) due to inherent polydispersity of the conjugates and variability in conjugation sites. Lysozyme appears as a distinct band corresponding to ~15 kDa.

PolyMPC-lysozyme conjugates were purified by fast protein liquid chromatography (FPLC), using a Superose 6 10/300 preparative size exclusion column,

eluting with PBS buffer at a flow rate 0.5 mL/min. As seen in Figure 2.1B**,** the protein-polymer conjugate elutes over the range of 14-to-19 mL, a significantly lower retention volume relative to lysozyme itself (20-21 mL), due to the larger size of the conjugate. The bimodal nature of the conjugate peak is expected for samples in which there is heterogeneity in the number of conjugated polymers per protein. Typically, the eluted conjugate was collected in 1 mL fractions, with each analyzed further by HPLC with size-exclusion columns.

Conjugate **18** (prepared from polyMPC **14**) was used for preliminary *in vivo* evaluation, specifically monitoring the pharmacokinetics. Conjugate **18** and free lysozyme were fluorescently tagged using an Alexa Fluor dye (AF647) and injected subcutaneously in mice. Blood was withdrawn at preselected time points and dye concentration in the serum samples was analyzed using fluorescence spectroscopy. As shown in Figure 2.1D, the conjugate displays the expected increased half life ($t_{1/2}$) of 50 hours, compared to the $t_{1/2}$ for the unmodified enzyme of 2.4 hours. These preliminary findings confirmed that attachment of polyMPC to a protein would increase the circulation half life, potentially increasing the overall therapeutic efficacy if this strategy were used in conjunction with therapeutically-relevant proteins.
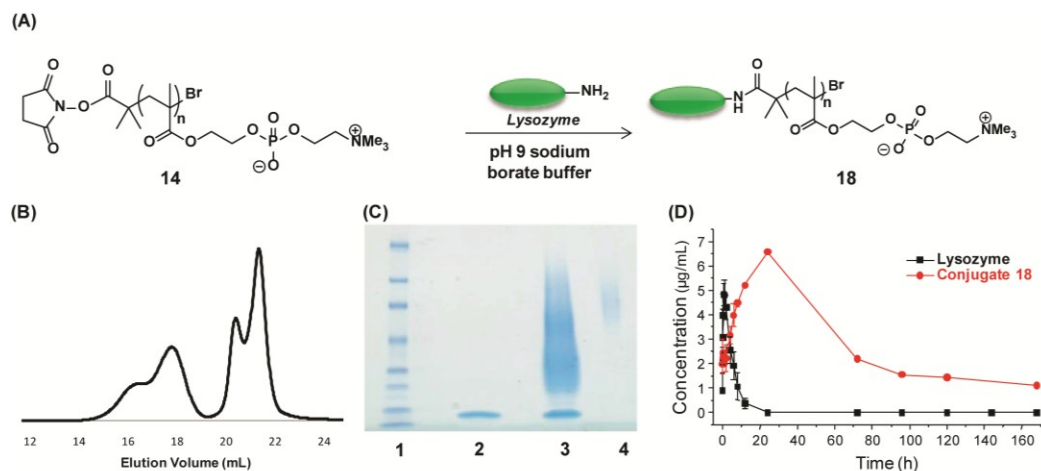
Figure 2.1 Synthetic scheme for preparation of polyMPC-lysozyme conjugates (A) and characterization including SEC-FPLC (B), SDS-PAGE (C) and preliminary pharmacokinetic evaluation in mice (D).

While NHS-esters are well-established for protein conjugation to various substrates, the susceptibility of NHS to hydrolysis in aqueous buffers can reduce the yield of attempted conjugation.[32] PolyMPC restricts solvent choices for the polymerization and work-up to water, methanol, and mixtures of these with some other solvents, so loss of the chain-end is likely (and has been characterized by NMR and UV/Vis spectroscopy[33]) even before its use in the conjugation reaction.   In an effort to preserve the NHS polymer chain end on polyMPC, we also explored the use of ionic liquids as polar, non-aqueous solvents for protein-polyMPC conjugation in high yield (Macromolecules, 2010).[27] Despite the success of this method, not all proteins will be amenable to reactions in ionic liquids, thus more robust chain-end functionality would be required to expand the scope of amine-reactive polyMPC structures in an aqueous environment.

2.3 Pentafluorophenyl ester-polyMPC

Pentafluorophenyl (PFP) esters, originally used in oligopeptide synthesis, react selectively with amines, and are more hydrolytically stable than N-hydroxysuccinimidyl (NHS) esters.[34,35] PFP-containing polymers have been studied in different contexts; for example, PFP-bearing chain transfer agents (CTAs) were synthesized for the polymerization of methacrylates by reversible addition fragmentation chain-transfer (RAFT), giving thermally responsive polymers having a PFP chain-end.[36,37] RAFT-polymerized PFP-containing methacrylates produced reactive homopolymers[35,38] and copolymers[39]; end-functional polymers prepared by RAFT bearing the PFP group for subsequent amidation were also reported.[40] One example exploited a PFP-acrylate copolymer as a surface coating, which allowed for subsequent protein immobilization.[41] In addition, a PFP-norbornene monomer was polymerized by ROMP, giving polynorbornene with demonstrated capacity for reaction with primary and secondary amines.[42] The work in this thesis represents the first example of PFP-functionalized ATRP initiators for MPC polymerization, giving highly water soluble and biocompatible polymers with chain-end functionality for fast and efficient protein conjugation (Biomacromolecules, 2012).[28] Additionally, various polymer architectures were explored in conjunction with this chain-end functionality, including linear, two-arm, and graft-type PC-polymers, derived from both methacrylate and cyclic olefin polymeric systems. In PEGylated proteins, multi-arm versions of PEG provide an alternative architecture with an envisaged "umbrella-like" coverage of the protein.[43] The architecture of polymer coverage may influence the properties of the conjugates, including activity, immunogenicity, and *in vivo* pharmacokinetics.[44] Yamasaki, *et al.* reported that

attachment of two-arm PEG to proteins resulted in a higher retention of enzymatic activity than linear PEG of similar molecular weight.[45] Similarly, covalently connecting a two-arm 10 kDa PEG to asparaginase reduced its antigenicity 10-fold relative to its linear PEG counterpart.[46,47] Taken together, these materials represent a novel PC-polymer platform well-suited for protein conjugation and, ultimately, examination in therapeutic settings.

Linear polyMPC was prepared from the novel ATRP initiator, PFP-ester **20**, shown in Scheme 2.3. Compound **20** was prepared in 70 % yield by reacting pentafluorophenol with 2-bromoisobutyryl bromide, isolated as a colorless liquid, and characterized by ^{1}H, ^{13}C, and ^{19}F NMR spectroscopy, and high resolution mass spectrometry (HRMS) (calculated: 331.9483; found: 331.9434). PolyMPC **21** was then prepared from initiator **20** by ATRP in a 1:1 DMSO/methanol solution in the presence of Cu(I)Br/bipyridine (bpy) as the catalyst/ligand system.
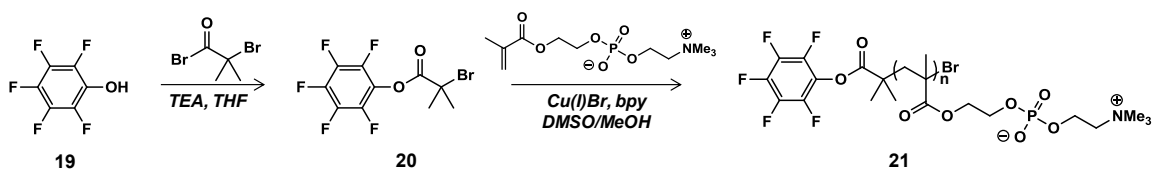
Scheme 2.3 Synthesis of linear PFP-containing ATRP initiator and polymerization of MPC.

The PFP-terminated polyMPC structures synthesized ranged from 5,000 to 30,000 g/mole, with polydispersity index (PDI) values from 1.2 - 1.5, estimated by aqueous gel permeation chromatography (GPC) (calibrated against linear PEO standards). The molecular weights were controlled by varying the monomer-to-initiator ratio, and monomer conversion was monitored by ^{1}H NMR spectroscopy (in CD$_3$OD solution), integrating monomer alkene resonances (5.4 and 6.0 ppm) against the polymer methyl

protons (1.0 ppm). At attempted higher molecular weight, some loss of control was noted by slightly higher PDI values. Following polymerization, the Cu catalyst was oxidized by exposure to air, and spent catalyst, ligand, and residual monomer were removed by passage through a short plug of silica, eluting with methanol. The pure polymer was isolated by precipitation into THF. ^{1}H NMR spectroscopy confirmed the expected backbone structure, and ^{19}F NMR showed the presence of the intact PFP-ester chain-end, with expected resonances at -152.9, -157.2, and -162.0 ppm in an integrated ratio of 2:1:2. PolyMPC **21** retained the PFP-ester end group even after several days in a solution of pH 9 sodium borate buffer with D_2O, as judged by ^{19}F NMR spectroscopy, showing no liberated pentafluorophenol, confirming PFP as a more robust end-group. Characterization data for three representative polymer samples is provided in Table 2.2.

Table 2.2 Polymerization results for polyMPC **21**: target molecular weight calculated from monomer:initiator ratio; percent conversion determined by ^{1}H NMR spectroscopy; peak elution time, M_n, M_w, and PDI determined by aqueous GPC against linear PEO calibration standards.

Polymer	Target MW (g/mole)	% Conversion	Peak Elution Time (min)	M_n (g/mole)	M_w (g/mole)	PDI (M_w/M_n)
21A	6,000	Quantitative	26.4	5,000	6,300	1.2
21B	20,000	90 %	24.9	11,700	15,000	1.3
21C	40,000	85 %	23.3	27,000	40,500	1.5

Two-arm PFP-polyMPC structures were synthesized and examined as alternatives to linear polymer conjugation, noting that one example of two-arm polyMPC can be found in a published patent for reductive amination.[48] Two-arm polyMPC was synthesized by incorporating a branching point into the ATRP initiator using bis-hydroxymethyl propionic acid (bis-MPA), as shown in Scheme 2.4. Acid chloride **23** was prepared from **22** with oxalyl chloride in CH_2Cl_2 followed by esterification with

ethylene glycol to give **24** as a colorless oil. The ethylene glycol linker provides spatial extension between the PFP group and the quaternary carbon of the branch point, an aspect found to be critical for successful protein conjugation.[28] Reaction of **24** with bis(pentafluorophenyl) carbonate gave PFP-initiator **25**, isolated as a pale yellow oil in 76 % yield. The structure of **25** was confirmed by ^{1}H, ^{19}F, and ^{13}C NMR spectroscopy, as well as HRMS (calculated: 684.9730; found: 684.9697). MPC polymerization using initiator **25** proceeded by ATRP in DMSO/methanol to give two-arm polyMPC **26** as a white solid, which was purified by precipitation into anhydrous THF or acetone.
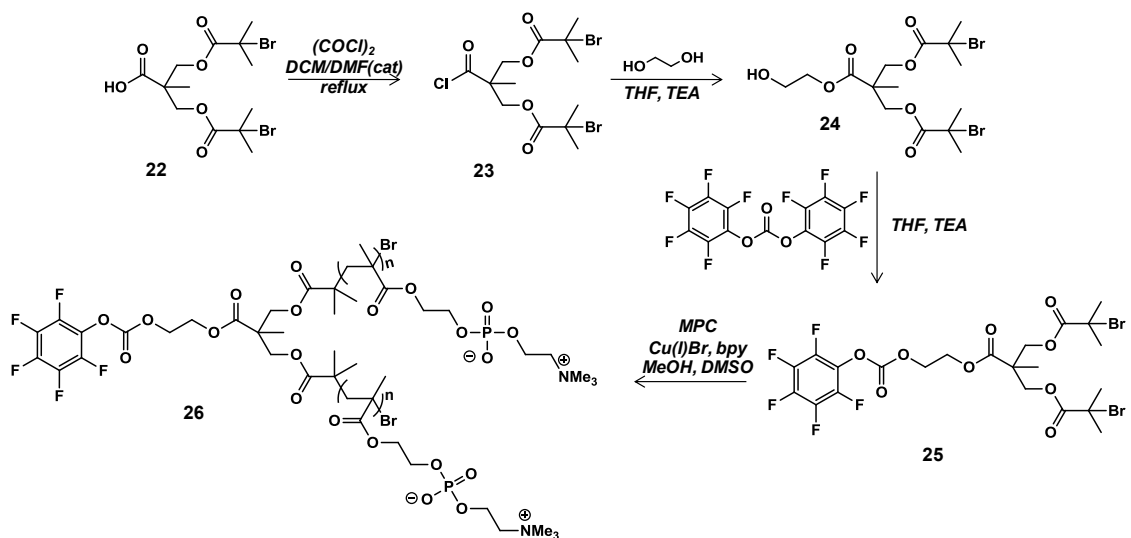
Scheme 2.4 Synthesis of two-arm branched PFP-containing ATRP initiator **25** and polymerization of MPC.

Polymers were synthesized over a range of molecular weights (Table 2.3), and characterized by ^{1}H and ^{19}F NMR spectroscopy, and aqueous gel permeation chromatography. GPC showed monomodal peaks with relatively narrow PDI values (~1.3), suggesting that initiation at each site occurred without steric interference from the other. The molecular weights estimated by GPC were slightly lower than the molecular weight determined by ^{1}H NMR spectroscopy and the monomer:initiator ratio.

Table 2.3 Summary of polymerization results for two-arm PFP-polyMPC **26**.

Polymer	Target MW (g/mole)	Conversion	Peak Elution Time (min)	M_n (g/mole)	M_w (g/mole)	PDI (M_w/M_n)
26A	6,000	Quantitative	25.2	6,450	9,200	1.4
26B	10,000	Quantitative	25.1	6,600	8,600	1.3
26C	20,000	Quantitative	24.7	13,700	17,600	1.3
26D	40,000	90 %	24.0	16,000	21,500	1.4

The steric freedom of PFP-carbonate terminated polyMPC **26** required more careful handling to avoid premature hydrolysis or methanolysis compared to the linear counterparts. Nonetheless, the end-group proved stable and effective when using minimal methanol, and avoiding a silica column for purification. Polymer **26** was isolated by simply precipitating into anhydrous THF, with retention of the PFP-carbonate chain end confirmed by ^{19}F NMR spectroscopy.

To expand the scope of PC polymers containing PFP groups for conjugation, a new set of structures was prepared by ring opening metathesis polymerization (ROMP) in collaboration with Katrina Kratz in the Emrick research group. This methodology exploits prior synthesis of PC-polyolefins,[49] while incorporating novel PFP-cyclooctene comonomers. PFP-containing cyclooctene **29** was synthesized from the acid chloride of carboxylate **28**, giving compound **29** as a yellow oil in 78 % yield. Copolymers from **27** and **29** were synthesized using the pyridine-substituted version of Grubbs' ruthenium benzylidene metathesis catalyst ((H_2IMes)(Cl)$_2$(pyr)$_2$RuCHPh) **31** in trifluoroethanol/CH_2Cl_2 mixtures, as shown in Scheme 2.5. Two samples of copolymer **31** of different molecular weights, each containing ~5 mole % PFP-ester monomer along the backbone, as determined by NMR spectroscopy were prepared. Molecular weight control was achieved by adjusting the monomer-to-catalyst feed ratio. Distinct from the PFP-ester terminated polyMPC described previously, these PC-polyolefin copolymers

have PFP groups situated randomly along the backbone, providing new, graft-type architectures for protein conjugation to the PC-polymer platform.
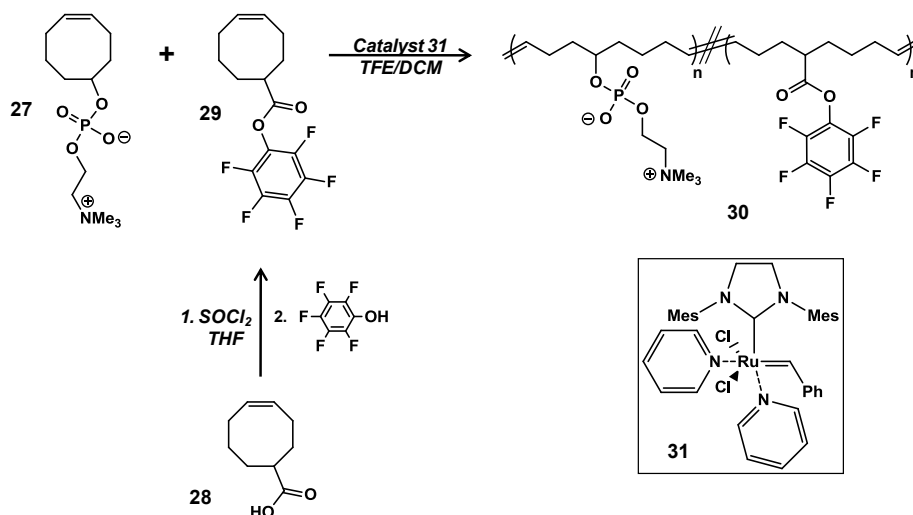
Scheme 2.5 Synthesis of PFP-COE **29**, and ROMP copolymerization with PC-COE **27** to give polymer **30**.

2.4 Protein conjugates from PFP-containing polymers

PFP-terminated polyMPC was tested for conjugation to lysozyme, as shown in Figure 2.2A, in pH 9 sodium borate buffer at room temperature. A lysozyme solution in buffer at 10 mg/mL was added to ~20 molar equivalents of PFP-polyMPC **21**. The reactions were monitored and characterized by high performance liquid chromatography (HPLC) and fast protein liquid chromatography (FPLC) (Figure 2.2B-C) using UV detection at 280 nm. High yielding conversion to conjugate (>80 %) was observed within 12 hours. Following FPLC purification, no unreacted lysozyme remains, as observed by SEC-FPLC (Figure 2.2C) and gel electrophoresis (SDS-PAGE) (Figure 2.2D). SDS-PAGE was carried out using gradient 4-15 % Tris-HCl polyacrylamide pre-cast gels with 25 mM Tris, 192 mM glycine, 0.1 % (w/v) SDS buffer at pH 8.3. The conjugates appear as polydisperse peaks by SEC, and as broad, smeared bands in SDS-

PAGE, which is attributed to the multiple reaction sites on lysozyme, as well as the polydispersity and hydrophilicity inherent to the polyzwitterionic structure.

Similarly, lysozyme conjugates were prepared from two-arm PFP-polyMPC **26** and poly(PC-COE)-*co*-(PFP-COE) **30**. The corresponding conjugates (Figure 2.2E and Figure 2.2F) were purified and isolated by FPLC, dialysis and lyophilization. Unique to the PC-polyolefins is the possible formation of conjugates consisting of multiple polymers per lysozyme, and/or multiple proteins conjugated to a single polymer chain. Considering the M_n and M_w values of these polymer samples, a percentage of the chains will have 2 or more PFP groups, giving the possibility of soluble network structures that cannot arise with PFP-terminated polyMPC. However, the excess of polymer used in these conjugation reactions precludes the formation of large network structures.
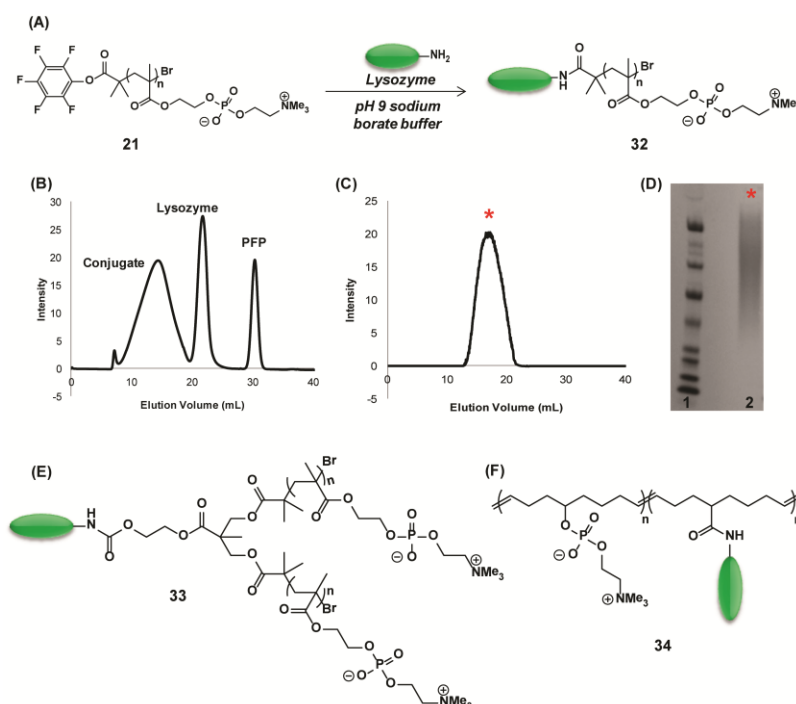
Figure 2.2 Preparation of linear polyMPC-lysozyme conjugate (A) and characterization: (B) SEC-FPLC of reaction mixture, (C) SEC-FPLC of purified conjugate, and (D) SDS-PAGE of purified conjugate. The corresponding two-arm (E) and grafted (F) conjugates were prepared under similar conditions.

32

Dynamic light scattering was performed on the linear, branched, and grafted polymer – protein conjugates prepared from comparable molecular weight polymers (approximately 15,000 g/mole) to examine their size in solution using the Malvern Zetasizer Nano series instrument. Native lysozyme had a measured diameter of 4.2 ± 0.1 nm in PBS solution at pH 7.4, and all of the lysozyme-polymer conjugates exhibited a distinct increase in size, with diameters of 10.7 ± 0.2 nm and 8.6 ± 0.1 nm for conjugates **32** (linear) and **33** (two-arm polyMPC), respectively. The grafted conjugate **34** displayed a large increase over the native enzyme, with a diameter of 22.7 ± 0.2 nm, attributed to the possibility of producing small multifunctional structures. However, in no case were unusually large structures seen that would be indicative of heavily aggregated or cross-linked material.

Polymer-protein conjugates typically exhibit activity and/or efficacy that differ from the native enzymes, depending to some extent on the proximity of the polymer to the active site. Even when conjugation is at some distance from the active site, the presence of the polymer may reduce activity if it becomes difficult (sterically) for the enzyme to interact with its environment. PEGylated G-CSF (Neulasta®), for example, retains 41 % of its native enzymatic activity.[11] Prior studies with lysozyme conjugated to a 5 kDa PEG chain showed suppressed enzymatic activity (77 %) relative to the native enzyme,[50] while a study on polyMPC-BSA and lysozyme conjugates showed 75-90 % of native enzymatic activity.[26] This data suggests that polymer conjugation does not markedly reduce enzyme activity, but that a modest reduction in activity may result from polymer shielding effects (steric interference).

The enzymatic activity of the polymer-lysozyme conjugates prepared in this study was tested using fluorescein-labelled *Micrococcus lysodeikticus* as the substrate. All the samples were prepared at lysozyme-equivalent concentrations, determined by UV/Vis spectroscopy with a standard curve constructed from different lysozyme concentrations at 280 nm. The substrate was incubated with the conjugates at 37 °C for one hour, then the fluorescence intensity of each was measured by excitation at 485 nm, detecting emission at 535 nm. The averaged measured values for the conjugates were compared to that of native lysozyme, and are reported as relative activities on the substrate (Figure 2.3). A no-enzyme control (NEC) experiment shows negligible background fluorescence in the absence of lysozyme. The linear and two-arm polyMPC conjugates were found to retain >80 % of the native enzymatic activity, while the graft conjugates retained >65 %. Two different molecular weight conjugates of each type were tested and compared to native lysozyme, with the results suggesting a correlation between polymer molecular weight and the activity retained. For the linear, two-arm, and grafted conjugates using a 4 - 6.5 kDa polymer, the relative enzymatic activity was very high (>98 %). At higher polymer molecular weight, lower activity was observed, specifically noted for the linear (84 %) and grafted (69 %) conjugates. As mentioned previously, this reduced activity may be due to steric interference of the enzyme with the substrate in the presence of these large polymer chains.
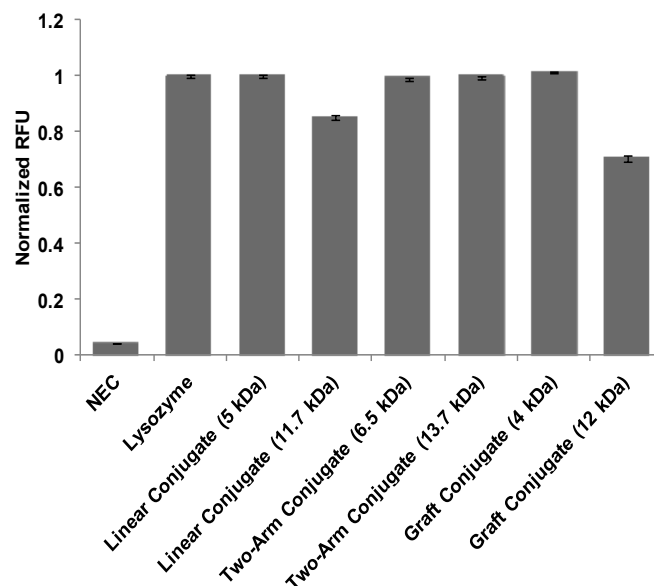
Figure 2.3 Results of fluorescence activity assay of lysozyme and lysozyme-polymer conjugates using fluorescein-labeled *Micrococcus lysodeikticus* (485 and 535 nm excitation and emission wavelengths, respectively). Samples were analyzed in triplicate. Error bars represent ± standard deviation.

To evaluate the polyMPC - protein conjugates *in vivo*, lysozyme, linear, and two-arm polyMPC-lysozyme conjugates were labeled with Alexa Fluor 647 (AF647) fluorescent dye. Such fluorescent labeling enables an evaluation of pharmacokinetics by HPLC. Analysis of aliquots of blood withdrawn at various time points, was used to determine the concentration of the conjugate in circulation at a given time. AF-labeled conjugates were purified by passage through a bio-gel P4 column eluting with pH 7.4 PBS, where two well-separated bands were seen, corresponding to the labeled product and unconjugated dye. The purified conjugates were concentrated and stored in solution at 4 °C. The purity of the AF-labeled structure was judged by SEC-HPLC with fluorescence detection, exciting at 650 nm and monitoring emission at 670 nm. AF647 concentration was determined by UV/Vis spectroscopy, and the solutions of labeled lysozyme and polyMPC-lysozyme were concentrated to 30 μg/mL (AF dye-equivalent

concentration). The labeled samples exhibited good stability at 4 °C for months, and were stable to freeze-thaw cycles as confirmed by HPLC analysis following such treatment. This feature is important for providing convenient and lengthy storage of polyMPC-protein conjugates. To analyze the pharmacokinetic properties of polyMPC-lysozyme conjugates **32** and **33** compared to lysozyme itself, AF647-labeled samples were injected intravenously into C57bl/6 mice (6 per group) at a dose of 1.5 mg/kg (AF dye equivalent doses). At designated time points, aliquots of blood were withdrawn from the animals. Following centrifugation and dilution with PBS, the serum samples were analyzed by SEC-HPLC with fluorescence detection, exciting at 650 nm and monitoring emission at 670 nm. AF647 dye concentrations in the samples at each time point was determined using a calibration curve and were plotted against post-injection time to generate the pharmacokinetics profiles of Figure 2.4.

The pharmacokinetic experiment reveals that polyMPC-lysozyme conjugate **32** remains in circulation much longer than lysozyme alone. The signal from labeled lysozyme became indistinguishable from the baseline in less than 12 hours, while the signal from the linear polyMPC conjugate extended to 5 days. The $t_{1/2}$ of 0.9 hours for free lysozyme was extended to 18 hours for the linear polymer-protein conjugate. Surprisingly, the two-arm polyMPC-lysozyme conjugate **33** showed a $t_{1/2}$ of only 1 hour, though low protein concentrations were detected for several days post-injection, giving in an increased area-under-the-curve (AUC) relative to native lysozyme, a phenomenon that is not well-understood. The presence of the linear polyMPC provides a $t_{1/2}$ that is ~30 times longer than the protein alone, and an AUC value ~24 times greater. In a study using interferon-α2a (a 20 kDa therapeutic protein)ʼ conjugation to a 20 kDa PEG-

equivalent molecular weight polyMPC (as determined by GPC againt PEO standards) was found to extend the elimination half life to 30 times that of the native enzyme[25], a result which is in excellent agreement with the findings presented here.
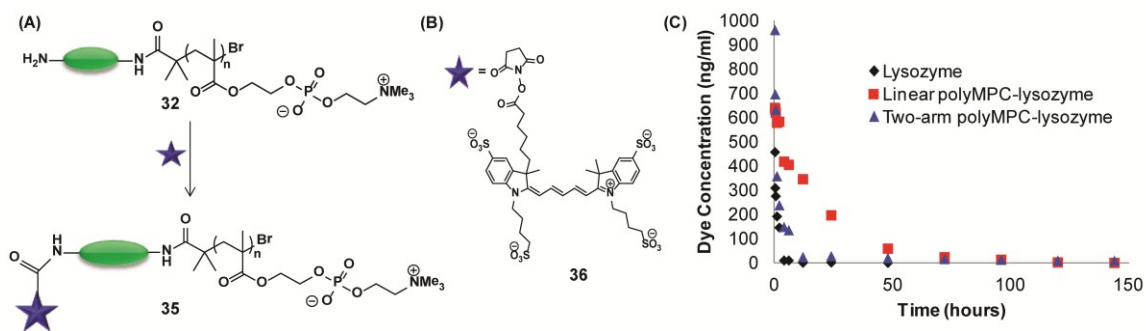
Figure 2.4 (A) Preparation of AF647-labeled polyMPC-lysozyme, (B) structure of AF647-NHS, and (C) PK plot comparing lysozyme, linear polyMPC-conjugate, and two-arm polyMPC-conjugate.

2.5 PolyMPC for site-selective protein conjugation

While the amidation methods discussed in the previous sections can be facile and effective for protein conjugation, it often yields non-selective attachment of multiple polymer chains, and a distribution of conjugate sizes within a given sample. Site-specific conjugation methods can eliminate the heterogeneity often associated with polymer-protein conjugates, producing well-defined samples with polymer attachment occurring only at particular locations. To this end, Lewis and coworkers previously reported the synthesis of a bis-sulfone polyMPC derivative for conjugation through disulfide bridges,[25] and Ishihara and coworkers subsequently reported the synthesis of a pyridine disulfide functionalized polyMPC for conjugation to thiol-containing proteins,[26] with both approaches yielding well-defined polymer-protein conjugates. Despite these advances, some drawbacks are noted, including the multistep synthetic pathways needed

to obtain the desired chain-end functionality, and that these particular examples are limited to thiol conjugation.

The reaction between an aminooxy functional group and a ketone or aldehyde to form a stable oxime bond has been explored as a route to chemoselective protein conjugation.[51-53] Ketones or aldehydes can be installed selectively on proteins through various methods, including solid phase protein synthesis,[51,54,55] protein engineering,[56] and chemical modification of amino acid residues.[52] Oxime formation to afford polymer-protein conjugates has been exploited in the case of poly(N-isopropylacrylamide) (PNIPAAm),[53] poly(2-hydroxyethylmethacrylate) (PHEMA),[53] and poly(PEG methacrylate),[53] with the oxime linkage found to be stable under physiological conditions.[56]

In this work, oxime conjugation chemistry has been extended to polyMPC for site-selective modification of proteins. This was accomplished by first synthesizing the aminooxy-containing ATRP initiator **39**, shown in Figure 2.5, as a shorter version of a known structure containing a tetraethylene glycol linker.[52] This was prepared by reaction of ethylene glycol with 2-bromoisobutyryl bromide, giving compound **38** in 60 % yield, followed by carbodiimide coupling of **38** with commercially-available (boc-aminooxy)acetic acid to give initiator **39** in 85 % yield. The structure of **39** was confirmed by ^{1}H NMR spectroscopy, specifically noting the t-boc protons at 1.5 ppm, and the methyl protons of the isobutyryl group at 1.9 ppm. Initiator **39** was mixed with MPC in a methanol/dimethylsulfoxide solution of Cu(I)Br/bipyridine as the catalyst/ligand system, giving boc-aminooxy terminated polyMPC **40**.
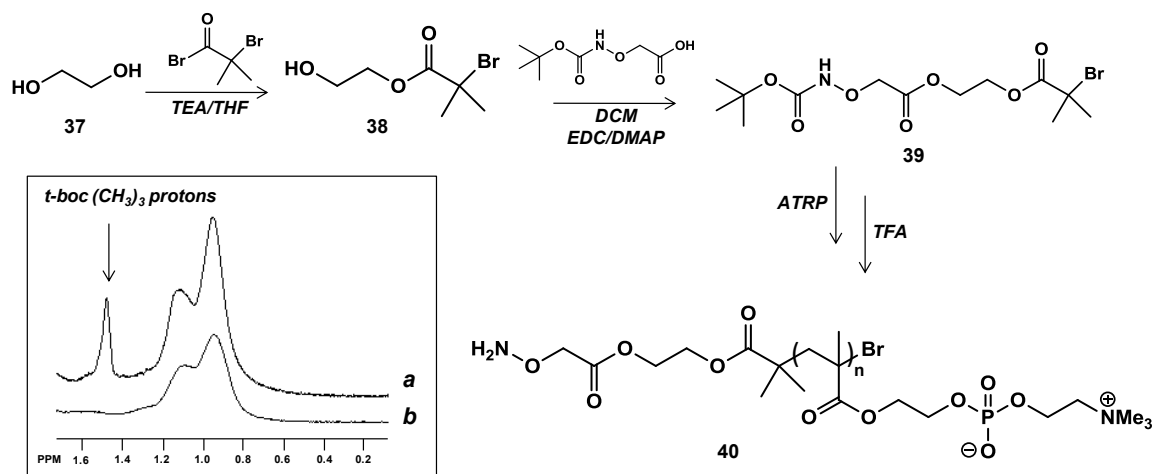
Figure 2.5 Synthesis of aminooxy-functionalized ATRP initiator **39** and polyMPC **40**. Inset is ^{1}H NMR spectrum before (a) and after (b) deprotection of the chain-end, showing disappearance of boc proton signal at 1.5 ppm.

Polymerizations were generally performed at room temperature for 18 hours, and monitored by ^{1}H NMR spectroscopy. Monomer conversion typically reached >95 %, determined by comparing the monomeric vinyl proton signals at 5.5 and 6 ppm with the methyl and methylene protons of the polymer backbone at 1 and 2 ppm, respectively. Polymers of varying molecular weights were obtained by adjusting monomer-to-initiator ratio at the outset of polymerization, and the samples displayed relatively narrow polydispersity indices (PDIs) (Table 2.4). Molecular weight and PDI values were characterized by aqueous gel permeation chromatography (GPC) against linear poly(ethylene oxide) standards in 0.1 M sodium nitrate and 0.02 weight percent sodium azide buffer. Successful deprotection of boc-aminooxy polyMPC in trifluoroacetic acid was confirmed by ^{1}H NMR spectroscopy, noting the loss of the t-boc proton signal at 1.5 ppm. GPC analysis before and after deprotection revealed no change in molecular weight, confirming the polymer backbone is stable to these deprotection conditions. The aminooxy-terminated polymers were purified by dialysis against pure water, followed by lyophilization to give the desired material as a white solid.

Table 2.4 Summary of polymerization results for aminooxy-polyMPC **40**.

Sample	[M]:[I]	Target M_n (g/mole)	Conversion	M_n (g/mole)	PDI (M_w/M_n)
40A	10:1	3,300	> 95 %	2,400	1.4
40B	17:1	5,400	> 95 %	5,000	1.3
40C	34:1	10,450	> 95 %	7,700	1.4
40D	66:1	20,000	> 95 %	15,000	1.5

Conditions suitable for reaction of aminooxy-terminated polyMPC were examined prior to protein conjugation, by reaction with 4-hydroxybenzaldehyde as a simple substrate, and one that provides a UV signature following conjugation. For example, polymer **40** was dissolved in pH 5.5 phosphate buffer/dimethylsulfoxide solution with 1.2 equivalents of 4-hydroxybenzaldehyde, and stirred at room temperature (Figure 2.6A). After several hours, an aliquot was removed and analyzed by aqueous GPC equipped with a UV detector (280 nm), showing substantial UV absorbance (Figure 2.6B) that reflects successful conjugation to the chain-end to give polymer **41**. Furthermore, ^{1}H NMR spectroscopy showed a singlet at 8.4 ppm corresponding to the *syn* addition product of the benzaldoxime chain-end, as well as signals at 7.05 and 7.64 ppm for the aromatic protons. End-group analysis by this technique indicated ~60 % conversion to the oxime-linked polymer **41**, confirming the ready availability of the aminooxy chain-end for reaction with ketones and aldehydes.
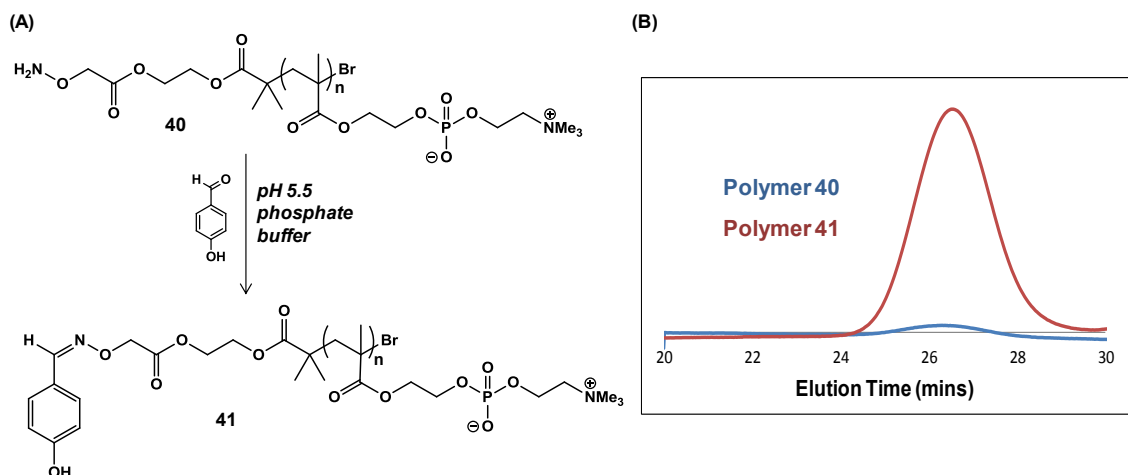
Figure 2.6 (A) Conversion of aminooxy-polyMPC **40** to benzaldoxime-polyMPC **41** and (B) aqueous GPC before and after conjugation (UV detection at 280 nm).

Aminooxy polyMPC **40** was tested for protein conjugation using lysozyme as a model enzyme. Lysozyme was first modified with pentafluorophenyl (PFP) ester-levulinate, compound **43** (prepared using a modified literature procedure[52]), to impart ketone functionality to the protein. Conjugation of lysozyme to **43** was performed in pH 9 sodium borate buffer, with 10 % DMSO, at room temperature. After 2 hours, analysis of the reaction mixture by cation exchange fast protein liquid chromatography (CE-FPLC) indicated complete conversion of native lysozyme. Lysozyme-levulinate **44** was purified by dialysis (MWCO 1000) against pure water, and isolated as a white solid following lyophilization. The presence of multiple amine groups on lysozyme allows for conjugation of more than one ketone per protein, and the molar ratio of lysoyzme to pentafluorophenyl ester-levulinate dictates the degree of modification. Electrospray ionization (ESI) mass spectrometry confirmed successful conjugation, with multiple ketones per lysozyme incorporated. We note that the techniques used here for conjugation and characterization are fully applicable to the synthesis of therapeutically relevant bioconjugates containing only one reactive site.

41
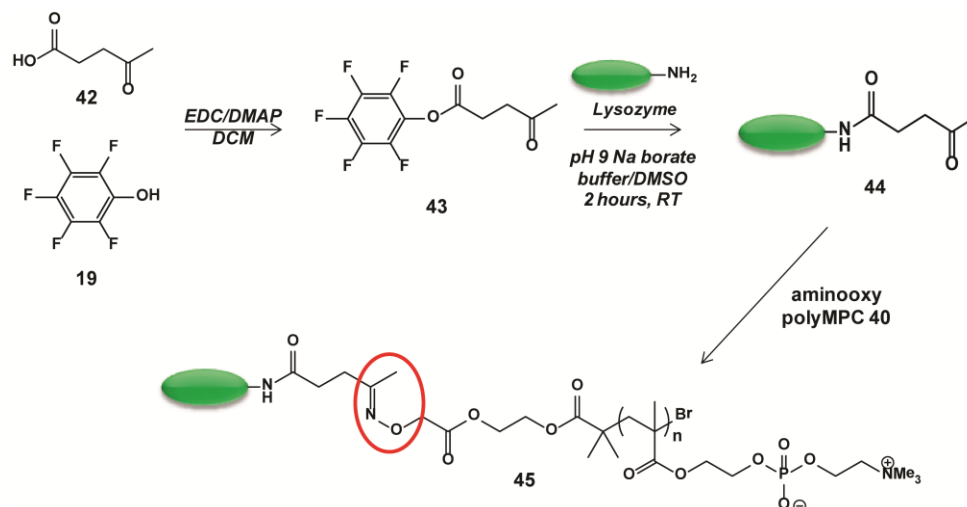
Scheme 2.6 Synthesis of lysozyme-levulinate **44** and polyMPC-lysozyme conjugate **45**.

Lysozyme-polyMPC conjugation was carried out using aminooxy-terminated polyMPC **40** with the ketone-modified enzyme **44**. This was done in phosphate buffer with 1:20 molar ratio of enzyme to polymer; conversion to conjugate **45** was monitored by size exclusion high performance liquid chromatography (SEC-HPLC). The conjugation was tested under several conditions: at pH 7.4 and 5.5, and with and without 100 mM aniline as catalyst. Oxime formation was found to occur at a reasonable rate in acidic pH, with aniline catalysis proceeding through a transimination reaction under acidic aqueous conditions.[57] Aliquots were removed from the reaction mixture at t = 2.5, 6, and 24 hours. Additionally, a control experiment was performed in which unmodified lysozyme was mixed with aminooxy polyMPC, which, as expected, led to no conjugation and elution of only native enzyme at 13 minutes. A representative HPLC chromatogram is shown in Figure 2.7, demonstrating efficient and selective conjugation of polyMPC-lysozyme, with conjugate eluting from 5 - 11 minutes, and unreacted lysozyme-levulinate eluting at 13 minutes.

By comparing the peak elution time of the conjugate to a calibration curve constructed from protein standards, the total molecular weight of the conjugate is an estimated 30,000 g/mole, corresponding to approximately 2 polymer chains per lysozyme. This is in good agreement with the estimated degree of functionalization of lysozyme-levulinate obtained by ESI-MS. Optimum conjugation conditions were found to be pH 5.5 phosphate buffer, with the presence of 100 mM aniline affording modest improvement in conjugation efficiency.
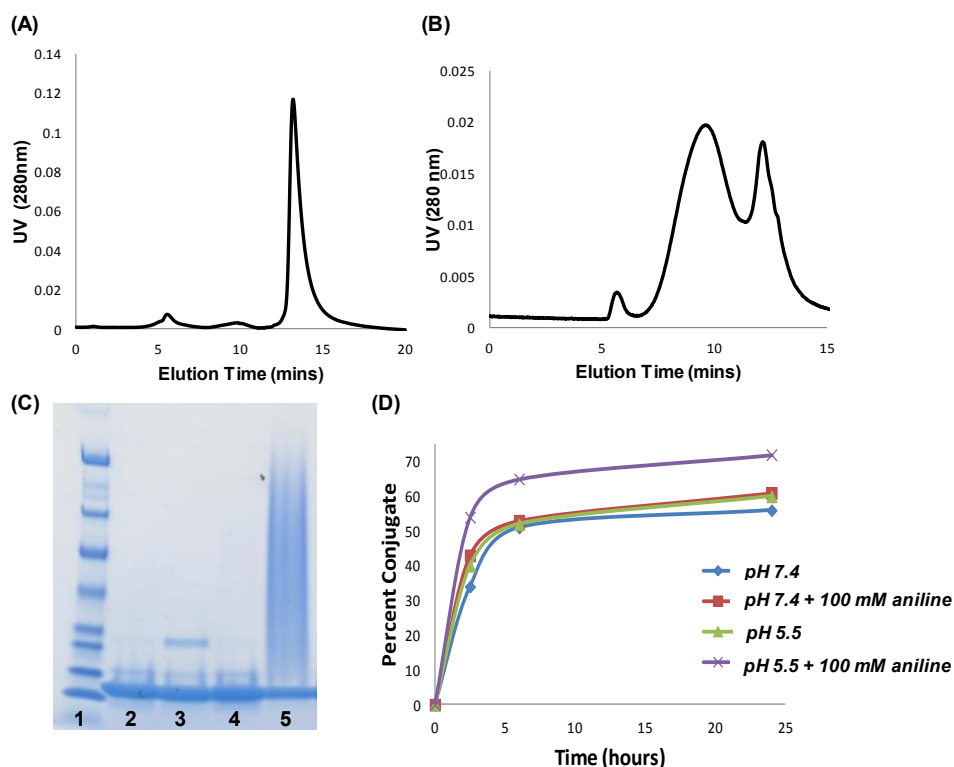
Figure 2.7 SEC-HPLC characterization of conjugation reactions: (A) lysozyme control; (B) conjugation in PBS pH 5.5 + 100 mM aniline. Conjugate elutes from 5-11 minutes and free protein elutes at 13 minutes. (C) SDS-PAGE analysis: Lane 1: protein standards; Lane 2: native lysozyme; Lane 3: lysozyme-levulinate; Lane 4: lysozyme control reaction; Lane 5: conjugation reaction at 24 hours in pH 5.5 PBS + 100 mM aniline. (D) Conversion vs. time for conjugation at different pH and catalytic aniline concentrations.

PolyMPC-lysozyme conjugation was also analyzed by gel electrophoresis (Figure 2.7), which confirmed the SEC-HPLC findings. SDS-PAGE was done on gradient 4-15 % Tris-HCl polyacrylamide pre-cast gels with 25 mM Tris, 192 mM glycine, and 0.1 % (w/v) SDS buffer at pH 8.3. Lane 1 shows broad-range protein standards (top to bottom: 209.0, 124.0, 80.0, 48.1, 34.8, 28.9, 20.6, and 7.1 kDa), and lanes 2 and 3 show native lysozyme and lysozyme-levulinate, respectively. Lane 4 confirms that conjugate is not formed in the absence of ketone functionality on lysozyme, and lane 5 shows the polyMPC-lysozyme conjugate as a broad band due to polydispersity and hydrophilicity inherent to the polymer, as well as the size distribution of conjugates within the sample resulting from the potential for multi-site attachment.

2.6 Conclusions and future outlook

In summary, a series of linear, two-arm, and grafted polymer – protein conjugates were prepared, exploiting active esters as chain-ends and pendent groups for protein conjugation to PC-polymers. PFP-esters represent an alternative active ester for efficient protein conjugation, with better hydrolytic stability than conventional NHS esters. DLS experiments showed that varying the architecture and molecular weight of the polymer affects the solution size of the conjugate, which in turn affects the pharmacokinetic properties of a therapeutic conjugate, altering the absorption/elimination half lives and effective exposure time.

Additionally, the synthesis of novel aminooxy-terminated MPC polymers using ATRP for a site-selective approach to forming well-defined protein conjugates was explored. These polymers are amenable to conjugation only with proteins bearing ketone functionality, as demonstrated using levulinate-modified lysozyme as a model system.

Conjugation conditions were optimized, demonstrating that the reaction is most efficient at low pH in conjunction with catalytic aniline.

The combination of synthetic ease, conjugation efficiency, retained enzymatic activity, and prolonged circulation time makes these structures interesting and potentially valuable for future polymer therapeutics. The examples presented here focus on lysozyme as a model system, however, going forward, these and other conjugation strategies will be applied to therapeutic proteins.

2.7 References

1.   Caliceti, P.; Veronese, F. Pharmacokinetic and biodistribution properties of poly(ethylene glycol)-protein conjugates. *Advanced Drug Delivery Reviews* **2003**, *55*, 1261–77.

2.   Roberts, M.; Harris, J. Attachment of degradable poly(ethylene glycol) to proteins has the potential to increase therapeutic efficacy. *Journal of Pharmaceutical Sciences* **1998**, *87*, 1440–5.

3.   Joralemon, M.J.; McRae, S.; Emrick, T. PEGylated Polymers for Medicine: From conjugatin to self-assembled systems. *Chemical Communications* **2010**, *46*, 1377-93.

4.   Katre, N.V. The conjugation of proteins with polyethylene glycol and other polymers. *Advanced Drug Delivery Reviews* **1993**, *10*, 91-114.

5.   Abuchowski, A.; van Es, T.; Palczuk, N.C.; Davis, F.F. Alteration of immunological properties of bovine serum albumin by covalent attachment of polyethylene glycol. *Journal of Biological Chemistry* **1977**, *252*, 3578-81.

6.   Hinds, K.; Kim, S. Effects of PEG conjugation on insulin properties. *Advanced Drug Delivery Reviews* **2002**, *54*, 505–30.

7.   Abuchowski, A.; Karp, D.; Davis, F.F. Reduction of plasma urate levels in the cockerel with polyethylene glycol-uricase. *Journal of Pharmacology and Experimental Therapeutics* **1981**, *219*, 352-4.

8.   Rhee, W.; Carlino, J.; Chu, S.; Higley, H. *Poly(ethylene glycol) Chemistry: Biotechnical and Biomedical Applications* **1992**, *Platinum Press, New York*, 183-98.

9.   Abuchowski, A.; Davis, F.F. Preparation and properties of polyethylene glycol-trypsin adducts. *Biochimica et Biophysica Acta* **1979**, *578*, 41-6.

10. Yoshinaga, K.; Shafer, S.G.; Harris, J.M. Effects of Polyethylene Glycol Substitution on Enzyme Activity. *Journal of Bioactive and Compatible Polymers* **1987**, *2*, 49-56.

11. Tanaka, H.; Satake-Ishikawa, R.; Ishikawa, M.; Matsuki, S. Pharmacokinetics of recombinant human granulocyte colony-stimulating factor conjugated to polyethylene glycol in rats. *Cancer Research* **1991**, *51*, 3710-14.

12. Bukowski, R.; Tendler, C.; Cutler, D.; Rose, E.; Laughlin, M.; Statkevich, P. Treating cancer with PEG Intron: pharmacokinetic profile and dosing guidelines for an improved interferon-alpha-2b formulation. *Cancer* **2002**, *95*, 389–96.

13. Ikada, Y. Surface modification of polymers for medical applications. *Biomaterials* **1994**, *15*, 725–36.

14. Lu, Z.; Kopecková, P.; Wu, Z.; Kopecek, J. Functionalized semitelechelic poly[N-(2-hydroxypropyl)methacrylamide] for protein modification. *Bioconjugate Chemistry* **1998**, *9*, 793–804

15. Ulbrich, K.; Strolhalm, J.; Plocova, D.; Oupicky, D.; Subr, V.; Soucek, J.; Pouckova, P.; Matousek, J. Poly [N-(2-Hydroypropyl) Methacrylamide] Conjugates of Bovine Seminal Ribonuclease. Synthesis, Physicochemical, and Preliminary Biological Evaluation. *Journal of Bioactive and Compatible Polymers* **2000**, *15*, 4-26.

16. Sure, V.; Etrych, T.; Ulbrich, K.; Hirano, T.; Kondo, T.; Todoroki, T.; Jelinkova, M.; Rihova, B. Synthesis and Properties of Poly[N-(2-Hydroxypropyl) Methacrylamide] Conjugates of Superoxide Dismutase. *Journal of Bioactive and Compatible Polymers* **2002**, *17*, 105-122.

17. Tao, L.; Liu, J.; Davis, T. Branched polymer-protein conjugates made from mid-chain-functional P(HPMA). *Biomacromolecules* **2009**, *10*, 2847–51.

18. Heredia, K.; Bontempo, D.; Ly, T.; Byers, J.; Halstenberg, S.; Maynard, H. In situ preparation of protein-"smart" polymer conjugates with retention of bioactivity. *Journal of the American Chemical Society* **2005**, *127*, 16955–60.

19. Bontempo, D.; Maynard, H. Streptavidin as a macroinitiator for polymerization: in situ protein-polymer conjugate formation. *Journal of the American Chemical Society* **2005**, *127*, 6508–9.

20. Bontempo, D.; Li, R.C.; Ly, T.; Brubaker, C.E.; Maynard, H.D. One-step synthesis of low polydispersity, biotinylated poly(N-isopropylacrylamide) by ATRP. *Chemical Communications* **2005**, *37*, 4702-4.

21. Iwasaki, Y.; Ishihara, K. Phosphorylcholine-containing polymers for biomedical applications. *Analytical and Bioanalytical Chemistry* **2005**, *381*, 534–46.

22. Ishihara, K.; Nomura, H.; Mihara, T.; Kurita, K.; Iwasaki, Y.; Nakabayashi, N. Why do phospholipid polymers reduce protein adsorption? *Journal of Biomedical Materials Research* **1998**, *39*, 323–30.

23. Miyamoto, D.; Watanabe, J.; Ishihara, K. Effect of water-soluble phospholipid polymers conjugated with papain on the enzymatic stability. *Biomaterials* **2003**, *25*, 71–6.

24. Samanta, D.; McRae, S.; Cooper, B.; Hu, Y.; Emrick, T.; Pratt, J.; Charles, S. End-functionalized phosphorylcholine methacrylates and their use in protein conjugation. *Biomacromolecules* **2008**, *9*, 2891–7.

25. Lewis, A.; Tang, Y.; Brocchini, S.; Choi, J.; Godwin, A. Poly(2-methacryloyloxyethyl phosphorylcholine) for protein conjugation. *Bioconjugate Chemistry* **2008**, *19*, 2144-55.

26. Seo, J.; Matsuno, R.; Lee, Y.; Takai, M.; Ishihara, K. Conformation recovery and preservation of protein nature from heat-induced denaturation by water-soluble phospholipid polymer conjugation. *Biomaterials* 2009, *30*, 4859-67.

27. Chen, X.; McRae, S.; Samanta, D.; Emrick, T. Polymer−Protein Conjugation in Ionic Liquids. *Macromolecules* **2010**, *43*, 6261-3.

28. McRae, S.; Chen, X.; Kratz, K.; Samanta, D.; Henchey, E.; Schneider, S.; Emrick, T. Pentafluorophenyl ester-functionalized phosphorylcholine polymers: preparation of linear, two-arm, and grafted polymer-protein conjugates. *Biomacromolecules* **2012**, *13*, 2099–109.

29. Ishihara, K.; Ueda, T.; Nakabayashi, N. Preparation of phospholipid polymers and their properties as polymer hydrogel membranes. *Polymer Journal* **1990**, *22*, 355-60.

30. Nicolas, J.; Miguel, V. S.; Mantovani, G.; Haddleton, D. M. Fluorescently tagged polymer bioconjugates from protein derived macroinitiators. *Chemical Communications* **2006**, 4697-99.

31. Tao, L.; Mantovani, G.; Lecolley, F.; Haddleton, D. M. α-Aldehyde terminally functional methacrylic polymers from living radical polymerization: application in protein conjugation "Pegylation". *Journal of the American Chemical Society* **2004**, *126*, 13220-1.

32. Hermanson, G.T. *Bioconjugate Techniques* **1996**, *Academic Press, Inc.*, 139-40.

33. Miron, T.; Wilchek, M. A spectrophotometric assay for soluble and immobilized N-hydroxysuccinimide esters. *Analytical Biochemistry* **1982**, *126*, 433-5.

34. Kisfaludy, L.; Schon, I. Preparation and applications of pentafluorophenyl esters of 9-fluorenylmethyloxycarbonyl amino acids for peptide synthesis. *Synthesis* **1983**, *4*, 325-27.

35. Eberhardt, M.; Mruk, R.; Zentel, R.; Théato, P. Synthesis of pentafluorophenyl(meth)acrylate polymers: New precursor polymers for the synthesis of multifunctional materials. *European Polymer Journal* **2005**, *41,* 1569-75.

36. Roth, P. J.; Wiss, K. T.; Zentel, R.; Theato, P. Synthesis of Reactive Telechelic Polymers Based on Pentafluorophenyl Esters. *Macromolecules* **2008**, *41*, 8513-19.

37. Wiss, K. T.; Krishna, O. D.; Roth, P. J.; Kiick, K. L.; Theato, P. A Versatile Grafting-to Approach for the Bioconjugation of Polymers to Collagen-like Peptides Using an Activated Ester Chain Transfer Agent. *Macromolecules* **2009**, *42*, 3860-63.

38. Gibson, M. I.; Fröhlich, E.; Klok, H.-A. Postpolymerization modification of poly(pentafluorophenyl methacrylate): Synthesis of a diverse water-soluble polymer library. *Journal of Polymer Science Part A: Polymer Chemistry* **2009**, *47*, 4332-45.

39. Eberhardt, M.; Théato, P. RAFT Polymerization of Pentafluorophenyl Methacrylate: Preparation of Reactive Linear Diblock Copolymers. *Macromolecular Rapid Communications* **2005**, *26,* 1488-93.

40. Roth, P.J.; Jochum, F.D; Zentel, R.; Theato, P. Synthesis of Hetero-Telechelic α,ω Bio-Functionalized Polymers. *Biomacromolecules* **2010**, *11*, 238-40.

41. Kessler, D.; Roth, P.; Theato, P. Reactive surface coatings based on polysilsesquioxanes: controlled functionalization for specific protein immobilization. *Langmuir : the ACS journal of surfaces and colloids* **2009**, *25*, 10068–76.

42. Vogel, N.; Théato, P. Controlled Synthesis of Reactive Polymeric Architectures Using 5-Norbornene-2-carboxylic Acid Pentafluorophenyl Ester. *Macromolecular Symposia* **2007**, 249-50.

43. Zhang, Y.; Wang, G.; Huang, J. A new strategy for synthesis of "umbrella-like" poly(ethylene glycol) with monofunctional end group for bioconjugation. *Journal of Polymer Science Part A: Polymer Chemistry* **2010**, *48*, 5974-81.

44. Jevsevar, S.; Kunstelj, M.; Porekar, V. PEGylation of therapeutic proteins. *Biotechnology Journal* **2009**, *5*, 113–28.

45.	Yamasaki, M.; Okabe, M.; Suzawa, T.; Yokoo, Y. New PEG2 type polyethylene glycol derivatives for protein modification. *Biotechnology Techniques* **1998**, *12*, 751-54.

46.	Veronese, F. M.; Monfardini, C.; Caliceti, P.; Schiavon, O.; Scrawen, M. D.; Beer, D. Improvement of pharmacokinetic, immunological and stability properties of asparaginase by conjugation to linear and branched monomethoxy poly(ethylene glycol). *Journal of Controlled Release* **1996**, *40*, 199-209.

47.	Matsushima, A.; Nishimura, H.; Ashihara, Y.; Yokota, Y.; Inada, Y. Modification of E.Coli Aspariginase with 2,4-Bis(methoxypolyethyleneglycol)-6-chloro-s-triazine (activated PEG2); Disappearance of Binding Ability Towards Anti-Serum and Retention of Enzymatic Activity. *Chemistry Letters* **1980**, *9*, 773-76.

48.	Charles, S.A.; (Oligasis Corporation, USA). US Patent Application Publication US 2010/0166700 A1, July 1, 2010.

49.	Kratz, K.; Breitenkamp, K.; Hule, R.; Pochan, D.; Emrick, T. PC-Polyolefins: Synthesis and Assembly Behavior in Water. *Macromolecules* **2009**, *42*, 3227-29.

50.	da Silva Freitas, D.; Abrahao-Neto, J. Biochemical and biophysical characterization of lysozyme modified by PEGylation. *International Journal of Pharmaceutics* **2010**, *392*, 111-17.

51.	Kochendoerfer, G.G.; Chen, S.-Y.; Mao, F.; Cressman, S.; Traviglia, S.; Shao, H.; Hunter, C.L.; Low, D.W.; Cagle, E.N.; Carnevali, M.; Gueriguian, V.; Keogh, P.J.; Porter, H.; Stratton, S.M.; Wiedeke, M.C.; Wilken, J.; Tang, J.; Levy, J.J.; Miranda, L.P.; Crnogorac, M.M.; Kalbag, S.; Botti, P.; Schindler-Horvat, J.; Savatski, L.; Adamson, J.W.; Kung, A.; Kent, S.B.H.; Bradburne, J.A. Design and chemical synthesis of a homogenous polymer-modified erythropoiesis protein. *Science* **2003**, *299*, 884-7.

52.	Heredia, K.L.; Tolstyka, Z.P.; Maynard, H.D. Aminooxy end-functionalized polymers synthesized by ATRP for chemoselective conjugation to proteins. *Macromolecules* **2007**, *40*, 4772-79.

53.	Vasquez-Dorbatt, V.; Tolstyka, Z.P.; Maynard, H.D. Synthesis of aminooxy end-functionalized pNIPAAM by RAFT polymerization for protein and polysaccharide conjugation. *Macromolecules* **2009**, *42*, 7650-56.

54.	Shao, H.; Crnogorac, M.M.; Kong, T.; Chen, S.Y.; Williams, J.M.; Tack, J.M.; Gueriguian, V.; Cagle, E.N.; Carnevali, M.; Tumelty, D.; Paliard, X.; Miranda, L.P.; Bradburne, J.A.; Kochendoerfer, G.G. Site-specific polymer attachment to a CCL-5 (RANTES) analogue by oxime exchange. *Journal of the American Chemical Society* **2005***, 127*, 1350-51.

55.   Tumelty, D.; Carnevali, M.; Miranda, L.P. A new approach to the chemical synthesis of keto-proteins. *Journal of the American Chemical Society* **2003**, *125*, 14238-39.

56.   Carrico, I.S.; Carlson, B.L.; Bertozzi, C.R. Introducing genetically encoded aldehydes into proteins. *Nature Chemical Biology* **2007**, *3*, 321-22.

57.   Dirksen, A.; Dawson, P.E. Rapid oxime and hydrazone ligations with aromatic aldehydes for biomolecular labeling. *Bioconjugate Chemistry* **2008**, *19*, 2543-48.

CHAPTER 3

POLYMPC PRODRUGS FOR CHEMOTHERAPEUTICS

3.1 Introduction to polymer prodrugs

Advances in polymer therapeutics provide new opportunities for improving pharmaceutical administration and delivery methods, including advances in experimental approaches to chemotherapy.[1,2,3] Small molecule antitumor agents used clinically often display poor pharmacokinetics, undesired toxicity and side-effects, and poor water solubility, presenting major delivery challenges. Numerous chemotherapeutic drugs used today have a relatively low therapeutic index, or therapeutic ratio, described as the lethal dose divided by the therapeutic dose (LD_{50}/ED_{50}). In essence, therapeutic benefits tend to be offset by detrimental side effects. Covalently conjugating a small molecule drug to a water-soluble polymer scaffold affords prodrugs with massively improved aqueous solubility, longer *in vivo* circulation time ($t_{1/2}$), and reduced side effects.[1] Macromolecular scaffolds afford increased hydrodynamic size compared to the drug alone, resulting in slower renal clearance, and increased uptake in tumor tissue by the enhanced permeability and retention (EPR) effect.[4] The EPR effect exploits preferential uptake of large molecules due to the porous vasculature of tumor tissue, and subsequent retention as a result of poor lymphatic drainage relative to healthy tissue.

Effective polymer prodrugs employ water-soluble, biocompatible polymers that introduce potent cancer drugs (which are often hydrophobic compounds) effectively into the bloodstream. In prodrug form, the drug payload is rendered inactive, with release from the polymer scaffold dictated by the type of linkage between the drug and polymer.

Upon release, active drug is recovered, and the inert polymer carrier clears from the body. A schematic representation of this process is shown in Figure 3.1.
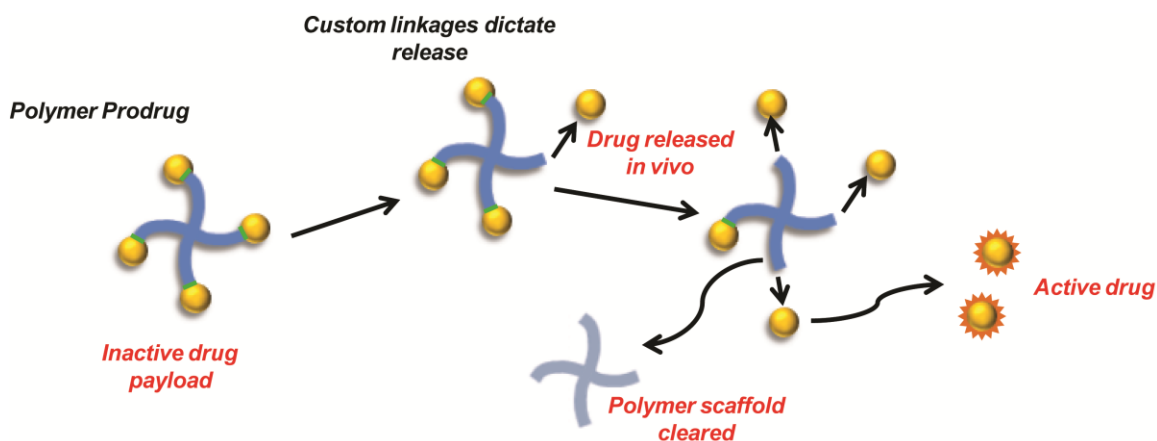
Figure 3.1 Schematic representation of polymer prodrug release mechanism *in vivo*.

Examples of hydrophilic polymers suitable for cancer drug delivery include poly(ethylene glycol) (PEG),[5] poly-*N*-(2-hydroxypropyl)methacrylamide (HPMA),[6-9] and cyclodextrin-based polymers.[10,11] Prominent among PEGylated cancer drug candidates is camptothecin (CPT), for which PEGylated versions show modestly enhanced circulation time and reduced side effects.[12] PEGylated camptothecin, reported by Enzon, Inc. as Prothecan®, consists of a 40,000 g/mol PEG chain with camptothecin at each chain-end, connected by ester linkages at the C-20-OH position of the drug.[12] Another chemotherapeutic agent, doxorubicin (DOX), has also been improved by PEGylation, including for example, with linear PEG conjugation,[13] as well as through sophisticated architectures such as "bow-tie" dendrimers.[14] The resulting polymer therapeutics display increased water solubility, decreased toxicity, and enhanced specificity due to the action of the EPR effect.

PolyMPC has been used extensively in bulk materials and coatings for contact lenses and blood-contacting devices that require a high level of biocompatibility and

resistance to protein adsorption.[15-21] As polyMPC has a decidedly lower commercial availability than functional PEG-based derivatives, its use in conjugation chemistry towards polymer prodrug therapeutics has been limited. Living free radical polymerization techniques, such as ATRP[22-25] and RAFT,[26,27] now enable the preparation of well-defined polyMPC-drug conjugates with diverse architectures that cannot be achieved by conventional PEGylation techniques. In particular, through covalent grafting to polyMPC copolymers, a very high drug loading can be envisaged, whereas PEGylation chemistry confines covalent drug attachment to the polymer chain-end(s).

The work described here extends polyMPC to the area of polymeric prodrugs, where small-molecule chemotherapeutics are covalently bound to the polymer backbone, and retain their therapeutic efficacy upon liberation from the polymer carrier. The chemotherapeutic agents CPT and DOX were investigated as potential drug candidates to be improved through the polyMPC delivery platform.

3.2 PolyMPC-CPT prodrugs by click chemistry

20(*S*)-Camptothecin (CPT), a natural alkaloid, was first isolated from the Chinese tree *Camptotheca acuminata* in the 1960s.[28] CPT shows potent anticancer activity over a broad range of cancer cells,[29,30] but has poor water solubility and high toxicity that has limited its clinical use. The efficacy of CPT and its more water soluble counterparts, topotecan and irinotecan, is compromised by ring-opening of the lactone ("E-ring") to the corresponding carboxylate under physiological conditions.[31,32] Binding of the carboxylate to serum albumin contributes to drug toxicity. In order to better solubilize CPT, its conjugation to water soluble polymers has been explored, specifically by acylation at the 20-OH position; this carries an added benefit of stabilizing the ring-closed form of the

drug.[33]   Water-soluble polymers such as poly(ethylene glycol) (PEG),[12,34] poly-*N*-(2-hydroxypropyl)methacrylamide   (HPMA),[35,36]   poly-L-glutamic   acid   (PG),[37-39] cyclodextrin-based polymers,[40,41] and PEG-grafted polyesters from the Emrick group[42] have been used to conjugate CPT; these polymer-CPT conjugates show increased efficacy over CPT to varying degrees.

The aim of this work was to apply click chemistry for CPT conjugation to the polyMPC backbone, using an acylated and azide-modified CPT, to give polyMPC-CPT conjugates with high drug loading and potential for future integration into CPT-based injectable cancer therapeutics (Bioconjugate Chemistry, 2009). This project was done in collaboration with Dr. Xiangji Chen, a post-doctoral researcher in the Emrick research group.   Considering prior work that demonstrated the amenability of CPT to click chemistry,[42] polyMPC-*g*-CPT conjugates were prepared by combining this technique with ATRP. Copolymerization of MPC with trimethylsilyl (TMS)-protected propargyl methacrylate (TMS-PgMA), prepared from 3-TMS-propargyl alcohol and methacryloyl chloride[43] was first explored, however, this method proved unsatisfactory, as the ethyl 2-bromoisobutyrate-initiated ATRP copolymerization of MPC and TMS-PgMA gave copolymers with high PDI (nearly 2), and often multimodal elution peaks by GPC. Moreover, ^{1}H NMR spectroscopy of these copolymers indicated a loss of the TMS protecting groups, likely the result of copper (I) acetylide formation during polymerization, as similar results have been observed in other polar organic solvents.[44] This undesired side-reaction promotes interchain coupling or even light cross-linking, and control experiments showed that the TMS protecting group was indeed lost completely when TMS-PgMA was stirred in solution under typical ATRP conditions.

Considering the role of copper (I) acetylide as an intermediate in Cu(I)-catalyzed Huisgen azide-alkyne click cycloaddition, ATRP and click cycloaddition were attempted simultaneously, by introduction of CPT-azide **48** at the outset of the polymerization, as shown in Figure 3.2. Monomer conversion was monitored by ^{1}H NMR spectroscopy, and cycloaddition was followed by disappearance of the CPT-azide N=N=N stretching signal at ~2100 cm^{-1} in the FTIR spectrum. PolyMPC-*g*-CPT conjugate **49** prepared in this fashion was purified by precipitation into THF, followed by passage over a short plug of silica gel in mixed solvents.
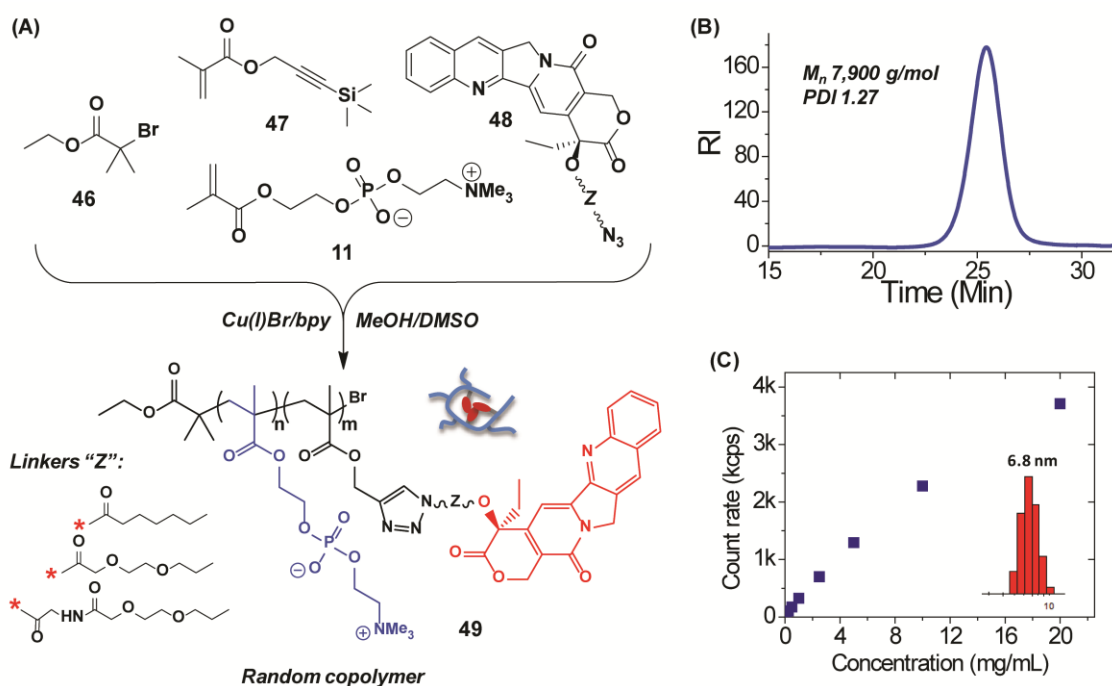
Figure 3.2 (A) Synthesis of polyMPC-*g*-CPT copolymers (**49**) by one pot ATRP and click chemistry; (B) aqueous GPC trace of copolymer **49**; (C) plot of light scattering intensity with concentration of copolymer **49** (inset is polymer diameter distribution).

PolyMPC-*g*-CPT was characterized by aqueous GPC as shown in Figure 3.2B, as well as ^{1}H and ^{13}C NMR spectroscopy. A homogeneous distribution of CPT functionality throughout the polymer molecular weight distribution was confirmed by overlaying the UV and RI traces obtained from GPC characterization. Aqueous solution sizes of these

structures were also characterized using dynamic light scattering (DLS), with the copolymers largely forming unimers, in which the hydrophilic polymers are expected to cover a collapsed core of hydrophobic CPT groups (Figure 3.2C). The graft copolymers did not show a critical micelle concentration (CMC) up to 20 mg/mL (the highest concentration tested) and the average diameter of these structures was 6.8 nm.

PolyMPC-*g*-CPT copolymers with different linkers between CPT and the polymer backbone, as depicted in Figure 3.2A, were synthesized to investigate drug release kinetics associated with ester linkages of variable neighboring hydrophilicity. For example, to contrast the case of the 6-azidohexanoic acid linker,[42] 2-[2-(2-azidoethoxy)ethoxy]acetic acid was synthesized. This was done by oxidation of 2-[2-(2-chloroethoxy)ethoxy]ethanol to the corresponding carboxylic acid using Jones reagent at room temperature, followed by displacement of the chloride by reaction with NaN_3 at 80 °C. The presence of the azide group was confirmed by its characteristic infrared spectral signal at ~2100 cm^{-1}, and α-azido methylene resonance at 50.6 ppm in the ^{13}C NMR spectrum. CPT-azide compounds were obtained by acylation of CPT with linkers using carbodiimide coupling. Varying linker chemistry was found to have little-to-no effect on the polymerization and cycloaddition reactions, as indicated by the relatively low PDI values, and experimental agreement with theoretical drug loadings. Thus, this one-pot click/ATRP procedure provides a facile one-step process to introduce CPT into hydrophilic, biocompatible MPC polymer backbone with good control over drug loading.

The CPT loading on the polyMPC backbone could be varied easily by adjusting the MPC:TMS-PgMA/CPT ratio at the outset of the polymerization, with exemplary samples listed in Table 3.1. Importantly, PDI control was achieved at CPT loadings up to

14 weight percent (compare this to SN-38-PEG 4-arm stars containing 3.7 wt % CPT[45]), and the aqueous solubility of this highly drug-loaded polyMPC structure was excellent (>250 mg/mL, or >35 mg/mL CPT equivalent). The lactone form of CPT alone has a solubility of 2.5 μg/mL; thus use of the polyMPC framework provides orders-of-magnitude greater solubility. Aqueous solutions of these conjugates exhibit viscosities that qualitatively resemble pure water, a notable difference from PEGylated drugs that often exhibit an undesirably high solution viscosity. The strongly hydrated zwitterionic moiety affects a wide range of properties, from solubility to sliding friction,[46] making these structures more appealing for many biological applications, including injectable therapeutics.

UV/Vis spectroscopy was found to be the most reliable method for determining CPT loading. Recording the UV absorbance of the CPT-loaded polymer at 370 nm allowed for the weight percent CPT in each polymer to be calculated, using known concentrations of the CPT-azide compounds and their molar extinction coefficients. The CPT loading for each sample is given in Table 3.1 as CPT weight percent. As expected, the relative absorbance at 370 nm from CPT increased with increasing amount of CPT incorporated, with experimental values corresponding closely to the theoretical CPT incorporation.

Table 3.1 Summary of polyMPC-*g*-CPT copolymers prepared by one-pot procedure.

Sample	Target CPT (wt %)	Conversion	M_n (g/mole)	PDI	Diameter (nm)	CPT wt %
49A	5 %	94 %	5,200	1.27	5.3	5.1 %
49B	10 %	96 %	5,500	1.25	5.5	7.7 %
49C	15 %	Quantitative	5,100	1.36	5.7	13.8 %
49D	8.5 %	Quantitative	13,000	1.31	9.3	7.0 %
49E	8.4 %	Quantitative	7,000	1.26	6.8	5.1 %

In vitro drug release studies were performed on polyMPC-*g*-CPT conjugates to gauge their relative release rates and potential utility in delivery applications. CPT-carrying polyMPC materials were incubated in PBS at various buffered pH values (5.5, 7.4, and 9.1) to measure the CPT hydrolysis half-lives from the polymer backbone, with the choice of backbone-to-drug linkage leading to significant changes in ester cleavage and drug release. The hydrophobic 6-azidohexanoic acid linker was first chosen for CPT conjugation, giving copolymers **49A-C** (Table 3.1). These structures gave very little hydrolysis over four days of incubation under several different aqueous conditions, suggesting that this linker is too hydrophobic for potential future *in vivo* use. To expedite ester hydrolysis, the hydrophilic linker 2-[2-(2-azidoethoxy)ethoxy]acetic acid was used to prepare copolymers **49D-E** (Table 3.1). The results of hydrolysis studies of these structures in different media are shown in Figure 3.3. SEC-HPLC was used to monitor CPT release from **49D** and **49E** incubated in various media (PBS, mouse serum, cell culture medium, and human plasma). The polymer-drug conjugate was observed to elute at 9.4 minutes and free CPT eluted at 16.9 minutes. Over the course of 96 hours, the conjugate peak was seen to decrease while the CPT peak increased, as expected, as CPT is hydrolyzed from the polymer backbone. These copolymers, with half-lives of 210–220 hours in PBS (pH 7.4), showed much faster release profiles than polyMPC-*g*-CPT copolymers prepared using 6-azidohexanoic acid linkers. These polymers also showed significantly shorter half-lives in mouse serum (~80 hours), cell culture medium (~40 hours) and human plasma (8-9 hours). The hydrophilicity and electron-withdrawing effect of the alkoxy group α to the carboxylic acid aids in accelerating ester cleavage.

Medium		PBS 7.4	Mouse serum	Cell Culture Medium	Human Plasma
$T_{1/2}$	49D	212 h	80 h	43 h	8.4 h
	49E	220 h	76 h	37 h	9.0 h
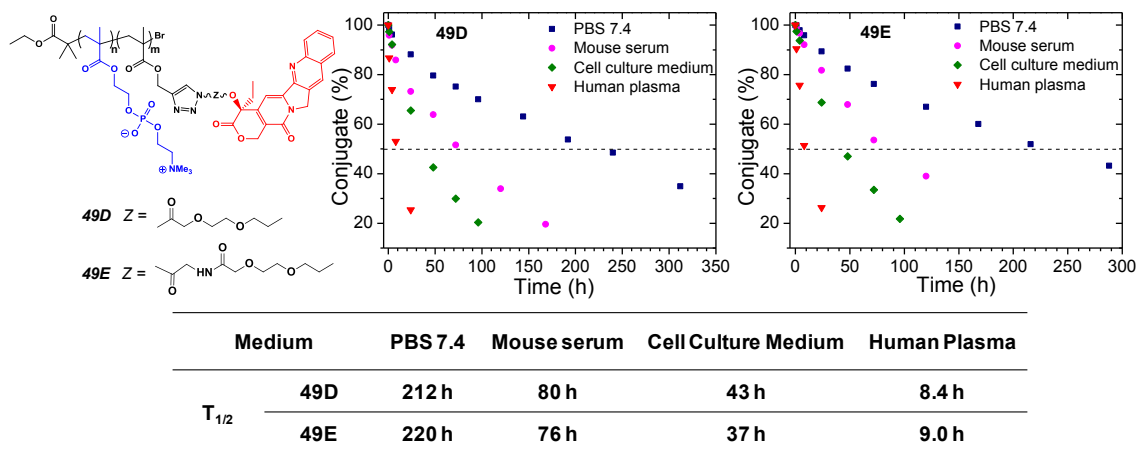
Figure 3.3 Conjugate **49D** and **49E** degradation in different media at 37 °C.

HPLC characterization of CPT liberation from polyMPC-*g*-CPT conjugates confirmed the importance of tailored linkers, and was informative for *in vitro* cell culture evaluation of conjugate toxicity against various cell lines. Taking **49D** and **49E** as examples, a much faster CPT release profile was seen in human plasma as compared to CPT release rates in PBS. These CPT hydrolysis half-lives are, however, slower than those reported for PEGylated-SN38 conjugates,[45] leading to an expected longer blood circulation time *in vivo*. The anti-cancer activity of these polyMPC-*g*-CPT structures (**49D** and **49E**) was tested against different cancer cell lines, including human breast (MCF7), ovarian (OVCAR 3) and colon (COLO 205) adenocarcinoma cells by Dr. Sangram Parelkar, a post-doctoral researcher in the Emrick research group. This was done by incubating CPT-equivalent concentrations of **49D** and **49E** with these cells for 72 hours, followed by cell viability measurements using a luminescence plate reader. Controls included a DMSO solution of CPT, and polyMPC itself. Dose response curves showed that both **49D** and **49E** were potent against the cancer cell lines tested here and importantly the noted cytotoxicity was through CPT only, since polyMPC by itself is

non-toxic (Figure 3.4). The IC_{50} values show that both **49D** and **49E** induced cytotoxicity at IC_{50} values higher than native CPT alone, resulting from the fact that CPT was slowly liberated over time from the polymer chain. It can also be seen that the colon cancer cells were most sensitive to polyMPC-*g*-CPT conjugates.
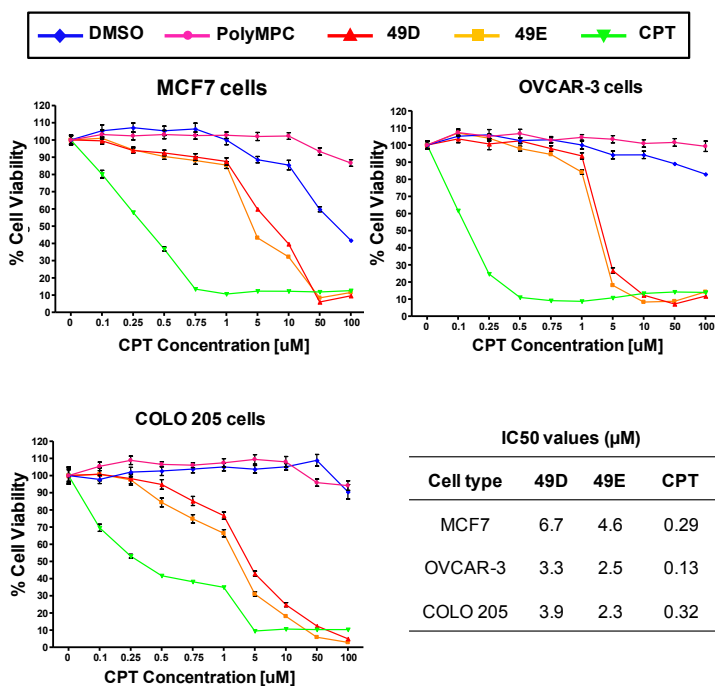
Figure 3.4 *In vitro* cytotoxicity of polyMPC-*g*-CPT conjugates in cell culture of human breast (MCF7), ovarian (OVCAR 3) and colon (COLO 205) adenocarcinoma cells. Error bars represent ± standard deviation.

3.3 Polymer micelles for drug delivery

In addition to conventional linear polymer-drug conjugates, alternative architectures have been used with impressive results, including branched structures, such as a dendritic PEG-polyester doxorubicin (DOX) conjugates,[14,47] as well as numerous reports of encapsulated drugs exploiting micellar and liposomal systems.[48-50] Polymer micelles are enabling materials in nanoscale therapeutics, generally prepared from amphiphilic block copolymers where, in water, the hydrophobic block sequesters drug

within the core, and the hydrophilic block serves as an encapsulating corona, imparting both water solubility and stealth properties to the micelles.[51-54] The ease with which drug-loaded micelles can be prepared (usually by dialysis or dilution) makes these nanostructures attractive for injectable therapeutics, however, their use can be problematic as they tend to suffer from "burst release" kinetics, where a large percentage of the payload is released very quickly.[55] Dilution upon injection is also a concern: self-assembled polymer micelles are dynamic structures with an equilibrium between free and associated polymer chains. Though polymeric micelles often have low critical micelle concentrations (CMC), extreme dilution arising from intravenous injection shifts the equilibrium toward free polymer, resulting in disassociation of the micelles and liberation of the payload.[55] An effective method to overcome these challenges is to stabilize polymer micelles by covalent cross-linking.

Both shell and core cross-linked micelles have been prepared from a variety of different chemistries, including cross-linking with bi-functional additives,[56,57] free radical polymerization,[58,59] and photo-cross-linking.[60,61] Reversing the cross-linking with an environmental trigger is an area of great interest, and examples of pH cleavable and redox sensitive cross-links have been reported.[62-65] Cross-linking with disulfides may be particularly important for drug delivery due to their triggered bond breakage under physiologically-relevant and intracellular-specific conditions; the intracellular environment is up to 1000 times more reducing than extracellular fluids.[66] Several recent reports utilized disulfide cross-linked micelles as drug delivery vehicles. Thiols have been introduced to polymers by post-polymerization modification, for example by thiol functionalization of PEGylated poly(lysine) with N-succinimidyl 3-(2-pyridyldithio)-

propionate.[67] Following micellization, oxidation led to core cross-linking, and treatment with dithiothreitol (DTT) resulted in micelle dissociation. In another example, a random copolymer of methacryloyloxyethyl phosphorylcholine (MPC), glycidyl methacrylate, and stearyl methacrylate formed micelles ~100 nm in diameter, with disulfide cross-linking achieved by reaction of the epoxide with cystamine.[68] The micelles were responsive to DTT, and biocompatible. Disulfide cross-linked polymer micelles have been reported as carriers for chemotherapeutic agents including doxorubicin (DOX)[69,70] camptothecin (CPT),[71] and paclitaxel (PTX).[72,73] A recent example employed a block copolymer of PEG and HPMA, where a percentage of the HPMA block was coupled to lipoic acid. Micelles from this polymer were loaded with DOX, and cross-linked using DTT.[74] However, this post-polymerization modification lacked control over, and characterization of, the degree of substitution. Moreover, the block copolymers were water-insoluble.

The work described in this section presents the synthesis of novel block copolymers based on polyMPC, where the second block is prepared from a lipoic acid-based methacrylate. This synthesis precludes the need for post-polymerization modification to introduce thiols, and ensures the presence of a functional hydrophobic block with known and easily tunable thiol content. These MPC-based block copolymers proved water soluble, even with high percentages of the lipoic acid-containing block, and self-assembled readily into nanoscale micelles. Such structures are presented as carriers for CPT, in which a pyridyldithio-functionalized CPT[71] was conjugated to the DHLA block, thus sequestering CPT to the micelle core. The disulfide linkages allow for controlled CPT release upon exposure to reducing conditions, as would be found upon

cellular internalization. This environmental stimulus, coupled with the passive targeting of the EPR effect inherent to polymer-based drug delivery systems, is of interest for improving the outcome of polymer-based drug delivery (Molecular Pharmaceutics, 2013).

3.4 Synthesis of CPT-loaded polyMPC micelles

PolyMPC-DHLA block copolymers were synthesized by RAFT polymerization, employing sequential monomer addition to form the block copolymers shown as **55** in Figure 3.5. Monomer **51** was prepared in 80 % yield by carbodiimide coupling of 2-hydroxyethyl methacrylate (**9**) and lipoic acid (**50**).[75] The monomer was isolated as a yellow oil, and stored as a CH_2Cl_2 solution at -80 °C to prevent disulfide exchange. Stored in this way, monomer **51** was stable for months.

PolyMPC-DHLA diblock copolymers were prepared by first polymerizing MPC using 4-cyano-4-(phenylcarbonothioylthio)pentanoic acid (**52**) and 4,4'-azobis(4-cyanovaleric acid) (ACVA, **53**) as the chain transfer agent and initiator, respectively, at 70 °C in methanol/dimethylsulfoxide solution. Following conversion of MPC to polymer, a DMSO solution of **51** was introduced under inert atmosphere, and the mixture was stirred at 70 °C for 12 hours. The polymerization was terminated by immersing the flask in liquid nitrogen, then allowing the mixture to warm while open to air. The polymerizations were generally taken to >90 % conversion, as judged by ^{1}H NMR spectroscopy, comparing vinyl protons of the monomer (5.5 and 6.0 ppm) to methyl protons on the polymer backbone (1.0 ppm). Polymer **54** was isolated as a pink solid following purification by passage through a short plug of silica gel, and precipitation into THF.
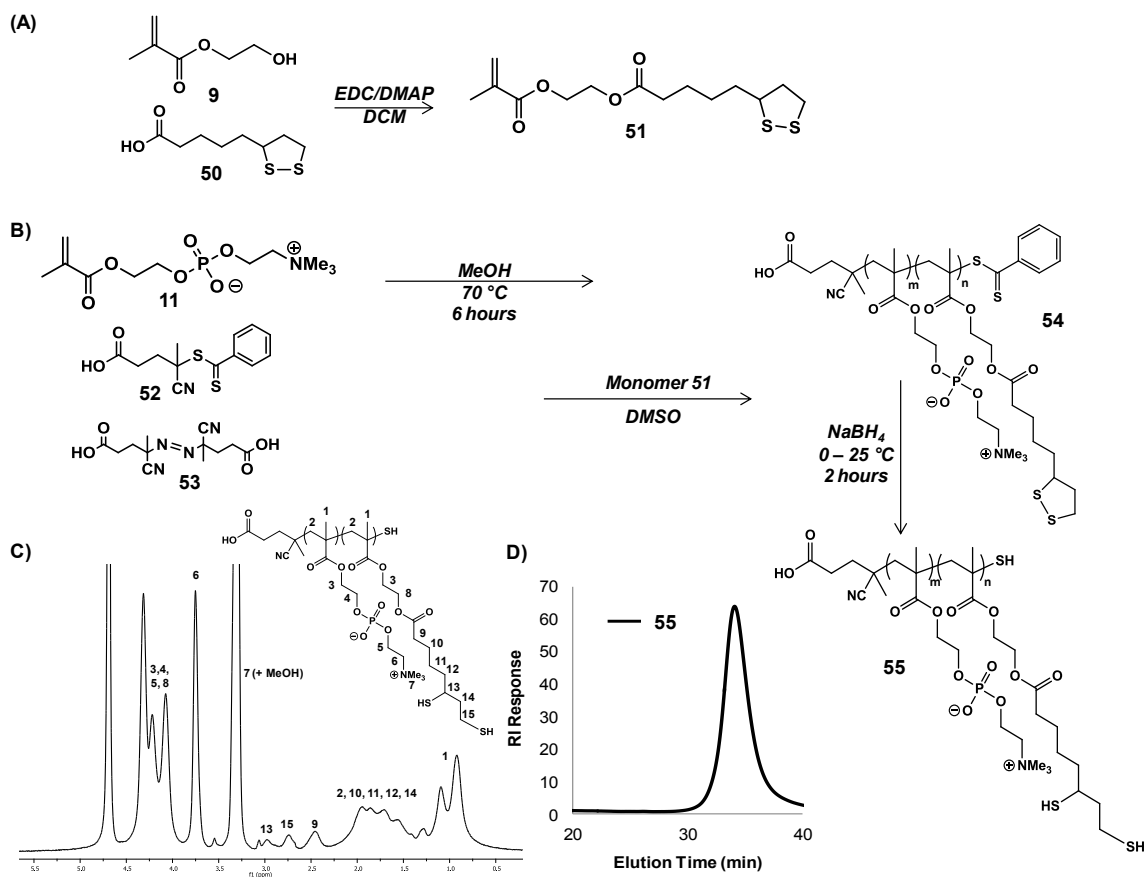
Figure 3.5 (A) Synthesis of thiol-containing monomer **51** based on lipoic acid **50**; (B) Synthesis of MPC block copolymers; (C) ^{1}H NMR spectroscopy of a representative polymer sample; (D) Aqueous gel permeation chromatography of polymer **55**.

Block copolymer **54** was reduced immediately to the free thiol form with $NaBH_4$ (4 molar equivalents relative to lipoic acid). The reaction was complete in 2 hours, at which point concentrated HCl was added to adjust the solution pH to ~3. The polymer solution was dialyzed against methanol, then water, at 4 °C (MWCO 1,000). Lyophilization gave polyMPC-DHLA (**55**) as a white solid. Polymer **55** was characterized by NMR spectroscopy, and GPC eluting with 0.1 M aqueous sodium nitrate + 0.02 % (wt) sodium azide or trifluoroethanol (TFE) (0.2 M sodium trifluoroacetate), against linear PEO or PMMA calibration standards, respectively (Table 3.2). The extent of DHLA incorporation was determined by ^{1}H NMR spectroscopy in 1:1 $CDCl_3$:MeOD,

64

comparing the DHLA methylene signal at 2.5 ppm with the methyl protons of the polymer backbone at 1.0 ppm. This showed the DHLA content to be well-controlled by adjusting monomer feed ratios. GPC in TFE revealed a well-defined (monomodal) polymer signal, with PDI ~ 1.2. In water, a high molecular weight signal was also seen, attributed to copolymer micellization in solution. Interestingly, aggregation of this sort was not observed in our characterization of random copolymers of similar composition and molecular weight. We hypothesize that this behavior arises from (1) the distinct amphiphilicity of these diblock copolymers that leads to rapid solution assembly, and (2) the dense concentration of thiols in the DHLA block that provides additional stability to the micelles through disulfide formation. We note that these diblock copolymers maintained excellent water solubility (to the eye), even at the highest DHLA incorporation of 41 mole percent (sample **55C**).

Table 3.2 Summary of polymerization results for block copolymer **55**.

Sample	Target Mol. Wt. (g/mole)	Target % DHLA	TFE GPC		% DHLA
			M_n	PDI	
55A	16,000	10 %	24,800	1.19	15 %
55B	18,000	20 %	26,900	1.24	23 %
55C	21,000	40 %	22,300	1.15	41 %

The critical micelle concentration (CMC) of block copolymers **55A-C** was examined using a pyrene fluorescence probe. Briefly, serial dilutions of polymer were prepared in PBS, and 5 μL of pyrene solution in acetone was added to each, giving a pyrene concentration of 0.6 μM. The samples were equilibrated at room temperature for 18 hours. Pyrene exhibits a shift in peak fluorescence intensity as it transitions from a hydrophilic (334 nm) to hydrophobic environment (339 nm), and CMC is determined by

plotting peak intensity against the log of the polymer concentration, as shown for polymer **55C** in Figure 3.6A. The onset of the sharp change in slope of the line is taken as the CMC.   Dynamic light scattering (DLS) analysis of the same series of samples/concentrations shows a non-linear relationship between the scattering intensity and concentration, confirming the presence of nanoscale micelles above CMC (Figure 3.6B). CMC varied slightly among the polymer samples, with an observed dependence on hydrophobic content; as expected, the CMC for polymer **55C** was lowest due its higher DHLA content (41 mole %). DLS measurements of block copolymers **55A-C** showed an increase in size with hydrophobic block length, with hydrodynamic diameters of 15, 18 and 28 nm, respectively, measured at 1 mg/mL in PBS (Figure 3.6C).

Sample	CMC (g/L)	Size (nm)
55A	0.15	15.5 ± 0.2
55B	0.16	18.4 ± 0.2
55C	0.04	28.3 ± 0.3
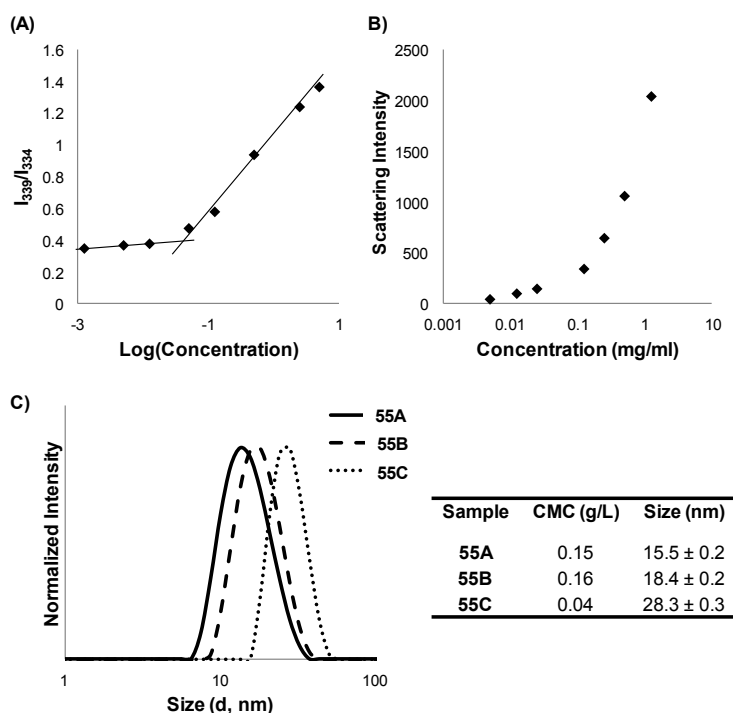
Figure 3.6 Summary of micelle characterization: (A) CMC determination using pyrene fluorescence for block copolymer **55C**; (B) scattering intensity vs. concentration from dynamic light scattering for block copolymer **55C**; (C) size (diameter) of micelles from copolymers **55A-C**.

Thiol-containing micelles can self-cross-link by oxidation to disulfide form, accomplished by continually purging the system with air. The process of disulfide formation was monitored using Ellman's test,[76] performed on polymer dissolved in PBS above the CMC and agitated by bubbling a slow stream of air through the mixture. At various time points, 10 uL aliquots were removed and added to a buffered solution of Ellman's reagent, resulting in a decrease in intensity of the UV absorption at 412 nm as the free thiol converted to disulfide (Figure 3.7A). This provides a spectroscopic handle to monitor cross-linking efficiency. Samples generally reached 85 % conversion in 48 hours. Solutions simply left open to air, without bubbling, gave significantly lower conversion (~20 % after two days).

Cross-linked micelles were characterized by DLS and TEM (Figure 3.7). DLS of cross-linked micelles formed from polymer solutions at 1 mg/mL showed no difference from the uncross-linked samples, suggesting that the cross-linking process neither disrupts the structure of the micelles nor promotes inter-micelle cross-linking. Aqueous solutions of cross-linked micelles (0.25 mg/mL) were cast on copper grids and imaged by TEM. Micelles observed by TEM supported the DLS data, with an average micelle diameter of 26 ± 4 nm (Figure 3.7B). The micelles imaged by TEM appeared as spherical structures and were dispersed cleanly on the substrate.

Cross-linked micelle solutions were stable, as characterized by DLS, to concentrations well below the CMC (0.01 mg/mL). However when treated with 5 mM dithiothreitol (DTT) at 37 °C, then cooled to room temperature and analyzed again by DLS, no signal was detected (as for the uncross-linked polymer at the same

concentration) indicating complete dissolution of the polymer micelle by disruption of the disulfide cross-links (Figure 3.7C).
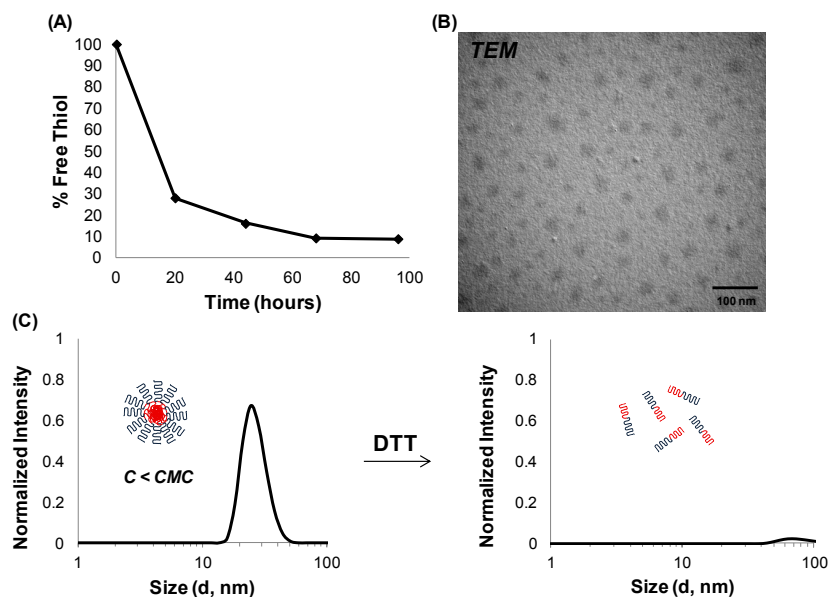
Figure 3.7 (A) Percent decline of free thiol over time for micelles prepared from copolymer **55B**, monitored by Ellman's test; (B) TEM of cross-linked micelles formed from polymer **55B**; (C) DLS of cross-linked polymer micelles from copolymer **55A** below the CMC (0.01 mg/mL) (left), and DLS of the same sample after treatment with DTT (right); DTT cleavage of disulfide linkages gives free polymer in solution (below CMC).

These redox-sensitive core cross-linked PC polymer micelles comprise a potentially suitable delivery platform for therapeutics, in which a triggered release can enable selective and targeted delivery of a drug, as the cytosol and nucleus are known to have a significantly higher reducing potential (mM) than the extracellular fluids (μM).[66] CPT was used as the chemotherapeutic, specifically a pyridyl disulfide-functionalized CPT derivative, prepared similarly as reported in the literature,[71] to facilitate conjugation to the polymer by disulfide formation. Briefly, 3-(2-pyridyldithio)-propionic acid (**56**) was prepared by reaction of 2,2'-dithiodipyridine with 3-mercaptopropionic acid in ethyl acetate, and purified by column chromatography on silica gel to yield the desired product

in 95 % yield.[77] Carbodiimide coupling of camptothecin (**1**) and linker **56** was achieved in anhydrous methylene chloride[71] (Figure 3.8).   Following purification by column chromatography on silica gel, eluting with methanol/methylene chloride mixtures, camptothecin derivative **57** was obtained as a yellow solid in ~50 % yield. The structure was confirmed by NMR spectroscopy and high resolution mass spectrometry (calculated, 546.115; found, 546.113).

CPT-pyridyl disulfide **57** was conjugated to polyMPC-DHLA by stirring in a 2:3 mixture of MeOH/DMSO for 72 hours at 37 °C. The solution was dialyzed against methanol (MWCO 1,000) to remove unreacted **57**, then against water to induce micelle formation. After complete removal of the organic solvents, the aqueous solution was transferred to a vial and purged with air to form CPT-loaded core-cross-linked polymer micelles, as depicted in Figure 3.8.   CPT loading was characterized by UV/Vis spectroscopy, comparing absorbance at 370 nm with a CPT solution of known concentration. Polymer-CPT prodrugs prepared in this way achieved from 5 to 10 wt % CPT-loading.
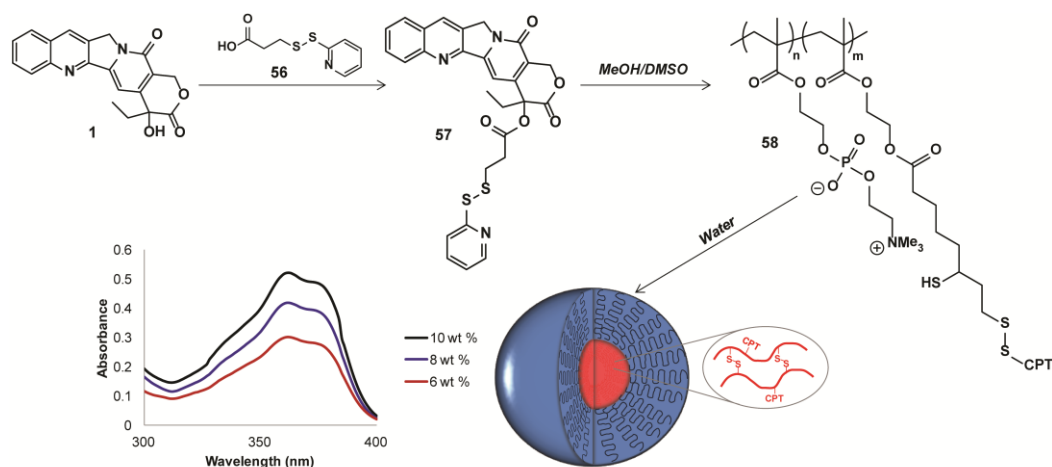
Figure 3.8 Synthesis of CPT-pyridyl disulfide **57**, conjugation to polyMPC-DHLA copolymer to give prodrug **58**, subsequent cross-linked micelle formation, and characterization of CPT loading by UV/Vis spectroscopy.

CPT release from the polymer micelles was monitored by dialysis, where 1 mL of micelle solution was transferred to a cassette (MWCO 3,500), and dialyzed against PBS, or PBS + 3 mM DTT (300 mL), in a closed container at 37 °C. At select time points, aliquots were removed from the external medium, and replaced with fresh buffer, while monitoring fluorescence intensity at 440 nm over time (λ_{ex} = 370 nm). Free CPT was dialyzed against PBS to demonstrate that diffusion out of the dialysis cassette is not a limiting factor, and to establish a benchmark for assessing the performance of the micelle-based systems. CPT (without encapsulation) diffused through the cassette within 6 hours, with 90 % released in the first 2 hours (Figure 3.9). For further comparison, polymer micelles were prepared containing unmodified CPT simply encapsulated in the core (i.e. having no disulfide linkage). Physically encapsulated systems showed little difference from CPT alone, with an initial burst release of 75 % in 4 hours, followed by slow release of the remaining drug over two days. In contrast, the disulfide-conjugated CPT prodrug micelles showed much different release profiles. In PBS containing DTT (3 mM), CPT release was fast, with 50 % release in 5.5 hours, and complete release in 2 days. In PBS at pH 7.4, CPT release was slow (85 % over 5 days), presumably due to slow hydrolysis of the ester linkage, with a half-life ($t_{1/2}$) of 28 hours. These results suggest these polyMPC-CPT prodrug micelles as a potential drug delivery system that is relatively stable in a neutral environment, yet can exploit the redox characteristics of the intracellular environment.
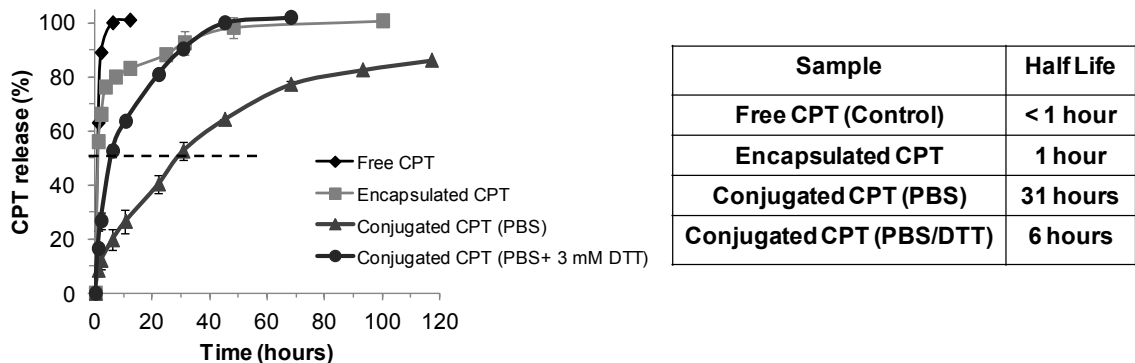
Figure 3.9 Release profiles of CPT, encapsulated CPT, conjugated CPT in PBS, and conjugated CPT in PBS + 3 mM DTT. Samples were analyzed in triplicate; error bars represent ± standard deviation.

The cytotoxicity of poly(MPC-DHLA)-CPT conjugates was tested *in vitro* against human breast cancer (MCF7) and colorectal (COLO205) adenocarcinoma cells by Dr. Sangram Parelkar. This was done by incubating CPT-equivalent concentrations of poly(MPC-DHLA)-CPT conjugates with these cells for 72 hours, followed by cell viability measurements using a luminescence plate reader. Dose response curves (Figure 3.10) showed that micellar conjugates (with CPT loadings of 2 and 5 weight percent) were potent against the cancer cell lines tested. The observed cytotoxicity arises from released CPT (a result of ester bond cleavage), and the polymer itself exhibits no toxicity even at extremely high concentrations (2.5 mg/mL).

The half-maximal inhibitory concentration (IC_{50}) values of poly(MPC-DHLA)-CPT prodrug micelles were in the range of 3-9 μM, as shown in Table 3.3, where the comparable IC_{50} values for both poly(MPC-DHLA)-CPT conjugates originate from their similar release rates. The data shows poly(MPC-DHLA) micelles containing CPT conjugated by disulfide linkage induce toxicity at higher concentrations than CPT alone. This is expected for polymer prodrugs, and is a key feature that allows higher maximum

tolerated dose (MTD) of prodrugs *in vivo*.[78,79] Interestingly, CPT that was physically encapsulated within the micelles (i.e. no covalent linkage) showed nearly identical toxicity to native CPT. This is likely due to the fast release observed for these structures, as compared to the gradual release of CPT from the prodrugs. The combination of redox triggered release and the cell culture data presented here will be beneficial for controlling drug release *in vivo*, while exploiting the very high water solubility arising from the phosphorylcholine-substituted polymer.
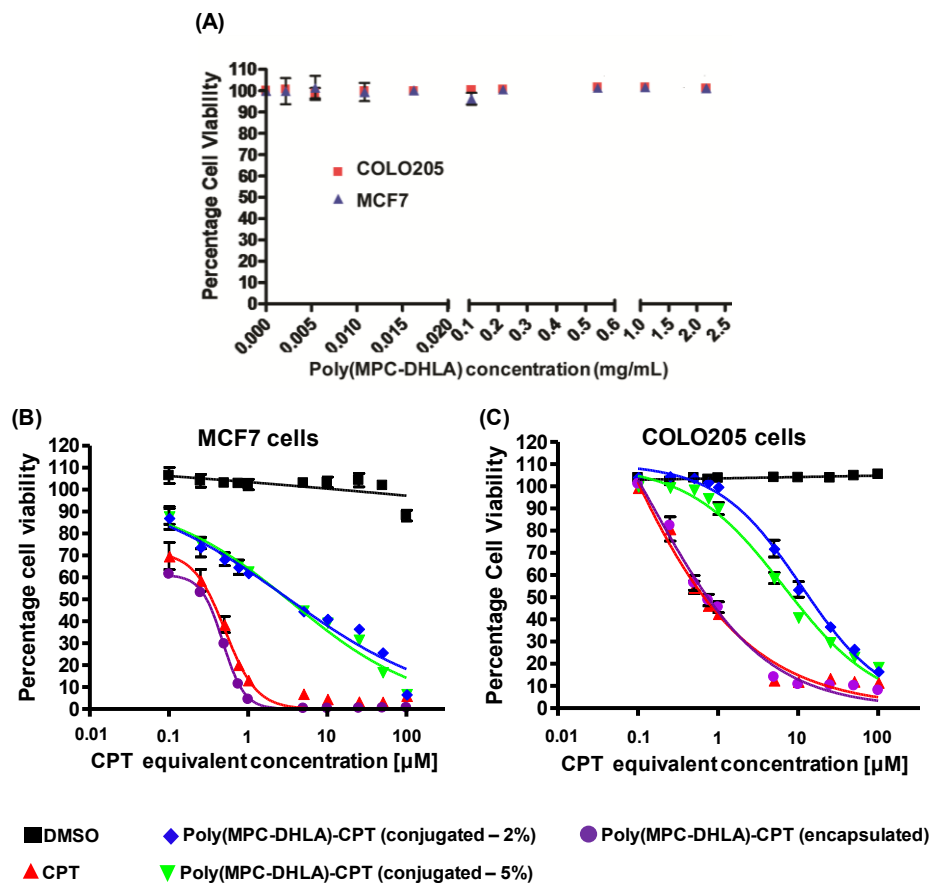
Figure 3.10 In vitro cytotoxicity of (A) polyMPC-DHLA micelles, and of CPT-loaded polyMPC-DHLA micelles with (B) human breast (MCF7) and (C) colorectal (COLO205) cells. Error bars represents ± standard deviation.

Table 3.3 IC$_{50}$ values of poly(MPC-DHLA)-CPT micelles in MCF7 and COLO205 cancer cell lines.

IC$_{50}$ [μM]	MCF7	COLO 205
CPT	0.51 ± 0.05	0.43 ± 0.1
Poly(MPC-DHLA)-CPT (encapsulated)	0.48 ± 0.01	0.44 ± 0.1
Poly(MPC-DHLA)-CPT (2 wt %)	3.0 ± 1.8	8.3 ±0.8
Poly(MPC-DHLA)-CPT (5 wt %)	3.6 ± 0.8	4.7 ± 0.3

In summary the synthesis of novel diblock copolymers and micelles based on phosphorylcholine and dihydrolipoic acid-containing methacrylates was shown, as well as their potential utility as a drug delivery platform. Use of DHLA as the hydrophobic block allows for post-polymerization conjugation and cross-linking reactions by disulfide formation. CPT was successfully conjugated to the DHLA block, then released in a controlled manner in buffer, with the benefit of a trigger in a reducing environment. The CPT-loaded micelles demonstrated cytotoxicity at higher CPT concentrations than with the drug alone, as expected for polymer prodrugs due to the covalent connection of CPT to the backbone. The combination of robust, highly water soluble micelles and stimuli-responsive drug release yields a system that is promising for overcoming challenges faced by micellar delivery vehicles, including *in vivo* stability and fast, non-specific release of their contents.

3.5 PolyMPC-DOX prodrugs

Doxorubicin (DOX) is another example of a clinically relevant chemotherapy agent that can benefit from a polymer-based delivery platform. DOX is a DNA intercalator, affecting a wide range of DNA processes. As is the case with many chemotherapeutics, the potent anticancer activity of DOX is accompanied by undesirable side effects. Doxil, a PEGylated liposomal formulation of DOX, has shown favorable

pharmacokinetics compared to the free drug, as well as reduced dose-limiting toxicity.[80,81]   Despite the benefits of this formulation, Doxil suffers from its own toxicities, especially palmer-planter erythrodysesthesia and mucositis/stomatitis arising from accumulation in the skin.[82-85] Covalent polymer-drug conjugation has also been explored with DOX, including a PEGylated dendrimer at a drug loading of 10 weight percent, showing promise in preclinical studies.[14]   In addition to the degradable dendritic structures,[14,86] HPMA,[87-89] and PEO-based polymers[90] were also conjugated to DOX exploiting pH-sensitive hydrazone chemistry.   The use of an acid-labile linker enables specific release of DOX either in the slightly acidic environment of tumor tissue[91,92] or intracellularly in the acidic environments of the endosomal or lysosomal compartments.[93]

In 2012, Dr. Xiangji Chen, a post-doctoral researcher in the Emrick research group, reported the synthesis of polyMPC-DOX conjugates, prepared by integrating hydrazone linkages as pendent groups along the polymer backbone.[94]   Such structures were prepared by ATRP copolymerization of MPC with either 2-*tert*-butoxy-2-oxoethyl methacrylate (TBOEMA) or 2-ethoxy-2-oxoethyl methacrylate (EtOEMA) using copper bromide and bipyridine as the catalyst and ligand, respectively.   The ethyl esters of copolymer **60** are readily converted to acyl hydrazides by substitution with hydrazine to give polyMPC-hydrazine, shown as polymer **61** in Scheme 3.1.   Polymer **61** was characterized by aqueous gel permeation chromatography (GPC) against linear PEO standards and by ^{1}H NMR spectroscopy to determine the mole percent of hydrazine monomer units within the polymer.   Polymer **61** was conjugated to DOX by hydrazone formation in methanol, in the presence of magnesium sulfate and acetic acid, to give polyMPC-DOX prodrug **62**.   PolyMPC-DOX **62** was purified by preparative size

exclusion chromatography, and lyophilized to give a bright red powder, which proved stable for months when stored as a dry solid at -20 °C.
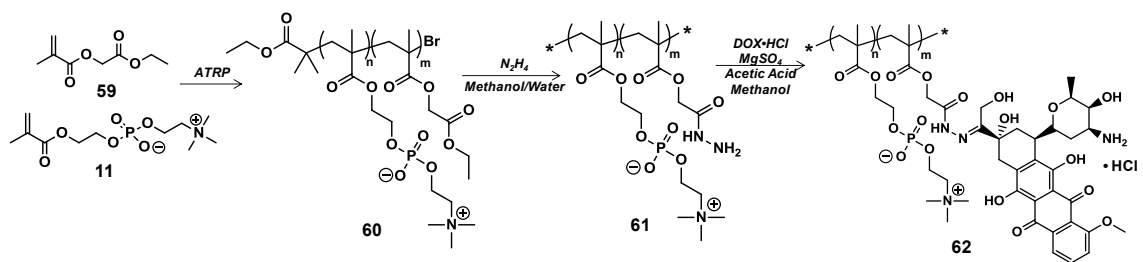
Scheme 3.1 Synthesis of polyMPC-DOX conjugate **62** from ethyl ester-containing polyMPC precursor polymer **60**.

The synthesis towards polyMPC-DOX prodrugs described by Chen et al[94] results in conjugates with exceptionally high water solubility and tunable drug loading, reaching or exceeding 30 weight percent DOX. These polyMPC-DOX conjugates displayed pH sensitive release profiles, with half-life ($t_{1/2}$) values ranging from 2-40 hours at pH 5.0, while only 2 to 20 % of DOX was released in 48 hours at pH 7.4. In cell culture, the half-maximal inhibitory concentration (IC_{50}) values for polyMPC-DOX ranged from 1.5 - 16 µM for human breast cancer (MCF7 and MDA-MB-231) and colorectal (COLO 205) adenocarcinoma cell lines.[94] Moreover, the maximum tolerated dose (MTD) was determined for polyMPC-DOX in athymic Nu/j mice, and was found to be well-tolerated to over 30 mg/kg over the course of the 30 day study; mice which received doses of 50 mg/kg showed only a 10 % weight loss at 22 days. These values represent an increase compared to the MTD of free DOX (~6 mg/kg),[95] the liposomal formulation DOXIL(36 mg/kg)[14] and a PEGylated polyester dendritic DOX example (20-40 mg/kg).[14]

The work presented in this thesis aims to extend *in vivo* prodrug characterization to include pharmacokinetics, biodistribution, and treatment efficacy data for polyMPC-DOX using a 4T1 murine breast cancer model in collaboration with Dr. Sallie Schneider

at the Pioneer Valley Life Sciences Institute (PVLSI) (Molecular Pharmaceutics, 2014). The 4T1 mammary carcinoma was selected as an extremely aggressive breast cancer model that is highly tumorigenic and metastatic, and thus can be considered as a model for triple negative breast cancer.[96,97] Unlike many tumor models, 4T1 tumors can metastasize spontaneously from the primary tumor to multiple distant sites including the lungs, lymph nodes, liver, brain and bone within weeks following injection.[96] We viewed the 4T1 model as a challenging tumor model to test the effect of polyMPC-DOX prodrugs, potentially enhancing the utility of DOX in late stage breast cancer. 4T1 cells can be introduced orthotopically by direct injection into the mammary gland, such that the primary tumor site is anatomically correct, and the syngeneic nature of the cells allows for use of immuno-competent animals, and thus examination of the effects of polyMPC-DOX conjugates on the immune system. The 4T1 breast cancer model has been used by others to study polymer prodrugs *in vivo*, including paclitaxel,[98,99] docetaxel,[98] cisplatin,[100,101] gemcitabine,[102] and doxorubicin[103,104] with variable success with respect to slowing tumor growth and reducing off-target toxicity. Given the high level of water solubility and degree of drug loading achievable with polyMPC-DOX, these prodrugs have potential for the treatment of breast cancer, and this study demonstrates their efficacy in 4T1 tumor-bearing mice.

3.6 Efficacy of polyMPC-DOX in 4T1 tumor-bearing mice

For the efficacy study described here, we used polyMPC-DOX with an estimated molecular weight of 25,000 g/mole, and DOX loading of 22 weight percent. To further extend our *in vivo* prodrug characterization, the pharmacokinetic profile of polyMPC-DOX was evaluated in BALB/c mice. Animals were sorted into three groups of eight,

with a control group (HBSS), a free DOX group, and a polyMPC-DOX group (6 mg/kg DOX equivalent doses) introducing drugs by a single tail vein injection of 100 μL total volume. Blood serum levels of DOX were monitored over time, analyzing for the presence of drug by HPLC equipped with a fluorescence detector. As shown in Figure 3.11, free DOX concentration decreased rapidly, with a $t_{1/2}$ of 15 minutes, clearing to near-undetectable levels within 1 hour. This is consistent with reported values for DOX.[95,103] PolyMPC-DOX displayed a significantly longer circulation half life of 2 hours. Accordingly, the area-under-the-curve (AUC) was dramatically higher for the polyMPC-DOX prodrug (408 μg•h/ml) compared to free DOX (22 μg•h/ml).
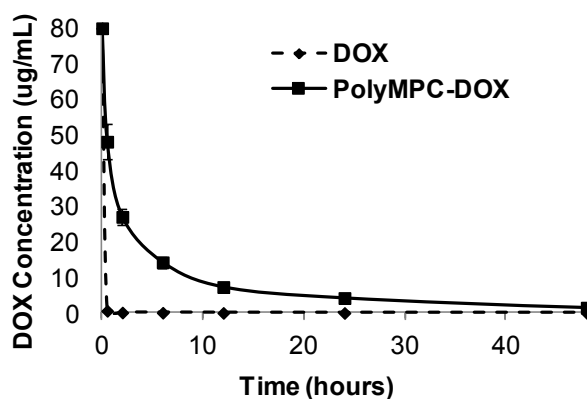
Figure 3.11 Pharmacokinetic analysis of polyMPC-DOX in BALB/c mice. Polymer conjugation extends the circulation half life from 15 minutes to 2 hours and increases the AUC from 22 μg•h/ml to 408 μg•h/ml . Error bars represent ± standard deviation.

The biodistribution of DOX was determined for both the free drug, and polyMPC-DOX, three and five days post-injection from the 6 mg/kg DOX equivalent doses administered to the tumor-bearing mice used in the PK study (Figure 3.12). The tumor uptake of DOX for polyMPC-DOX was 700 ng per gram of tissue three days after injection, and 390 ng/g five days after injection. This represents a two-fold increase over free DOX at Day 3 (350 ng/g) and a three-fold increase over free DOX at Day 5 (130

ng/g). Moreover, polyMPC-DOX conjugates displayed reduced accumulation in off-target organs, including the spleen and especially the lungs relative to free DOX. Significantly higher drug accumulation was noted in the liver for the polyMPC-DOX group compared to the free DOX group, which we attribute to the prolonged circulation times and delayed clearance noted for the polymer prodrug. While DOX is known to be metabolized primarily by the liver, the liposomal formulation DOXIL was found to have impaired hepatic metabolism, suspected to be excluded from uptake based on liposome size.[105] Similarly the increased size of polyMPC-DOX prodrugs relative to free DOX may hamper hepatic uptake, resulting in delayed accumulation. Low drug accumulation found in the heart for the polyMPC-DOX group is potentially advantageous, reducing cardiotoxicity effects, a known dose-limiting side effect commonly associated with DOX administration.[81] Tumor-to-normal tissue distribution ratios are given in Table 3.4, highlighting the preferential DOX uptake in tumor tissue relative to healthy tissue. The benefits of passive tumor targeting of polymer prodrugs has been noted before, and the data presented here suggests the polyMPC-DOX has similar benefits *in vivo*.[4,103]
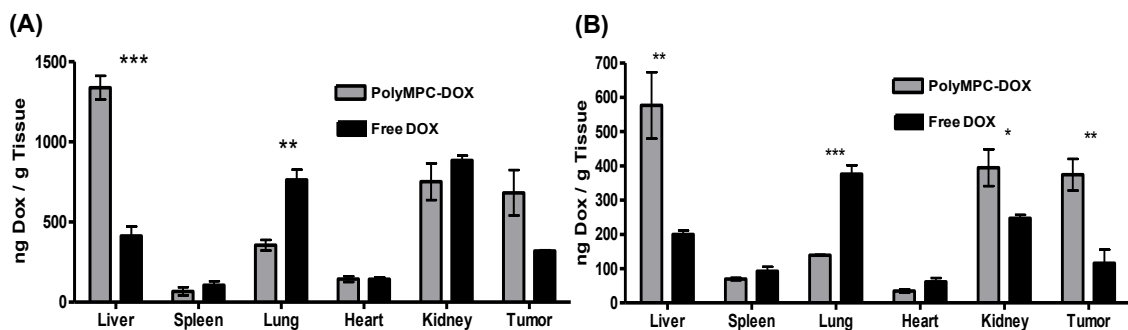
Figure 3.12 Biodistribution analysis of polyMPC-DOX compared to free DOX after (A) 3 days and (B) 5 days expressed as ng DOX / g tissue. The significance was determined using a two-tailed Student's t-test [* p=0.05 to 0.01; ** p=0.01 to 0.001; *** p<0.001]. Error bars represent ± the standard error of the mean (SEM).

Table 3.4 Tumor-to-normal tissue distribution ratios for polyMPC-DOX and DOX.

		Liver	Spleen	Lung	Heart	Kidney
PolyMPC-DOX	Day 3	0.52	1.50	1.86	4.00	0.90
	Day 5	0.66	2.40	2.45	5.94	0.94
Free DOX	Day 3	0.83	0.35	0.45	2.01	0.39
	Day 5	0.63	0.21	0.33	1.43	0.49

At the conclusion of the PK and biodistribution study, the spleen, liver, kidney, heart, lungs, and tumors were removed from the animals and weighed, with livers and spleens fixed and paraffin-embedded for histological analysis. As shown in Figure 3.13A, only small differences amongst the groups were noted with respect to tissue weights. Histological analysis of tissue sections stained with hematoxylin and eosin (H&E) suggested no significant off-target toxicity at these high levels of DOX, consistent with the use of the polyMPC as a carrier. Despite the previously noted increase in drug accumulation in the liver, H&E analysis revealed no sign of adverse effects or off-target toxicity in the liver (Figure 3.13B).
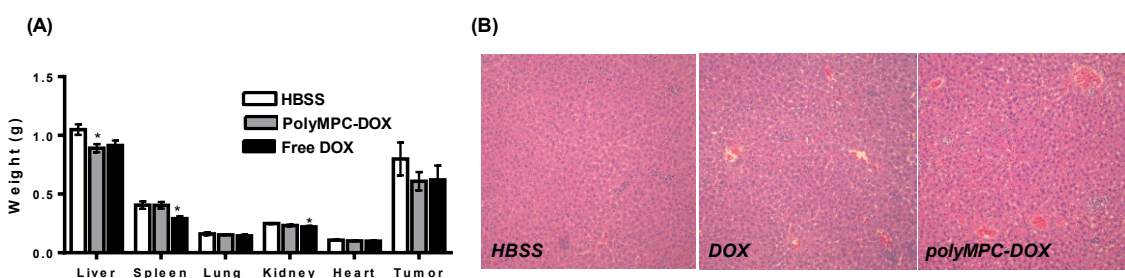
Figure 3.13. (A) Weights (g) of tissues collected at conclusion of the study (5 days post-injection): liver, spleen, lung, kidneys, heart and tumor. Error bars represent ± SEM. [*p = 0.5 - 0.1]; (B) H&E stained liver sections from HBSS, DOX, and polyMPC-DOX treatment groups from biodistribution study.

While our data, and other literature reports on polyMPC point to the safety of its use *in vivo,* we are not aware of prior reports that examine potential *in vivo* immunogenicity arising from its presence in the bloodstream. Thus, in conjunction with these *in vivo* efficacy studies, we also sought to gauge whether there were innate or

adaptive immune system responses to polyMPC, accomplished through a complete blood count (CBC), and measurement of cytokine responses by an enzyme-linked immunosorbent assay (ELISA) (Figure 3.14). Analysis of serum cytokine and white blood cell (WBC) levels indicated an initial increase in total WBC count on Day 3 with polyMPC DOX (Figure 3.14A), with no differences noted on Day 5 (Figure 3.14B). The initial increase in white blood cell count, suggestive of a foreign antigen response, was rectified by Day 5. Red blood cell (RBC) counts indicated no differences across the treatment groups. Furthermore, we observed no significant differences between polyMPC-DOX and HBSS in Th1 versus Th2 cytokines by ELISA at Day 3, with only a slight decrease in IL12 and IL10 noted at Day 5. However, this cannot be attributed to the polyMPC carrier, since this decrease is much more pronounced in the case of animals treated with free DOX (Figures 3.14C-3.14H). These results suggest that polyMPC-bound DOX does not elicit significant adverse immunogenic effects that could lead towards undesired anemia or inflammatory response in animals.
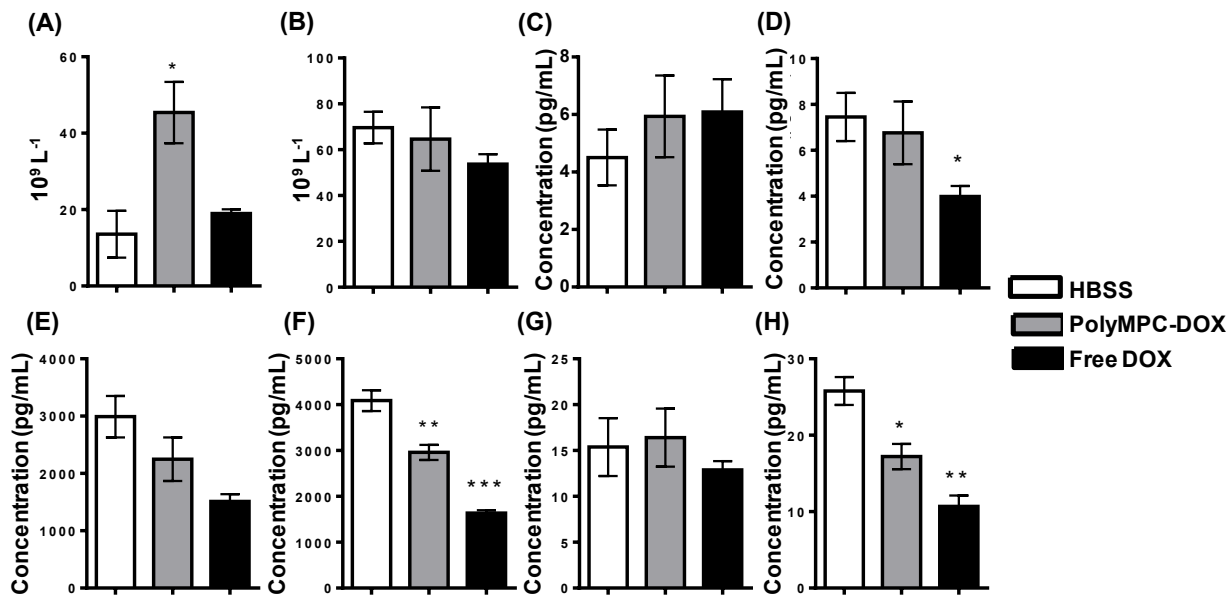
Figure 3.14. Analysis of immune response across all treatment groups using complete blood count (CBC) and ELISA cytokine measurements three and five days after injection. (A) White blood cell count (WBC) (Day 3); (B) WBC (Day 5); (C) Interferon-γ (IFN- γ) (Day 3); (D) IFN- γ (Day 5); (E) Interleukin-12 (IL-12) (Day 3); (F) IL-12 (Day 5); (G) Interleukin-10 (IL-10) (Day 3); (H) IL-10 (Day 5). Error bars represent ± SEM.

4T1 tumor-bearing mice were used to evaluate the therapeutic performance of polyMPC-DOX conjugates for the treatment of breast cancer. Tumors were established by orthotopic injection of murine 4T1 cells (5×10^6 4T1 cells in Hank's balanced salt solution, HBSS) into the mammary fat pad of the mice (~17.5 g, 4 weeks old). The mice were randomized into three groups of 15; at a tumor volume in the range of 42-132 mm^3, mice were administered either HBSS, free DOX (3 mg/kg, ~1/2 MTD), or polyMPC-DOX (15 mg/kg DOX equivalent, ~1/2 MTD) by tail vein injection. Subsequent doses were administered on Days 7 and 17 (polyMPC-DOX group only). Mice were examined and weighed every 2-4 days, and tumor volume was determined by caliper measurements (calculated by $0.52 \times L \times W^2$) over a period of 29 days. Mice were removed from the study when the tumor volume reached 1500 mm^3, if weight loss exceeded 20 %, or if the

animal appeared to be showing signs of stress, including a scruffy appearance or abnormal behavior. A summary of tumor efficacy results is presented in Figure 3.15. Figure 3.15A shows that survival was increased substantially for mice receiving polyMPC-DOX compared to both the untreated and free DOX-treated mice. Notably, mice receiving the free DOX treatment showed no improvement, essentially mirroring results for the HBSS group; all these mice were removed from the study by Day 18. In contrast, 80 % of the mice receiving the polyMPC-DOX treatment remained in the study at Day 18, with overall survival in the polyMPC-DOX group extended almost two-fold (29 days) compared to the other treatment groups. Figure 3.15B shows that tumor growth was greatly suppressed in the mice receiving the polyMPC-DOX, whereas the mice receiving free DOX showed no difference relative to the untreated mice. Untreated and free DOX treated mice surviving to Day 18 displayed tumors with average volumes ranging from 1600-1850 mm^3, requiring their removal from the study. PolyMPC-DOX treated mice at Day 18 had average tumor volumes of 1050 mm^3, and at the Day 29 end-point, average tumor volume was 1170 mm^3. The weights of the mice overall remained largely unchanged over the course of the study, as shown in Figure 3.15C. However, following the third dose of polyMPC-DOX, animal weights did not return to normal range quickly enough, necessitating their removal from the study. At the conclusion of the study, tissues (livers, spleens, hearts, kidneys) were collected and analyzed to compare to the results obtained from the PK/biodistribution study, with the efficacy mice displaying comparable tissue weights amongst treatment groups, with the exception of the lungs. The significant weight increase in the lungs of the polyMPC-DOX group is attributed to the numerous metastases in the lungs, likely due to the prolonged survival of

the mice in this group (two times that of the free DOX and HBSS mice). We note that the mice receiving polyMPC-DOX treatment were dosed below the previously determined MTD for these conjugates (30-50 mg/kg DOX equivalent) so that the cumulative dose received did not exceed the MTD. Since the PK data reveals that polyMPC-DOX is nearly cleared within 48 hours, future animal studies will examine a more frequent dosing regimen, aiming towards complete tumor regression. Nonetheless, this experiment confirms the efficacy of polyMPC-DOX prodrugs, even when presented with aggressive, highly metastatic 4T1 cancer in live animals.
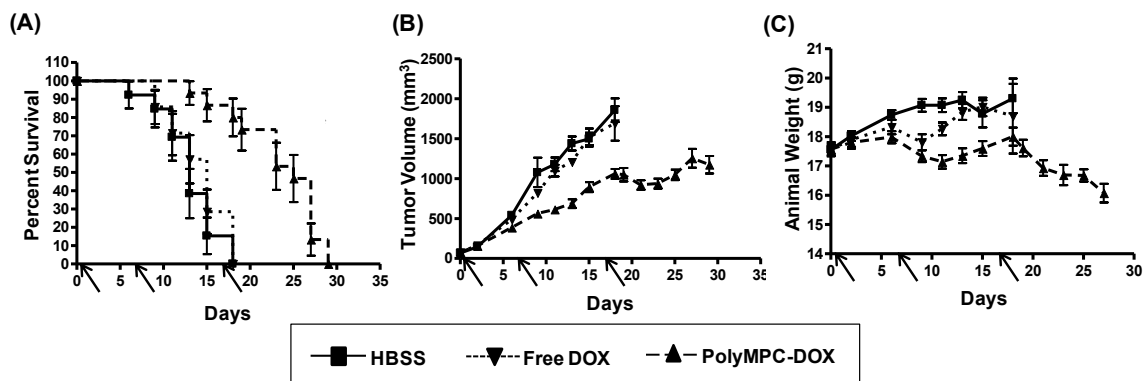
Figure 3.15. Summary of efficacy data in 4T1 mouse model. (A) Survival curve for mice treated with HBSS (squares, solid line), polyMPC-DOX (triangles, dashed line), and free DOX (inverted triangles, dotted line); (B) tumor growth over time for mice treated with HBSS (squares, solid line), polyMPC-DOX (triangles, dashed line), and free DOX (inverted triangle, dotted line); (C) mouse weight for mice treated with HBSS (squares, solid line), polyMPC-DOX (triangles, dashed line), and free DOX (inverted triangle, dotted line) Arrows indicate days on which treatments were administered: 0, 7, and 17 (polyMPC-DOX only). Error bars represent ± SEM.

The present study demonstrates the ability of polyMPC-DOX to prolong circulation half-life from 15 minutes to 2 hours, with favorable accumulation occurring in the tumor as opposed to healthy tissues, and no significant innate or adaptive immunogenic responses. Moreover, we demonstrate the efficacy of polyMPC-DOX in 4T1 tumor-bearing mice, increasing the overall survival two-fold, and significantly reducing tumor growth in mice. The aggressive 4T1 mouse model reveals the potential

83

for polyMPC-DOX in the treatment of triple negative breast cancer, and ongoing studies include evaluating the *in vivo* efficacy against a human breast cancer cell line.

3.7 Conclusions and Future Outlook

PolyMPC has been demonstrated as an effective drug carrier for small molecule chemotherapeutic agents, with camptothecin and doxorubicin as examples. Using appropriately functionalized comonomers with MPC, drugs can be incorporated along the polymer backbone as pendent groups, a strategy which has allowed for unprecedented, massively high drug loadings, for example up to 45 weight % in the case of DOX. Furthermore, the mechanism of release can be tailored according to the linker, including through simple hydrolysis, or according to environmental (i.e. intratumoral or intracellular) triggers including redox or pH sensitivity.

Future studies will include the further exploration of more advanced architectures, for example, polyMPC-based micelles. Polymer micelles provide a route to larger structures (20 - 100 nm in diameter), enhancing the circulatory retention and thus therapeutic window. Additionally, active targeting strategies will be employed, aiming to reduce non-specific uptake by healthy tissue and reduce off-target toxicity. To realize this synthetically, the antibody Erbitux (Cetuximab), known to target the epidermal growth factor receptors (EGFR) that are typically upregulated in tumors, will be used. Antibody-polyMPC conjugation can be accomplished through installing a thiol-reactive polymer chain end, such as maleimide. Antibody-polymer prodrug conjugates have the added benefit of high drug loading; in addition to incorporating multiple copies of drug along the polymer, multiple polymer chains (usually between 4 and 8) can be conjugated to a single antibody.

3.8 References

1. Duncan, R. Polymer conjugates as anticancer nanomedicines. *Nature Reviews Cancer* **2006**, *6*, 688-701.

2. Pasut, G.; Veronese, F.M.; PEG conjugates in clinical development or use as anticancer agents: An overview. *Advanced Drug Delivery Reviews* **2009**, *61*, 1177-88.

3. Joralemon, M.J.; McRae, S.; Emrick, T. PEGylated polymers for medicine: from conjugation to self-assembled systems. *Chemical Communications* **2010**, *46*, 1377-93.

4. Maeda, H.; Wu, J.; Sawa, T.; Matsumura, Y.; Hori, K. Tumor vascular permeability and the EPR effect in macromolecular therapeutics: a review. *Journal of Controlled Release* **2000**, *65*, 271-84.

5. Greenwald, R.B.; Choe, Y.H.; McGuire, J.; Conover, C.D. Effective drug delivery by PEGylated drug conjugates. *Advanced Drug Delivery Reviews* **2003**, *55*, 217-50.

6. Thomson, A.H.; Vasey, P.A.; Murray, L.S.; Cassidy, J.; Fraier, D.; Frigerio, E.; Twelves, C. Population pharmacokinetics in phase I drug development: a phase I study of PK1 in patients with solid tumours. *British Journal of Cancer* **1999**, *81*, 99-107.

7. Seymour, L.W.; Ferry, D.R.; Kerr, D.J.; Rea, D.; Whitlock, M.; Poyner, R.; Boivin, C.;   Hesslewood, S.; Twelves, C.; Blackie, R.; Schatzlein, A.; Jodrell, D.; Bissett, D.; Calvert, H.; Lind, M.; Robbins, A.; Burtles, S.; Duncan, R.; Cassidy, J. Phase II studies of polymer-doxorubicin (PK1, FCE 28068) in the treatment of breast, lung, and colorectal cancer. *International Journal of Oncology* **2009**, *34*, 1629-36.

8. Bissett, D.; Cassidy, J.; Bono, J.S.; Muirhead, F.; Main, M.; Robson, L.; Fraier, D.; Magne, M.L.; Pellizzoni, C.; Porro, M.G.; Spinelli, R.; Speed, W.; Twelves, C. Phase I and pharmacokinetic (PK) study of MAG-CPT (PNU 166148): a polymeric derivative of camptothecin (CPT). *British Journal of Cancer* **2004**, *91*, 50-5.

9. Kopecek, J.; Kopeckova, P.; Minko, T.; Lu, Z. HPMA copolymer-anticancer drug conjugates: design, activity, and mechanism of action. *European Journal of Pharmaceutics and Biopharmaceutics* **2006**, *50*, 61-81.

10. Schluep, T.; Hwang, J.; Cheng, J.J.; Heidel, J.D.; Bartlett, D.W.; Hollister, B.; Davis, M.E. Preclinical efficacy of the camptothecin-polymer conjugate IT-101 in multiple cancer models. *Clinical Cancer Research* **2006**, *12*, 1606-14.

11. Numbenjapon, T.; Wang, J.Y.; Colcher, D.; Schluep, T.; Davis, M.E.; Duringer, J.; Kretzner, L.; Yen, Y.; Forman, S.J.; Raubitschek, A. Preclinical results of camptothecin- polymer conjugate (IT-101) in multiple human lymphoma xenograft models. *Clinical Cancer Research* **2009**, *15*, 4365-73.

12. Greenwald, R. B.; Pendri, A.; Conover, C. D.; Lee, C.; Choe, Y. H.; Gilbert, C.; Martinez, A.; Xia, J.; Wu, D. C.; Hsue, M. Camptothecin-20-PEG ester transport forms: the effect of spacer groups on antitumor activity. *Bioorganic and Medicinal Chemistry* **1998**, *6*, 551-62.

13. Rodrigues, P.; Beyer, U.; Schumacher, P.; Roth, T.; Fiebig, H.; Unger, C.; Messori, L.; Orioli, P.; Paper, D.; Mülhaupt, R.; Kratz, F. Acid-sensitive polyethylene glycol conjugates of doxorubicin: preparation, in vitro efficacy and intracellular distribution. *Bioorganic and Medicinal chemistry* **1999**, *7*, 2517–24.

14. Lee, C.; Gillies, E.; Fox, M.; Guillaudeu, S.; Fréchet, J.; Dy, E.; Szoka, F. A single dose of doxorubicin-functionalized bow-tie dendrimer cures mice bearing C-26 colon carcinomas. *Proceedings of the National Academy of Sciences of the United States of America* **2006**, *103*, 16649–54.

15. Ishihara, K.; Iwasaki, Y. J. Reduced protein adsorption on novel phospholipid polymers. *Journal of Biomaterials Applications* **1998**, *13*, 111-27.

16. Ishihara, K.; Nomura, H.; Mihara, T.; Kurita, K.; Iwasaki, Y.; Nakabayashi, N. Why do phospholipid polymers reduce protein adsorption? *Journal of Biomedical Materials Research* **1998**, *39*, 323–30.

17. Ishihara, K. New polymeric biomaterials phospholipid polymers with a biocompatible surface. *Froniers of Medical and Biological Engineering* **2000**, *10*, 83-95.

18. Lewis, A. L. Phosphorylcholine-based polymers and their use in the prevention of biofouling. *Colloids and surfaces. B, Biointerfaces* **2000**, *18*, 261–75.

19. Nakabayashi, N.; Williams, D. Preparation of non-thrombogenic materials using 2-methacryloyloxyethyl phosphorylcholine. *Biomaterials* **2003**, *24*, 2431–5.

20. Iwasaki, Y.; Ishihara, K. Phosphorylcholine-containing polymers for biomedical applications. *Analytical and Bioanalytical Chemistry* **2005**, *381*, 534–46.

21. Ishihara, K.; Takai, M. Bioinspired interface for nanobiodevices based on phospholipid polymer chemistry. *Journal of the Royal Society Interface* **2009**, *6*, S279-91.

22. Lobb, E.; Ma, I.; Billingham, N.; Armes, S.; Lewis, A. Facile synthesis of well-defined, biocompatible phosphorylcholine-based methacrylate copolymers via atom transfer radical polymerization at 20 degrees C. *Journal of the American Chemical Society* **2001**, *123*, 7913–4.

23. Ma, I. Y.; Lobb, E. J.; Billingham, N. C.; Armes, S. P.; Lewis, A. L.; Lloyd, A. W.; Salvage, J. Synthesis of Biocompatible Polymers. 1. Homopolymerization of 2-Methacryloyloxyethyl Phosphorylcholine via ATRP in Protic Solvents: An Optimization Study. *Macromolecules* **2002**, *35*, 9306-14.

24. Ma, Y.; Tang, Y.; Billingham, N. C.; Armes, S. P.; Lewis, A. L.; Lloyd, A. W.; Salvage, J. P. Well-Defined Biocompatible Block Copolymers via Atom Transfer Radical Polymerization of 2-Methacryloyloxyethyl Phosphorylcholine in Protic Media. *Macromolecules* **2003**, *36*, 3475-84.

25. Licciardi, M.; Tang, Y.; Billingham, N.; Armes, S.; Lewis, A. Synthesis of novel folic acid-functionalized biocompatible block copolymers by atom transfer radical polymerization for gene delivery and encapsulation of hydrophobic drugs. *Biomacromolecules* **2004**, *6*, 1085–96.

26. Yusa, S.-I.; Fukuda, K.; Yamamoto, T.; Ishihara, K.; Morishima, Y. Synthesis of well-defined amphiphilic block copolymers having phospholipid polymer sequences as a novel biocompatible polymer micelle reagent. *Biomacromolecules* **2004**, *6*, 663–70.

27. Yu, B.; Lowe, A.; Ishihara, K. RAFT synthesis and stimulus-induced self-assembly in water of copolymers based on the biocompatible monomer 2-(methacryloyloxy)ethyl phosphorylcholine. *Biomacromolecules* **2009**, *10*, 950–8.

28. Wall, M. E.; Wani, M. C.; Cook, C. E.; Palmer, K. H.; McPhail, A. T.; Sim, G. A. Plant Antitumor Agents. I. The Isolation and Structure of Camptothecin, a Novel Alkaloidal Leukemia and Tumor Inhibitor from Camptotheca acuminata 1,2. *Journal of the American Chemical Society* **1966**, *88*, 3888-90.

29. Slichenmyer, W.; Rowinsky, E.; Donehower, R.; Kaufmann, S. The current status of camptothecin analogues as antitumor agents. *Journal of the National Cancer Institute* **1993**, *85*, 271–91.

30. Muggia, F. M.; Dimery, I.; Arbuck, S. G. *In Conference on the Camptothecins - From Discovery to the Patient*; Pantazis, P., Giovanella, B. C., Rothenberg, M. L., Eds.; New York Acad Sciences: Bethesda, Md, **1996**, 213-23.

31. Herben, V. M. M.; Huinink, W.; Beijnen, J. H. Clinical pharmacokinetics of topotecan. *Clinical Pharmacokinetics* **1996**, *31*, 85-102.

32. Mathijssen, R.; van Alphen, R.; Verweij, J.; Loos, W.; Nooter, K.; Stoter, G.; Sparreboom, A. Clinical pharmacokinetics and metabolism of irinotecan (CPT-11). *Clinical Cancer Research* **2001**, *7*, 2182–94.

33. Zhao, H.; Lee, C.; Sai, P.; Choe, Y.; Boro, M.; Pendri, A.; Guan, S.; Greenwald, R. 20-O-acylcamptothecin derivatives: evidence for lactone stabilization. *The Journal of Organic Chemistry* **2000**, *65*, 4601–6.

34. Greenwald, R.; Pendri, A.; Conover, C.; Gilbert, C.; Yang, R.; Xia, J. Drug delivery systems. 2. Camptothecin 20-O-poly(ethylene glycol) ester transport forms. *Journal of Medicinal Chemistry* **1996**, *39*, 1938–40.

35. Zamai, M.; VandeVen, M.; Farao, M.; Gratton, E.; Ghiglieri, A.; Castelli, M.; Fontana, E.; D'Argy, R.; Fiorino, A.; Pesenti, E.; Suarato, A.; Caiolfa, V. Camptothecin poly[n-(2-hydroxypropyl) methacrylamide] copolymers in antitopoisomerase-I tumor therapy: intratumor release and antitumor efficacy. *Molecular Cancer Therapeutics* **2002**, *2*, 29–40.

36. Caiolfa, V. R.; Zamai, M.; Fiorino, A.; Frigerio, E.; Pellizzoni, C.; d'Argy, R.; Ghiglieri, A.; Castelli, M. G.; Farao, M.; Pesenti, E.; Gigli, M.; Angelucci, F.; Suarato, A. *In 9th International Symposium on Recent Advances in Drug Delivery Systems*; Elsevier Science: Salt Lake City, Utah, **1999**, 105-19.

37. Singer, J. W.; Bhatt, R.; Tulinsky, J.; Buhler, K. R.; Heasley, E.; Klein, P.; de Vries, P. *In International Symposium on Tumor Targeted Delivery Systems*; Elsevier Science: Bethesda, Maryland, **2000**, 243-7.

38. Zou, Y. Y.; Wu, Q. P.; Tansey, W.; Chow, D.; Hung, M. C.; Vej, C. C.; Wallace, S.; Li, C. Effectiveness of water soluble poly(L-glutamic acid)-camptothecin conjugate against resistant human lung cancer xenografted in nude mice. *International Journal of Oncology* **2001**, *18*, 331-6.

39. Bhatt, R.; de Vries, P.; Tulinsky, J.; Bellamy, G.; Baker, B.; Singer, J.; Klein, P. Synthesis and in vivo antitumor activity of poly(l-glutamic acid) conjugates of 20S-camptothecin. *Journal of Medicinal Chemistry* **2003**, *46*, 190–3.

40. Cheng, J.; Khin, K.; Jensen, G.; Liu, A.; Davis, M. Synthesis of linear, beta-cyclodextrin-based polymers and their camptothecin conjugates. *Bioconjugate Chemistry* **2002**, *14*, 1007–17.

41. Cheng, J.; Khin, K.; Davis, M. Antitumor activity of beta-cyclodextrin polymer-camptothecin conjugates. *Molecular Pharmaceutics* **2003**, *1*, 183–93.

42. Parrish, B.; Emrick, T. Soluble camptothecin derivatives prepared by click cycloaddition chemistry on functional aliphatic polyesters. *Bioconjugate Chemistry* **2006**, *18*, 263–7.

43. Gao, H.; Matyjaszewski, K. Synthesis of Star Polymers by a Combination of ATRP and the "Click" Coupling Method. *Macromolecules* **2006**, *39*, 4960-5.

44. Ito, H.; Arimoto, K.; Sensul, H.; Hosomi, A. Direct alkynyl group transfer from silicon to copper: New preparation method of alkynylcopper (I) reagents. *Tetrahedron Letters* **1997**, *38*, 3977-80.

45. Zhao, H.; Rubio, B.; Sapra, P.; Wu, D.; Reddy, P.; Sai, P.; Martinez, A.; Gao, Y.; Lozanguiez, Y.; Longley, C.; Greenberger, L.; Horak, I. Novel prodrugs of SN38 using multiarm poly(ethylene glycol) linkers. *Bioconjugate Chemistry* **2008**, *19*, 849–59.

46. Chen, M.; Briscoe, W.; Armes, S.; Klein, J. Lubrication at physiological pressures by polyzwitterionic brushes. *Science (New York, N.Y.)* **2009**, *323*, 1698–701.

47. Guillaudeu, S.; Fox, M.; Haidar, Y.; Dy, E.; Szoka, F.; Fréchet, J. PEGylated dendrimers with core functionality for biological applications. *Bioconjugate Chemistry* **2008**, *19*, 461–9.

48. Alakhov, V.; Klinski, E.; Li, S.; Pietrzynski, G.; Venne, A.; Batrakova, E.V.; Bronitch, T.; Kabanov, A.V. Block copolymer-based formulation of doxorubicin. From cell screen to clinical trials. *Colloids and Surfaces B: Biointerfaces* **1999**, *16*, 113-34.

49. Nakanishi, T.; Fukushima, S.; Okamoto, K.; Suzuki, M.; Matsumura, Y.; Yokoyama, M.; Okano, T.; Sakurai, Y.; Kataoka, K. Development of the polymer micelle carrier system for doxorubicin. *Journal of Controlled Release* **2001**, *74*, 295-302.

50. Christian, D.A.; Cai, S.; Garbuzenko, O.B.; Harada, T.; Zajac, A.L.; Minko, T.; Discher, D.E. Flexible Filaments for in Vivo Imaging and Delivery: Persistent Circulation of Filomicelles Opens the Dosage Window for Sustained Tumor Shrinkage. *Molecular Pharmaceutics* **2009**, *6*, 1343-52.

51. Van Nostrum, C.F. Covalently cross-linked amphiphilic block copolymer micelles. *Soft Matter* **2011**, *7*, 3246-59.

52. Gohy, J.- F. Block Copolymer Micelles. *Advances in Polymer Science* **2005**, *190*, 65-136.

53. Jones, M.-C.; Leroux, J.-C. Polymeric micelles- a new generation of colloidal drug carriers. *European Journal of Pharmaceutics and Biopharmaceutics* **1999**, *48*, 101-11.

54. O'Reilly, R.K.; Hawker, C.J.; Wooley, K.L. Cross-linked block copolymer micelles: functional nanostructures of great potential and versatility. *Chemical Society Reviews* **2006**, *35*, 1068-83.

55. Peer, D.; Karp, J.M.; Hong, S.; Farokhzad, O.C.; Margalit, R.; Langer, R. Nanocarriers as an emerging platform for cancer therapy. *Nature Nanotechnology* **2007**, *2*, 751-60.

56. Li, Y.T.; Lokitz, B.S.; McCormick, C.L. RAFT synthesis of a thermally responsive ABC triblock copolymer incorporating N-acryloxysuccinimide for facile in situ formation of shell cross-linked micelles in aqueous media. *Macromolecules* **2006**, *39*, 81-9.

57. Duong, H.T.T.; Nguyen, T.L.U.; Stenzel, M.H. Micelles with surface conjugated RGD peptide and crosslinked polyurea core via RAFT polymerization. *Polymer Chemistry* **2010**, *1*, 171-82.

58. Iijima, M.; Nagasaki, Y.; Okada, T.; Kato, M.; Kataoka, K. Core-polymerized reactive micelles from heterotelechelic amphiphilic block copolymers. *Macromolecules* **1999**, *32*,1140-6.

59. Lee, W.-C.; Li, Y.-C.; Chu, I.-M. Amphiphilic poly(D,L-lactic acid)/poly(ethylene glycol)/poly(D,L-lactic acid) nanogels for controlled release of hydrophobic drugs. *Macromolecular Bioscience* **2006**, *6*, 846-54.

60. Henselwood, F.; Liu, G. Water-soluble nanospheres of poly(2-cinnamoylethyl methacrylate)-block-poly(acrylic acid). *Macromolecules* **1997**, *30*, 488-93.

61. Saito, K.; Ingalls, L.R.; Lee, J.; Warner, J.C. Core-bound polymeric micellar system based on photocrosslinking of thymine. *Chemical Communications* **2007**, *24*, 2503-5.

62. Meng, F.; Hennink, W.E.; Zhong, Z. Reduction-sensitive polymers and bioconjugates for biomedical applications. *Biomaterials* **2009**, *30*, 2180-98.

63. Cheng, R.; Feng, F.; Meng, F.; Deng, C.; Feijen, J.; Zhong, Z. Glutathione-responsive nano-vehicles as a promising platform for targeted intracellular drug and gene delivery. *Journal of Controlled Release* **2011**, *152*, 2-12.

64. Hu, X.; Li, H.; Luo, S.; Liu, T.; Jiang, Y.; Liu, S. Thiol and pH dual-responsive dynamic covalent shell cross-linked micelles for triggered release of chemotherapeutic drugs. *Polymer Chemistry* **2013**, *4*, 695-706.

65. Convertine, A.J.; Diab, C.; Prieve, M.; Paschal, A.; Hoffman, A.S.; Johnson, P.H.; Stayton, P.S. pH-Responsive polymeric micelle carriers for siRNA drugs. *Biomacromolecules* **2010**, *11*, 2904-11.

66. Schafer, F.Q.; Buettner, G.R. Redox environment of the cell as viewed through the redox state of the glutathione disulfide/glutathione couple. *Free Radical Biology and Medicine* **2011**, *30*, 1191-1212.

67. Kakizawa, Y.; Harada, A.; Kataoka, K. Environment-sensitive stabilization of core-chell structured polyion complex micelle by reverible cross-linking of the core through disulfide bond. *Journal of the American Chemical Society* **1999**, *121*, 11247-8.

68. Zhang, J.; Gong, M.; Yang, S.; Gong, Y.-K. Crosslinked biomimetic random copolymer micelles as potential anti-cancer drug delivery vehicle. *Journal of Controlled Release* **2011**, *152*, e1-e132.

69. Xu, Y.; Meng, F.; Cheng, R.; Zhong, Z. Reduction-sensitive reversible crosslinked biodgradable micelles for triggered release of doxorubicin. *Macromolecular Bioscience* **2009**, *9*, 1254-61.

70. Vetvicka, D.; Hruby, M.; Hovorka, O.; Etrych, T.; Vetrik, M.; Kovar, L.; Kovar, M.; Ulbrich, K.; Rihova, B. Biological evaluation of polymeric micelles with covalently bound doxorubicin. *Bioconjugate Chemistry* **2009**, *20*, 2090-97.

71. Cabral, H.; Nakanishi, M.; Kumagai, M.; Jang, W.-D.; Nishiyama, N.; Kataoka, K. A photo- activated targeting chemotherapy using glutathione sensitive camptothecin-loaded polymer micelles. *Pharmaceutical Research* **2009**, *26*, 82-92.

72. Konna, T.; Watanabe, J.; Ishihara, K. Enhanced solubility of paclitaxel using water-soluble and biocompatible 2-methacryloyloxyethyl phosphorylcholine polymers. *Journal of Biomedical Materials Research Part A* **2002**, *65*, 209-14.

73. Chu, H.; Liu, N.; Wang, X.; Jiao, Z.; Chen, Z. Morphology and in vitro release kinetics of drug-loaded micelles based on well-defined PMPC-b-PBMA copolymer. *International Journal of Pharmaceutics* **2009**, *371*, 190-6.

74. Wei, R.; Cheng, L.; Zheng, M.; Cheng, R.; Meng, F.; Deng, C.; Zhong, Z. Reduction-responsive disassemblable core-cross-linked micelles based on poly(ethylene glycol)-b-poly(N-2-hydroxypropyl methacrylamide)-lipoic acid conjugates for triggered intracellular anticancer drug release. *Biomacromolecules* **2012**, *13*, 2429-38.

75. Chen, X.; Lawrence, J.; Parelkar, S.; Emrick, T. Novel Zwitterionic Copolymers with Dihydrolipoic Acid: Synthesis and Preparation of Nonfouling Nanorods. *Macromolecules* **2012**, *46*, 119-27.

76. Ellman, G.L. Tissue Sulfhydryl groups. *Archives of Biochemistry and Biophysics* **1959**, *82*, 70-7.

77. Digilio, G.; Menchise, V.; Gianolo, E.; Catanzaro, V.; Carrera, C.; Napolitano, R.; Fedeli, F.; Aime, S. Exofacial protein thiols as a route for the internalization of Gd(III)-based complexes for magnetic resonance imaging cell labeling. *Journal of Medicinal Chemistry* **2010**, *53*, 4877-90.

78. Davis, M.E.; Chen, Z.; Shin, D.M. Nanoparticle therapeutics: an emerging treatment modality for cancer. *Nature Reviews Drug Discovery* **2008**, *7*, 771-82.

79. Duncan, R. The dawning era of polymer therapeutics. *Nature Reviews Drug Discovery* **2003**, *2*, 347-60.

80. Berry, G.; Billingham, M.; Alderman, E.; Richardson, P.; Torti, F.; Lum, B.; Patek, A.; Martin, F. The use of cardiac biopsy to demonstrate reduced cardiotoxicity in AIDS Kaposi's sarcoma patients treated with pegylated liposomal doxorubicin. *Annals of Oncology* **1998**, *9*, 711–6.

81. Safra, T.; Jeffers, S.; Tsao-Wei, D.D.; Groshen, S.; Lyass, O.; Henderson, R.; Berry, G.; Gabizon, A. Pegylated liposomal doxorubicin (doxil): Reduced clinical cardiotoxicity in patients reaching or exceeding cumulative doses of 500 mg/m2. *Annals of Oncology* **2000**, *11*, 1029-33.

82. Lotem, M.; Hubert, A.; Lyass, O.; Goldenhersh, M.A.; Ingber, A.; Peretz, T.; Gabizon, A. Skin toxic effects of polyethylene glycol-coated liposomal doxorubicin. *Archives of Dermatology* **2000**, *11*, 1029-33.

83. Hamilton, A.; Biganzoli, L.; Coleman, R.; Mauriac, L.; Hennebert, P.; Awada, A.; Nooij, M.; Beex, L.; Piccart, M.; Van Hoorebeeck, I.; Bruning, P.; de Valeriola, D. EORTC 10968: a phase I clinical and pharmacokinetic study of polyethylene glycol liposomal doxorubicin (Caelyx, Doxil) at a 6-week interval in patients with metastatic breast cancer. *Annals of Oncology* **2002**, *13*, 910–8.

84. Uziely, B.; Jeffers, S.; Isacson, R.; Kutsch, K.; Wei-Tsao, D.; Yehoshua, Z.; Libson, E.; Muggia, F.; Gabizon, A. Liposomal doxorubicin: antitumor activity and unique toxicities during two complementary phase I studies. *Journal of Clinical Oncology* **1995**, *13*, 1777–85.

85. Elbayoumi, T. A.; Torchilin, V. P. Tumor-specific antibody-mediated targeted delivery of Doxil® reduces the manifestation of auricular erythema side effect in mice. *International Journal of Pharmaceutics* **2008**, *357*, 272-279.

86. van der Poll, D.; Kieler-Ferguson, H.; Floyd, W.; Guillaudeu, S.; Jerger, K.; Szoka, F.; Fréchet, J. Design, synthesis, and biological evaluation of a robust, biodegradable dendrimer. *Bioconjugate Chemistry* **2010**, *21*, 764–73.

87. Etrych, T.; Jelínková, M.; Ríhová, B.; Ulbrich, K. New HPMA copolymers containing doxorubicin bound via pH-sensitive linkage: synthesis and preliminary in vitro and in vivo biological properties. *Journal of Controlled Release* **2001**, *73*, 89–102.

88. Ulbrich, K.; Etrych, T.; Chytil, P.; Jelínková, M.; Ríhová, B. HPMA copolymers with pH-controlled release of doxorubicin: in vitro cytotoxicity and in vivo antitumor activity. *Journal of Controlled Release* **2003**, *87*, 33–47.

89. Mrkvan, T.; Sirova, M.; Etrych, T.; Chytil, P.; Strohalm, J.; Plocova, D.; Ulbrich, K.; Rihova, B. Chemotherapy based on HPMA copolymer conjugates with pH-controlled release of doxorubicin triggers anti-tumor immunity. *Journal of Controlled Release* **2005**, *110*, 119–29.

90. Vetvicka, D.; Hruby, M.; Hovorka, O.; Etrych, T.; Vetrik, M.; Kovar, L.; Kovar, M.; Ulbrich, K.; Rihova, B. Biological evaluation of polymeric micelles with covalently bound doxorubicin. *Bioconjugate Chemistry* **2009**, *20*, 2090–7.

91. Tannock, I. F.; Rotin, D. Acid pH in tumors and its potential for therapeutic exploitation. *Cancer Research* **1989**, *49*, 4373–84.

92. Engin, K.; Leeper, D.B.; Cater, J.R.; Thistlethwaite, A.J.; Tupchong, L.; McFarlane, J.D. *International Journal of Hyperthermia* **1995**, *11*, 211-6.

93. Mellman, I.; Fuchs, R.; Helenius, A. Acidification of the endocytic and exocytic pathways. *Annual Review of Biochemistry* **1986**, *55*, 663-700.

94. Chen, X.; Parelkar, S.; Henchey, E.; Schneider, S.; Emrick, T. PolyMPC-Doxorubicin Prodrugs. *Bioconjugate Chemistry* **2012**, *23*, 1753-63.

95. Kratz, F.; Azab, S.; Zeisig, R.; Fichtner, I.; Warnecke, A. Evaluation of combination therapy schedules of doxorubicin and an acid-sensitive albumin-binding prodrug of doxorubicin in the MIA PaCa-2 pancreatic xenograft model. *International Journal of Pharmaceutics* **2013**, *441*, 499-506.

96. Pulaski, B.A.; Ostrand-Rosenberg, S. Mouse 4T1 Breast Tumor Model. *Current Protocols in Immunology* **2001**, *39*, 20.2.1-20.2.16.

97. Tao, K.; Fang, M.; Alroy, J.; Sahagian, G.G. Imagable 4T1 model for the study of late stage breast cancer. *BMC Cancer* **2008**, *8*, 228-46.

98. Etrych, T.; Sirova, M.; Starovoytova, L.; Rihova, B.; Ulbrich, K. HPMA Copolymer Conjugates of Paclitaxel and Docetaxel with pH-Controlled Drug Release. *Molecular Pharmaceutics* **2010**, *7*, 1015-26.

99. Liu, Z.; Chen, K.; Davis, C.; Sherlock, S.; Cao, Q.; Chen, X.; Dai, H. Drug delivery with carbon nanotubes for in vivo cancer treatment. *Cancer Research* **2008**, *68*, 6652-60.

100. Paraskar, A.; Soni, S.; Basu, S.; Amarasiriwardena, C.J.; Lupoli, N.; Srivats, S.; Roy, R.S.; Sengupta, S. Rationally engineered polymeric cisplatin nanoparticles for improved antitumor efficacy. *Nanotechnology* **2011**, *22*, 265101.

101. Paraskar, A.S.; Soni, S.; Chin, K.T.; Chaudhuri, P.; Muto, K.W.; Berkowitz, J.; Handlogten, M.W.; Alves, N.J.; Bilgicer, B.; Dinulescu, D.M.; Mashelkar, R.A.; Sengupta, S. Harnessing structure-activity relationship to engineer a cisplatin nanoparticle for enhanced antitumor efficacy. *Proceedings of the National Academy of Sciences USA* **2010**, *107*, 12435-40.

102. Kiew, L.V.; Cheong, S.K.; Ramli, E.; Sidik, K.; Lim, T.M.; Chung, L.Y. Efficacy of Poly-L-Glutamic Acid-Gemcitabine Conjugate in Tumor-Bearing Mice. *Drug Developement Research* **2012**, *73*, 120-9.

103. Zhou, L.; Cheng, R.; Tao, H.; Ma, S.; Guo, W.; Meng, F.; Liu, H.; Liu, Z.; Zhong, Z. Endosomal pH-Activatable Poly(ethylene oxide)-graft-Doxorubicin Prodrugs: Synthesis Drug Release, and Biodistribution in Tumor-Bearing Mice. *Biomacromolecules* **2011**, *12*, 1460-7.

104. Gao, Z.-G.; Tian, L.; Park, I.-S.; Bae, Y.H. Prevention of metastasis in 4T1 murine breast cancer model by doxorubicin carried by folate conjugated pH sensitive polymeric micelles. *Journal of Controlled Release* **2011**, *152*, 84-9.

105. Hilmer, S.N.; Cogger, V.C.; Muller, M.; Le Couteur, D.G. The hepatic pharmacokinetics of doxorubicin and liposomal doxorubicin. *Drug Metabolism and Disposition* **2004**, *32*, 794-9.

CHAPTER 4

PROMOTING CELL ADHESION ON SLIPPERY PHOSPHORYLCHOLINE HYDROGEL SURFACES

4.1 Introduction

Hydrogels are three-dimensional cross-linked polymeric materials capable of absorbing and retaining large amounts of water. This "water-rich" environment makes hydrogels suitable for biological applications, while the mechanical tunability of the polymer component gives substantial breadth to these materials. Hydrogels from both natural and synthetic polymers are of interest for drug delivery,[1-4] sensors[5-7] and tissue engineering,[8-11] where tuning the chemistry tailors the materials towards desired applications. Synthetic polymer hydrogels are commonly prepared by conventional free radical polymerization, in which a small percentage of difunctional monomer leads to cross-linking. Newer gelation methods have been developed with the advent of "click chemistry",[12] for example exploiting copper-catalyzed azide-alkyne cycloaddition[13,14] and thiol-ene reactions.[15,16]

Synthetic polymers commonly utilized as hydrogels for biomaterials include poly(ethylene glycol),[17-20] poly(hydroxyethyl methacrylate),[21,22] poly(vinyl alcohol),[23,24] and poly(acrylamide).[25,26] Phosphorylcholine (PC)-based polymers are of growing interest as biomaterials, since the zwitterionic pendent groups in these polymers impart exceptional hydrophilicity and biocompatibility. PC-polymer hydrogel membranes were introduced by Nakabayashi and coworkers,[27] consisting of a copolymer of 2-methacryloyloxyethyl phosphorylcholine (MPC) and n-butyl methacrylate. Additional examples include MPC hydrogels prepared by conventional radical polymerization with

various difunctional cross-linkers,[28] a novel PC-dimethacrylate cross-linker that produces cross-linked MPC hydrogels,[29,30] degradable PC hydrogels containing phosphoester linkages,[31] PC hydrogels that gel by hydrogen bonding interactions,[32] a boronic acid-containing PC copolymer hydrogel for 3-D cell encapsulation,[33] and our prior work on PEG-PC hydrogels with tunable mechanical properties.[34] PC-based hydrogels are also used in contact lenses, with several examples of siloxane-containing PC hydrogels reported.[35-37] This thesis sought to improve upon the PC-polymer scaffold by exploiting new chemistries and mild gelation conditions, while promoting cell interactions with these conventionally non-adherent ('slippery') biomaterials, making them attractive for future applications in 3-dimensional cell culture.

The new MPC-containing polymers reported in this thesis work utilize a lipoic acid-containing methacrylate and a GRGDS (glycine-arginine-glycine-aspartic acid-serine) substituted methacrylamide for copolymerization with MPC. Incorporation of the lipoic acid comonomer gives access to dihydrolipoic acid (DHLA) moieties in the polymer structure, which allows for facile post-polymerization cross-linking with poly(ethylene glycol)diacrylate (PEGDA) by Michael addition between the alkenes and the thiols of DHLA, precluding the need for initiators or other additives. The reaction of thiols with the electron-deficient olefins of acrylates occurs rapidly at slightly basic pH, and we observed fast hydrogel formation (<10 minutes) from these components. The GRGDS peptide, a minimal cell adhesion sequence found in extracellular matrix (ECM) proteins, permits mammalian cell attachment to the ECM by cell adhesion receptors (integrins).[38] Using C_2C_{12} and SKOV3 cells, known to express RGD interacting $\alpha_5\beta_1$ and $\alpha_v\beta_3$ integrins,[39-41] we demonstrate that the incorporation of the GRGDS peptide sequence

into the hydrogel permits specific cell adhesion,[42] with a notable effect of peptide concentration on cell attachment, spreading and proliferation (Journal of Materials Chemistry B, 2014).[43]

4.2 Synthesis of cross-linkable polyMPC for hydrogels

Phosphorylcholine (PC)-based hydrogel precursor polymers were prepared according to Scheme 4.1, by incorporating monomer **51** into random copolymer structures, providing a synthetic handle for efficient cross-linking. Esterification of 2-hydroxyethyl methacrylate (HEMA) with lipoic acid (LA), using EDC coupling, gave HEMA-LA monomer **51** as a yellow oil.[44] Compound **51** was characterized by ^{1}H NMR spectroscopy, specifically noting the vinyl protons at 5.4 and 6.1 ppm, and the characteristic signals from the lipoic acid moiety in the alkyl region of the spectrum (~2.5 ppm). A GRGDS-containing methacrylic monomer was prepared by Fmoc-protected solid phase peptide synthesis (SPPS) for the purpose of promoting cell adhesion and enhancing the utility of these PC-containing hydrogels as biomaterials. GRGDS methacrylamide **63** was prepared on a 2-chlorotrityl chloride resin, by coupling with serine, followed by reactions with aspartic acid, glycine, arginine and glycine. The final glycine coupling was followed by an N-Fmoc-amidocaproic acid linker, then capped with methacrylic acid. Simultaneous side-chain deprotection and resin-cleavage, using a solution of trifluoroacetic acid/H$_2$O/triisopropylsilane, gave GRGDS-methacrylamide monomer **63** as a white solid in 50 % yield after precipitation from ether. The structure of the GRGDS monomer was confirmed by ^{1}H and ^{13}C NMR spectroscopy, as well as electrospray ionization mass spectrometry (calculated: 672.3, found, 672.4).
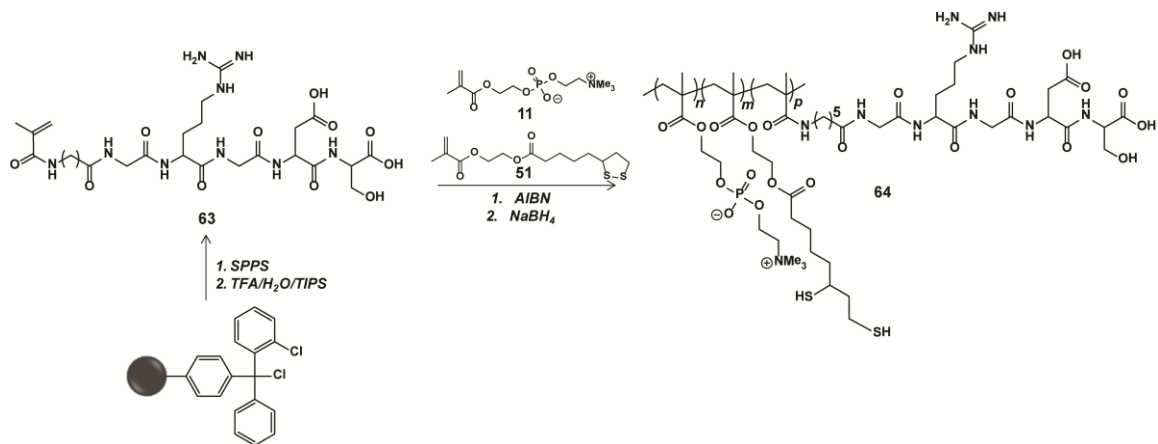
Scheme 4.1 Synthesis of GRGDS-methacrylamide **63** by solid phase peptide synthesis and copolymerization with MPC and HEMA-LA to give copolymer **64**.

Copolymerization of MPC, HEMA-LA, and GRGDS-MA was carried out using conventional free radical polymerization with azobisisobutyrylnitrile (AIBN) as the initiator in a methanol/dimethylsulfoxide solution at 65 °C (Scheme 4.1). Monomer conversion generally reached >95 % within 4 hours, as judged by ^{1}H NMR spectroscopy, comparing the integration of the monomer vinyl peaks at 5.4 and 6.1 ppm with the polymer backbone methyl protons at 1.0 ppm. The copolymers were precipitated from THF, and further purified by passing over a short silica column eluting with methanol. The lipoic acid-containing copolymers were reduced to the free thiol form with $NaBH_4$ in water (4 molar equivalents relative to lipoic acid). The reaction was complete in 2 hours, at which point the solution pH was adjusted to ~3 with $HCl_{(conc)}$. Purification by dialysis (MWCO 1000) followed by lyophilization afforded copolymer **64**, poly(MPC-*co*-DHLA-*co*-GRGDS), as a white solid in 80 % yield. The polymers were characterized by aqueous gel permeation chromatography (GPC) (0.1 M $NaNO_3$ + 0.02 wt % NaN_3) relative to linear poly(ethylene oxide) standards, giving number-average molecular weights ranging from 40 to 65 kDa, with molecular weight distributions typical of free radical polymerization (Figure 4.1). DHLA incorporation (~20-30 mole percent) was

characterized by ^{1}H NMR spectroscopy, and found to match closely with comonomer feed ratio, shown in Table 4.1. GRGDS content was adjusted from 0.25 to 5 mole percent by changing the feed ratio of the GRGDS-methacrylamide. While precise quantification of oligopeptide incorporation is difficult to perform spectroscopically, quantitative monomer conversion (as confirmed by ^{1}H NMR spectroscopy) suggested that the target copolymer composition was achieved. The copolymers maintained good water solubility (>100 mg/mL) even at relatively high DHLA content and at high molecular weight, highlighting the exceptional hydrophilicity of the phosphorylcholine moiety and its ability to solubilize these multifunctional copolymers.
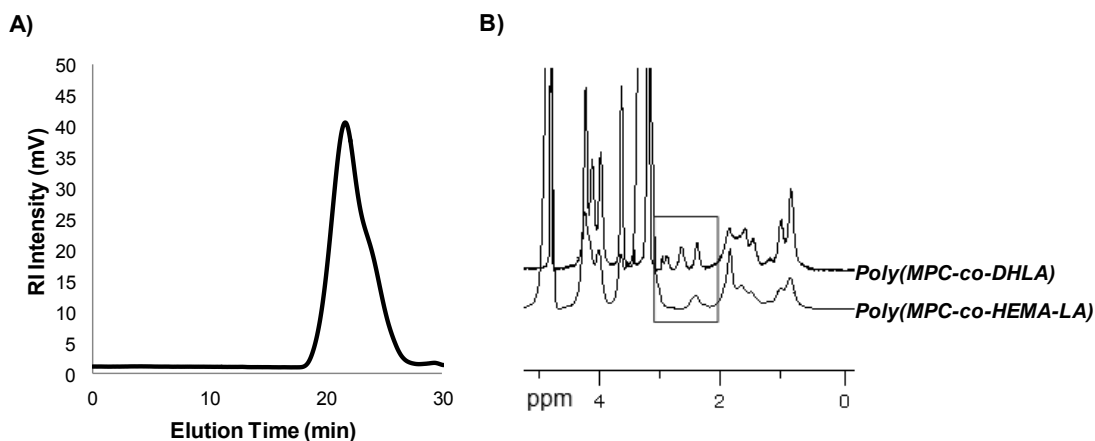
Figure 4.1 A) Aqueous GPC and B) ^{1}H NMR spectroscopy (in MeOD) of poly(MPC-*co*-DHLA).

Table 4.1 Summary of polymerization results for poly(MPC-*co*-DHLA-*co*-GRGDS).

Sample	Theoretical MW (g/mole)	M_n (g/mole)	PDI	% DHLA	% GRGDS
64A	14,500	64,200	4.4	21 %	0 %
64B	12,300	48,100	5.2	24 %	0.25 %
64C	12,500	54,400	4.6	29 %	1 %
64D	13,400	42,200	4.7	27 %	5 %

4.3 Preparation of polyMPC hydrogels by Michael addition

Hydrogels containing polymer **64** formed readily under slightly basic conditions (pH 9 sodium borate buffer), using PEGDA as a difunctional cross-linker in a 1:1 molar ratio of thiol:acrylate (Scheme 4.2). We emphasize that the PC-polymers allow for simple, initiator-free gelation in a completely aqueous environment, in contrast to many hydrogels that require external initiators, and sometimes organic solvents, which must be removed prior to their use in a biological setting. Upon addition of PEGDA to DHLA-containing polyMPC, gelation in pH 9 buffer occurred in <10 minutes at 37 °C. We note that no gelation was observed in the absence of PEGDA, confirming cross-linking occurs by Michael addition and not interchain disulfide formation of polyMPC-*co*-DHLA.
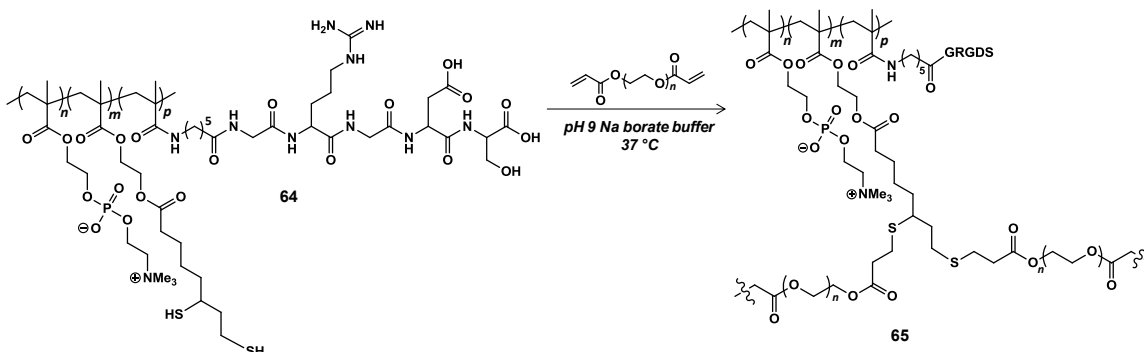
Scheme 4.2 Preparation of hydrogels, represented as polymer **65**, by mixing PEGDA at 37 °C in pH 9 sodium borate buffer.

The equilibrium water content (EWC) of the hydrogels was analyzed by soaking the gels in water to equilibrate the swollen state, and remove any uncross-linked material. After three days, excess water was removed and the weight of the swollen hydrogel was compared to that of the dried hydrogel. These polyMPC hydrogels are very water-rich (>90 % water by weight), with no significant EWC variation observed for samples prepared from PEGDA cross-linkers of different molecular weight, and having different GRGDS peptide content (Figure 4.2). The water uptake of PC hydrogels is much higher

than that of many PEG-based examples,[4,10,19] highlighting the exceptional properties of the PC zwitterion.
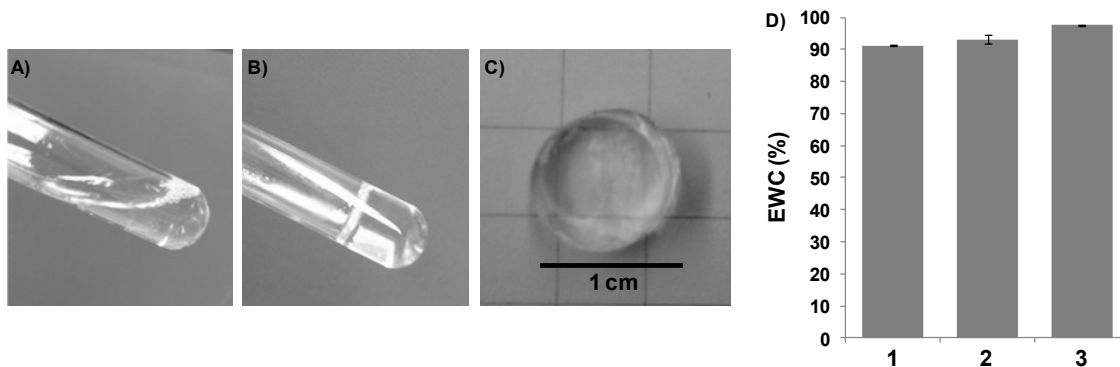
Figure 4.2 PolyMPC-*co*-DHLA and PEG$_{2000}$DA: (A) before gelation and (B) hydrogel formation after 10 minutes of heating at 37 °C. Hydrogels were cut into 1 cm disks (C) and used to analyze equilibrium water content (EWC, %). (D) EWC of polyMPC hydrogels: (1) hydrogel cross-linked with PEG$_{700}$DA (91.3 ± 0.2 %); (2) hydrogel cross-linked with PEG$_{2000}$DA (93.2 ± 1.5 %); (3) GRGDS-containing hydrogel cross-linked with PEG$_{2000}$DA (97.6 ± 0.2 %). Samples were measured in triplicate and error bars represent ± standard deviation.

Dynamic mechanical analysis (DMA) and shear rheology were used to probe the mechanical properties of swollen hydrogels (Figure 4.3). After swelling for 48 hours, a test of the frequency response using DMA was performed, showing a constant elastic modulus (G') of 2.95 ± 0.16 kPa throughout the measured frequency range, with the elastic modulus always greater than the loss modulus (G''; 0.27 ± 0.16 kPa). Furthermore, rheology experiments indicated the potential for mechanical tunability of this system: as expected, increasing polymer concentration or molecular weight led to greater elastic modulus of the resulting hydrogels, illustrating the range of physical/mechanical properties accessible through this materials chemistry.

101
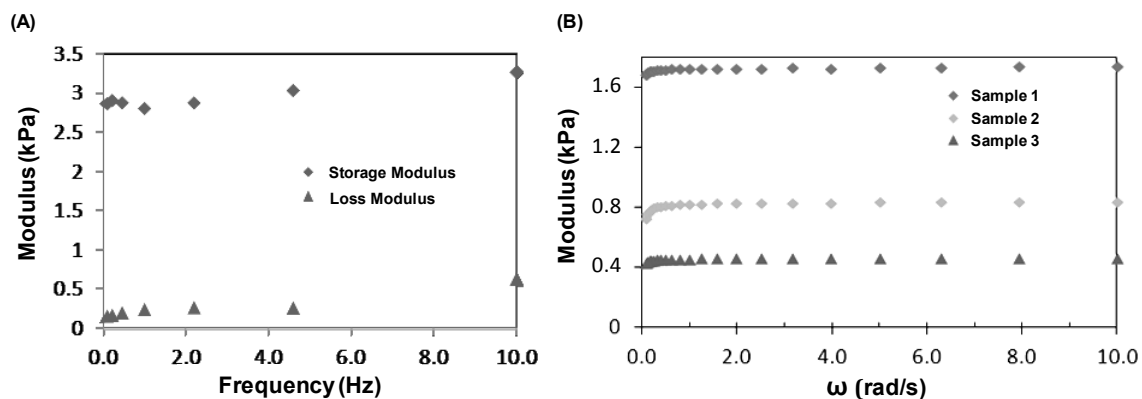
Figure 4.3 (A) Dynamic mechanical analysis (DMA) frequency response experiment of hydrogels prepared from polyMPC-*co*-DHLA (100 mg/mL), cross-linked with PEG$_{700}$DA. (B) Shear rheology experiments demonstrate the effect of varying polymer component molecular weights on the elastic modulus (G'). Sample 1: polyMPC-*co*-DHLA (60 kDa) with PEG$_{6000}$DA; Sample 2: polyMPC-*co*-DHLA (25 kDa) with PEG$_{6000}$DA; Sample 3: polyMPC-*co*-DHLA (25 kDa) with PEG$_{700}$DA.

4.4 In vitro cell culture: Evaluating cell adhesion

We next examined the influence of the GRGDS sequence on polymer-cell interactions, using hydrogels prepared in 24-well tissue culture plates. Stock solutions of both polymer and cross-linker were prepared in pH 9 sodium borate buffer, then mixed in the plate at a 1:1 ratio of [SH]:[acrylate], with a final polyMPC concentration of 50 mg/mL. The plate was incubated at 37 °C for 20 minutes to ensure effective gelation. The resulting hydrogels were washed/exchanged with PBS to remove the borate buffer. The hydrogels were then washed twice in sterile cell culture growth medium, and incubated for 2 hours at 37 °C in 5 % CO_2 to remove residual PBS and reduce non-specific cell binding. The media was aspirated and the surface of the hydrogel seeded with C_2C_{12} or SKOV3 cells, followed by incubation at 37 °C; cell adhesion was visualized using optical microscopy (Figure 4.4). Notably, cells seeded on polyMPC hydrogels lacking the GRGDS peptide failed to attach, and at 24 hours were aggregated in the media above the hydrogel, as seen in Figure 4.4A-B. In contrast, hydrogels

functionalized with the GRGDS peptide sequence showed cell spreading and proliferation on the hydrogel surface, similar to the control (polystyrene tissue culture plate), with no floating cells observed (Figure 4.4C-H). C_2C_{12} cells adhered to these hydrogels relatively quickly (<6 hours), while SKOV3 cells adhered within 24 hours. Increasing cell density was observed upon increasing GRGDS content from 0.25 % to 1 % to 5 % (corresponding to 0.4, 1.6, and 7 mM bulk GRGDS, respectively). Hydrogels prepared from copolymer **64D**, containing 5 % GRGDS, showed excellent cell spreading and density, comparable to the polystyrene controls.
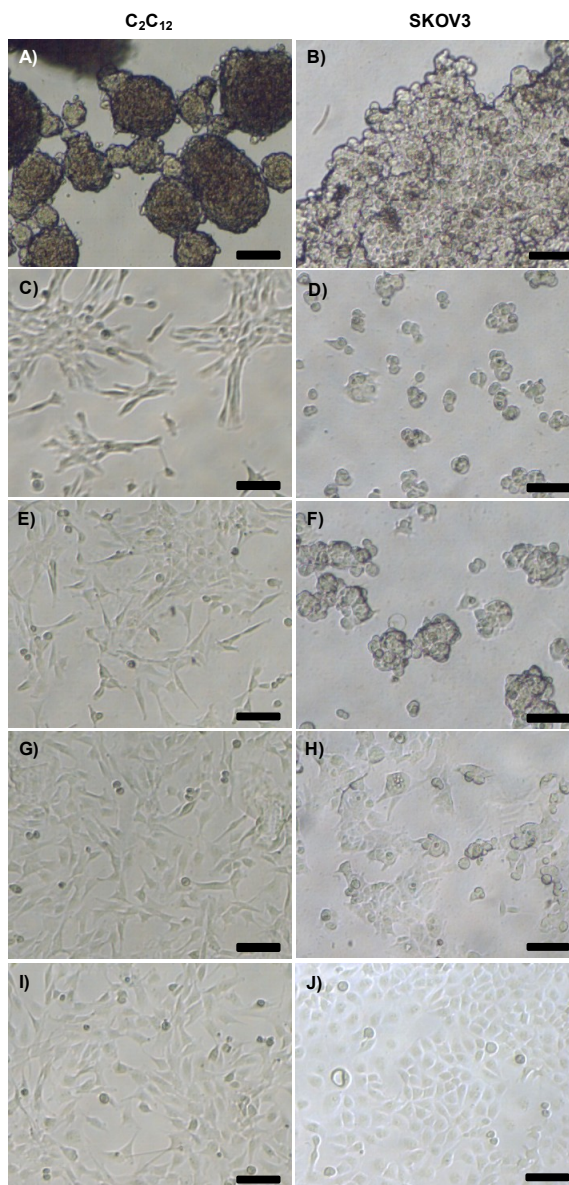
Figure 4.4 Optical micrographs of C_2C_{12} and SKOV3 cells after 24 hours incubation on hydrogels from polymers containing (A-B) no GRGDS, (C-D) 0.25 % GRGDS, (E-F) 1 % GRGDS, (G-H) 5 % GRGDS, and on (I-J) polystyrene tissue culture plate. Scale bar = 100 μm.

Cell density was quantified using the CellTiter-Glo Luminescent Cell Viability Assay (Promega) 24 hours post cell-seeding. The cell density measured for each hydrogel is given as a percentage of the polystyrene control. For both C_2C_{12} and SKOV3 cells, the density tracked with GRGDS peptide content. This is shown in the graph of

104

Figure 4.5, in which cell density increased as a function of peptide incorporation, from <50 % for 0.25 % peptide, to >90 % for 5 % peptide. The relative difference in cell densities 24 hours after seeding confirms that the hydrogel surface permits cell proliferation in addition to attachment, and that the GRGDS oligopeptide in the hydrogel interacts with the cellular integrins.
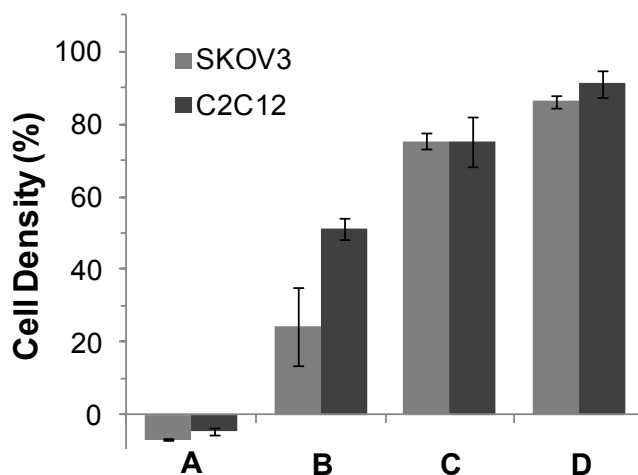
Figure 4.5 Quantification of cell adhesion after 24 hours for C_2C_{12} and SKOV3 cells, expressed as percent cell density, on hydrogels containing no GRGDS (A), 0.25 % GRGDS (B), 1 % GRGDS (C), and 5 % GRGDS (D), relative to the cell density in the control (polystyrene tissue culture plate). Error bars indicate ± standard deviation.

4.5 Summary and future outlook

In summary, the synthesis of thiol-containing PC-polymers based on the polymerization of MPC and HEMA-LA was described, with incorporation of GRGDS-MA for cellular recognition. These polymers rapidly form hydrogels by Michael addition to PEGDA in an initiator-free system at 37 °C in pH 9 buffer leaving no residual initiators/additives after hydrogel formation. Mechanical properties testing suggests the hydrogels as ideal materials for biological assays, capable of mimicking soft tissues or tumor environments. PolyMPC and polyMPC-hydrogels, despite their excellent

biocompatibility, are incapable of cell adhesion/proliferation on the hydrogel surface, while hydrogels containing variable percentages of GRGDS promote cell adhesion and proliferation, demonstrated using C_2C_{12} and SKOV3 cells. Equipping these traditionally 'slippery' PC-polymers with such pronounced cell adhesion properties broadens the scope of functional biomaterials available for developing more sophisticated *in vitro* and *in vivo* applications.

4.6 References

1.   Zhao, X.; Harris, J. Novel degradable poly(ethylene glycol) hydrogels for controlled release of protein. *Journal of Pharmaceutical Sciences* **1998**, *87*, 1450–8.

2.   van de Wetering, P.; Metters, A.; Schoenmakers, R.; Hubbell, J. Poly(ethylene glycol) hydrogels formed by conjugate addition with controllable swelling, degradation, and release of pharmaceutically active proteins. *Journal of Controlled Release* **2005**, *102*, 619–27.

3.   Gupta, K.; Barnes, S.; Tangaro, R.; Roberts, M.; Owen, D.; Katz, D.; Kiser, P. Temperature and pH sensitive hydrogels: an approach towards smart semen-triggered vaginal microbicidal vehicles. *Journal of Pharmaceutical Sciences* **2007**, *96*, 670–81.

4.   Salmaso, S.; Semenzato, A.; Bersani, S.; Matricardi, P.; Rossi, F.; Caliceti, P. Cyclodextrin/PEG based hydrogels for multi-drug delivery. *International Journal of Pharmaceutics* **2007**, *345*, 42–50.

5.   Han, I.; Han, M.-H.; Kim, J.; Lew, S.; Lee, Y.; Horkay, F.; Magda, J. Constant-volume hydrogel osmometer: a new device concept for miniature biosensors. *Biomacromolecules* **2001**, *3*, 1271–5.

6.   Rubina, A.; Pan'kov, S.; Dementieva, E.; Pen'kov, D.; Butygin, A.; Vasiliskov, V.; Chudinov, A.; Mikheikin, A.; Mikhailovich, V.; Mirzabekov, A. Hydrogel drop microchips with immobilized DNA: properties and methods for large-scale production. *Analytical Biochemistry* **2004**, *325*, 92–106.

7.   Ehrick, J.; Deo, S.; Browning, T.; Bachas, L.; Madou, M.; Daunert, S. Genetically engineered protein in hydrogels tailors stimuli-responsive characteristics. *Nature Materials* **2005**, *4*, 298–302.

8.   Lee, K.; Mooney, D. Hydrogels for tissue engineering. *Chemical Reviews* **2001**, *101*, 1869–79.

9. Burdick, J.; Anseth, K. Photoencapsulation of osteoblasts in injectable RGD-modified PEG hydrogels for bone tissue engineering. *Biomaterials* **2002**, *23*, 4315–23.

10. Lutolf, M.; Hubbell, J. Synthetic biomaterials as instructive extracellular microenvironments for morphogenesis in tissue engineering. *Nature Biotechnology* **2004**, *23*, 47–55.

11. Zhu, J. Bioactive modification of poly(ethylene glycol) hydrogels for tissue engineering. *Biomaterials* **2010**, *31*, 4639–56.

12. Yigit, S.; Sanyal, R.; Sanyal, A. Fabrication and functionalization of hydrogels through "click" chemistry. *Chemistry, an Asian Journal* **2011**, *6*, 2648–59.

13. Malkoch, M.; Vestberg, R.; Gupta, N.; Mespouille, L.; Dubois, P.; Mason, A.; Hedrick, J.; Liao, Q.; Frank, C.; Kingsbury, K.; Hawker, C. Synthesis of well-defined hydrogel networks using click chemistry. *Chemical Communications* **2006**, *26*, 2774–6.

14. Ossipov, D. A.; Hilborn, J. Poly(vinyl alcohol)-Based Hydrogels Formed by "Click Chemistry." *Macromolecules* **2006**, *39*, 1709-1718.

15. Lowe, A. B.; Hoyle, C. E.; Bowman, C. N. Thiol-yne click chemistry: A powerful and versatile methodology for materials synthesis. *Journal of Materials Chemistry* **2010**, *20*, 4745-50.

16. Yang, T.; Long, H.; Malkoch, M.; Gamstedt, E. K.; Berglund, L.; Hult, A. Characterization of well-defined poly(ethylene glycol) hydrogels prepared by thiol-ene chemistry. *Journal of Polymer Science Part A: Polymer Chemistry* **2011**, *49*, 4044-54.

17. Cruise, G.; Scharp, D.; Hubbell, J. Characterization of permeability and network structure of interfacially photopolymerized poly(ethylene glycol) diacrylate hydrogels. *Biomaterials* **1998**, *19*, 1287–94.

18. Metters, A.; Anseth, K.S.; Bowman, C.N. Fundamental studies of a novel, biodegradable PEG-b-PLA hydrogel. *Polymer* **2000**, *41*, 3993-4004.

19. Peyton, S.; Raub, C.; Keschrumrus, V.; Putnam, A. The use of poly(ethylene glycol) hydrogels to investigate the impact of ECM chemistry and mechanics on smooth muscle cells. *Biomaterials* **2006**, *27*, 4881–93.

20. Lin, C.-C.; Anseth, K. PEG hydrogels for the controlled release of biomolecules in regenerative medicine. *Pharmaceutical research* **2009**, *26*, 631–43.

21. Wichterle, O.; Lím, D. Hydrophilic Gels for Biological Use. *Nature* **1960**, *185*, 117-118.

22. Bryant, S.; Cuy, J.; Hauch, K.; Ratner, B. Photo-patterning of porous hydrogels for tissue engineering. *Biomaterials* **2007**, *28*, 2978–86.

23. Cascone, M. G.; Laus, M.; Ricci, D.; Guerra, R. S. D. Evaluation of poly(vinyl alcohol) hydrogels as a component of hybrid artificial tissues. *Journal of Materials Science: Materials in Medicine* **1995**, *6*, 71-5.

24. Nuttelman, C. R.; Mortisen, D. J.; Henry, S. M.; Anseth, K. S. Attachment of fibronectin to poly(vinyl alcohol) hydrogels promotes NIH3T3 cell adhesion, proliferation, and migration. *Journal of Biomedical Materials Research* **2001**, *57*, 217-23.

25. Stile, R. A.; Burghardt, W. R.; Healy, K. E. Synthesis and Characterization of Injectable Poly(N -isopropylacrylamide)-Based Hydrogels That Support Tissue Formation in Vitro. *Macromolecules* **1999**, *32*, 7370-79.

26. Trappmann, B.; Gautrot, J.; Connelly, J.; Strange, D.; Li, Y.; Oyen, M.; Cohen Stuart, M.; Boehm, H.; Li, B.; Vogel, V.; Spatz, J.; Watt, F.; Huck, W. Extracellular-matrix tethering regulates stem-cell fate. *Nature Materials* **2012**, *11*, 642–9.

27. Ishihara, K.; Ueda, T.; Nakabayashi, N. Preparation of phospholipid polymers and their properties as polymer hydrogel membranes. *Polymer Journal* **1990**, *22*, 355-60.

28. Kiritoshi, Y.; Ishihara, K. Preparation of cross-linked biocompatible poly(2-methacryloyloxyethyl phosphorylcholine) gel and its strange swelling behavior in water/ethanol mixture. *Journal of Biomaterials Science. Polymer edition* **2001**, *13*, 213–24.

29. Kiritoshi, Y.; Ishihara, K. Synthesis of hydrophilic cross-linker having phosphorylcholine-like linkage for improvement of hydrogel properties. *Polymer* **2004**, *45*, 7499-7504.

30. Goda, T.; Furukawa, H.; Gong, J. P.; Ishihara, K. Relaxation modes in chemically cross-linked poly(2-methacryloyloxyethyl phosphorylcholine) hydrogels. *Soft Matter* **2013**, *9*, 2166-2171.

31. Wachiralarpphaithoon, C.; Iwasaki, Y.; Akiyoshi, K. Enzyme-degradable phosphorylcholine porous hydrogels cross-linked with polyphosphoesters for cell matrices. *Biomaterials* **2007**, *28*, 984–93.

32. Kimura, M.; Fukumoto, K.; Watanabe, J.; Takai, M.; Ishihara, K. Spontaneously forming hydrogel from water-soluble random- and block-type phospholipid polymers. *Biomaterials* **2005**, *26*, 6853–62.

33. Xu, Y.; Jang, K.; Konno, T.; Ishihara, K.; Mawatari, K.; Kitamori, T. The biological performance of cell-containing phospholipid polymer hydrogels in bulk and microscale form. *Biomaterials* **2010**, *31*, 8839–46.

34. Herrick, W.; Nguyen, T.; Sleiman, M.; McRae, S.; Emrick, T.; Peyton, S. PEG-Phosphorylcholine Hydrogels As Tunable and Versatile Platforms for Mechanobiology. *Biomacromolecules* **2013**, *14*, 2294–304.

35. Court, J.; Redman, R.; Wang, J.; Leppard, S.; Obyrne, V.; Small, S.; Lewis, A.; Jones, S.; Stratford, P. A novel phosphorylcholine-coated contact lens for extended wear use. *Biomaterials* **2001**, *22*, 3261–72.

36. Shimizu, T.; Goda, T.; Minoura, N.; Takai, M.; Ishihara, K. Super-hydrophilic silicone hydrogels with interpenetrating poly(2-methacryloyloxyethyl phosphorylcholine) networks. *Biomaterials* **2010**, *31*, 3274–80.

37. Li, L.; Wang, J.-H.; Xin, Z. Synthesis and biocompatibility of a novel silicone hydrogel containing phosphorylcholine. *European Polymer Journal* **2011**, *47*, 1795-1803.

38. Barckyz, M.; Carracedo, S.; Gullberg, D. Integrins. *Cell Tissue Research* **2010**, *339*, 269-80.

39. Glenn, H.; Wang, Z.; Schwartz, L. Acheron, a Lupus antigen family member, regulates integrin expression, adhesion, and motility in differentiating myoblasts. *American journal of physiology. Cell Physiology* **2009**, *298*, C46–55.

40. Casey, R.; Skubitz, A. CD44 and beta1 integrins mediate ovarian carcinoma cell migration toward extracellular matrix proteins. *Clinical and Experimental Metastasis* **1999**, *18*, 67–75.

41. Vaz, R.; Martins, G.; Thorsteinsdóttir, S.; Rodrigues, G. Fibronectin promotes migration, alignment and fusion in an in vitro myoblast cell model. *Cell and Tissue Research* **2012**, *348*, 569–78.

42. Hersel, U.; Dahmen, C.; Kessler, H. RGD modified polymers: biomaterials for stimulated cell adhesion and beyond. *Biomaterials* **2003**, *24*, 4385–415.

43. Page, S.M.; Parelkar, S.; Gerasimenko, A.; Shin, D.Y.; Peyton, S.; Emrick, T. Promoting Cell Adhesion on Slippery Phosphorylcholine Hydrogel Surfaces. *Journal of Materials Chemistry B* **2014**, 2, 620-624.

44. Chen, X.; Lawrence, J.; Parelkar, S.; Emrick, T. Novel Zwitterionic Copolymers with Dihydrolipoic Acid: Synthesis and Preparation of Nonfouling Nanorods. *Macromolecules* **2013**, *46*, 119-127.

CHAPTER 5

EXPERIMENTAL SECTION

5.1 Materials

Pentafluorophenol, 4-(dimethylamino)pyridine (DMAP), triethylamine (TEA), *N*-(3-dimethylaminopropyl)-*N*´-ethylcarbodiimide hydrochloride (EDC), 2-bromoisobutyryl bromide, copper(I) bromide, 2,2´-bipyridine (bpy), bis-hydroxymethyl propionic acid, oxalyl chloride, bis(pentafluorophenyl) carbonate, Grubbs' generation II catalyst, ethyl vinyl ether, pyridine, lysozyme from hen egg white, 2-hydroxyethylmethacrylate (HEMA), N-boc-aminooxy acetic acid, levulinic acid, ethylene glycol, trifluoroacetic acid, methanol (anhydrous), dimethylsulfoxide (anhydrous), 4-hydroxybenzaldehyde, sodium azide, *N,N*´-diisopropylethylamine (DIPEA), 2-bromopropionyl bromide, 6-bromohexanoic acid, 2-[2-(2-chloroethoxy)ethoxy]ethanol, ethyl 2-bromoisobutyrate, 3-(trimethylsilyl)propargyl alcohol, methacryloyl chloride, mouse serum, human plasma, lipoic acid, 3-mercaptopropionic acid, 2,2'-dithiodipyridine, 4-cyano-4-(phenylcarbonothioylthio)pentanoic acid, 4,4'-azobis(4-cyanovaleric acid) (ACVA), ethyl bromoacetate, hydrazine monohydrate, acetic acid, magnesium sulfate, acetonitrile (anhydrous), methacrylic acid, Fmoc-chloride, 6-aminocaproic acid, triisopropylsilane (TIPS), poly(ethylene glycol) diacrylate (M_n 6,000, 2,000 and 700), and dimethylformamide (anhydrous) were purchased from Aldrich. 2-Methacryloyloxyethyl phosphorylcholine (MPC) was purchased from Aldrich or synthesized according to literature procedures. MPC purchased from Sigma Aldrich was washed with anhydrous ether prior to use. Oxalyl chloride and 1-ethyl-3-(3-dimethylaminopropyl)carbodiimide) (EDC) were purchased from TCI America. Ethylene chlorophosphate (COP) was

purchased from Alfa Aesar. Camptothecin (CPT) and doxorubicin (DOX) were purchased from 21CEC. HEMA and COP were purified by Kugelrohr distillation prior to use. Dichloromethane and triethylamine were distilled over calcium hydride and tetrahydrofuran was dried over sodium/benzophenone ketyl and freshly distilled before use. All other chemicals were used as received unless otherwise noted. EnzChek® Lysozyme Assay Kit and Alexa Fluor 647 dye were purchased from Invitrogen. Pre-stained broad-range protein standards, 4-15 % Mini-Protean TGX precast gels, and Bio-Safe Coomassie stain were purchased from BioRad. Human colorectal (COLO205) and breast (MCF7) adenocarcinoma cells were purchased from American Type Culture Collection (ATCC). RPMI 1640 and MEM cell culture media were purchased from Life Technologies and Mediatech, respectively. Fetal bovine serum (FBS) was purchased from Atlanta Biologicals and bovine insulin from Aldrich. Cell viability was measured using CellTiter-Glo luminescent cell viability assay from Promega. Dialysis cassettes (MWCO 3,500; total volume 0.5-3 mL) were purchased from Fisher Scientific and hydrated in water prior to use. Spectra/Por 3 dialysis membrane (MWCO 1000) was purchased from Spectrum Laboratories, Inc. Sephadex (LH-20 and G-25) was purchased from GE Life Sciences and swelled for 24 hours prior to use. Hank's Balanced Salt Solution used for *in vivo* studies was obtained from Life Technologies (Gibco).

5.2 Instrumentation

Nuclear magnetic resonance (NMR) spectroscopy was performed on a Brüker Spectrospin DPX300, an Avance 400, or an Agilent 700. Aqueous GPC was performed in 0.1 M sodium nitrate and 0.02 weight percent sodium azide buffer against poly(ethylene oxide) calibration standards, operating at 1.0 mL/ min with three Waters Ultrahydrogel

columns (7.8 x 300 mm) equipped with RI and UV/Vis detectors. GPC in 1,1,1-trifluoroethanol (TFE) (with 0.2 M sodium trifluoroacetate) was performed against poly(methyl methacrylate) (PMMA) standards, operating at 0.75 mL/min at 40 °C with three Agilent PL HFIPgel columns (300 x 7.5 mm) equipped with RI and UV/Vis detectors. UV/Visible spectroscopy was performed on a Perkin-Elmer Lambda 25 spectrometer. Fluorescence measurements were taken on a Perkin-Elmer LS 55 fluorimeter. Dynamic light scattering was performed on a Malvern Zetasizer Nano-ZS. Transmission electron microscopy (TEM) was performed using a TEM JEOL 2000FX with samples prepared on carbon-coated copper grids purchased from Electron Microscopy Sciences. High-resolution mass spectral (HRMS) data were obtained on a JEOL JMS700 MStation. IR absorbance data were obtained on a Perkin-Elmer Spectrum One FT-IR spectrometer equipped with a universal ATR sampling accessory. The HPLC system consisted of a Waters Alliance system with a 2996 photodiode array detector and a 2475 fluorescence detector. A size exclusion column (Shodex KW-803) eluting with 10% ethanol in PBS buffer (pH 7.4) at a flow rate of 1 mL/min was used to analyze protein-polymer conjugate samples. A reverse phase C18 column (250 × 4.6 mm) eluting with a gradient of 5-95% of acetonitrile in 0.05% TFA at a flow rate of 1 mL/min was used to analyze prodrug samples. A reverse phase C18 column (250 × 4.6 mm) eluting with 40% acetonitrile in water + 1% TFA at a flow rate of 1 mL/min was used to analyze biological samples obtained from polyMPC-DOX animal studies. Dynamic rheological properties of hydrogels were analyzed using a Rheometrics Mechanical Spectrometer, performing frequency sweeps from 0-10 Hz on hydrogels in the equilibrium swollen state. Optical microscopy was performed on a Nikon CKX41 inverted microscope and

cell density measured by plate reader in luminescence mode (BMG Labtech FLUOstar OPTIMA plate reader). Size exclusion FPLC was performed on a GE AKTA system using Superose 6 10/300 columns with PBS buffer at a flow rate of 0.5 ml/min, monitoring at 280 nm. Cation exchange FPLC was performed on a GE AKTA system equipped with a Hitrap SP HP 5mL cation exchange column at a flow rate of 5 mL/min.

5.3 Methods

- **Synthesis of 2-(2-oxo-1,3,2-dioxapospholoyloxy)ethyl methacrylate (OPEMA) (10)**
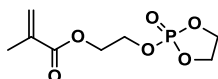
OPEMA was prepared according to literature procedures as described by Nakabayashi and coworkers.[1]
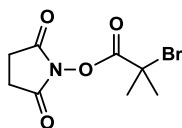
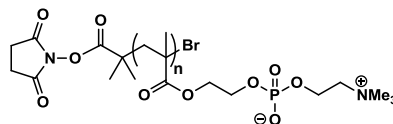- **Synthesis of 2-methacryloyloxyethyl phosphorylcholine (MPC) (11)**
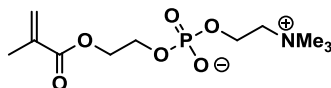
MPC monomer was prepared according to literature procedures, as described by Nakabayashi and coworkers.[1]

- **Synthesis of NHS ATRP initiator (13)**

NHS initiator **13** was prepared according to literature procedures.[2]

- **Synthesis of NHS-polyMPC (14)**

Initiator **13** (13 mg, 0.05 mmol) was dissolved in degassed DMSO (1.5 mL). To this solution, CuBr (7 mg, 0.05) mmol) and 2,2'-bipyridine (15 mg, 0.10 mmol) was added, followed by a solution of MPC monomer (547 mg, 1.85 mmol) in degassed methanol (0.5 mL). The reaction mixture was subjected to three freeze-pump-thaw cycles, then stirred under inert (argon or nitrogen) atmosphere at room temperature for 12 hours. The mixture was eluted through a short column of silica gel, and a colorless solution was recovered. The solution was dried under vacuum, and washed with dry THF (2 mL) to give the desired polymer (190 mg) as a white powder. ^{1}H NMR (400 MHz, CD$_3$OD): δ 0.81-1.33 (br), 1.81-2.22 (br), 2.87 (s), 3.25 (s), 3.69-3.81 (br), 4.04-4.45 (br) ppm; ^{31}P NMR (400 MHz, CD$_3$OD): -0.3 ppm. Gel permeation chromatography, against PEO calibration standards, eluting with 0.1 M aqueous NaNO$_3$ containing 0.2 weight percent NaN$_3$: Mn 8,900, Mp 9,600, Mw 11,600, PDI 1.3.

- **Synthesis of 4-(2-hydroxyethoxy)benzaldehyde (15)**
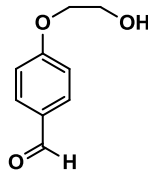
Sodium hydroxide (0.8 g, 20 mmol) was dissolved in 25 mL of H$_2$O in a 2-neck round bottom flask. The solution was stirred vigorousy. 4-Hydroxybenzaldehyde (2.44 g, 20 mmol) was added to the flask in small batches over the course of 15 minutes. 2-Bromoethanol (2.49 g, 20 mmol) was added to the reaction mixture dropwise. The

resulting solution was heated to 98 °C for 30 hours. The reaction was cooled to 10 °C using an ice-water bath, and the pH was adjusted to ~10 using aqueous NaOH. The reaction mixture was then extracted with dichloromethane (4 times, 30 mL each). The organic layers were combined and dried with MgSO$_4$. After filtration, solvent was removed using rotary evaporation. The residue was purified using column chromatography (70 % ethyl acetate/hexanes on silica gel) to afford the purified product as a pale yellow oil (2.23 g, 67 % yield).

- **Synthesis of benzaldehyde ATRP initiator (16)**
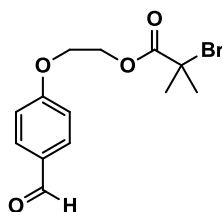
4-(2-hydroxyethoxy) benzaldehyde (0.96 g, 6.0 mmol) was dissolved in CH$_2$Cl$_2$ (13 mL) under nitrogen atmosphere. Triethylamine (0.71 g, 7.0 mmol) was added slowly, and the mixture was cooled to 0°C. A solution of 2-bromoisobutyryl bromide (1.3 g, 5.7 mmol) in CH$_2$Cl$_2$ (4 mL) was added dropwise over the course of 10 minutes. The reaction mixture was then stirred at room temperature for 16 hours. The reaction mixture was filtered, washed twice with saturated aqueous NaHCO$_3$, dried over MgSO$_4$, filtered, then concentrated by rotary evaporation. The crude mixture was purified by column chromatography over silica gel, eluting with ethyl acetate:hexane mixtures, to give the desired product as a yellow oil (650 mg, 59 %). ^{1}H NMR (300MHz, CDCl$_3$): δ 9.7 (s), 7.9 (d), 7.2 (d), 4.5 (t), 4.3 (t), 1.9 (s) ppm; ^{13}C NMR (300MHz, CDCl$_3$): δ 30.67, 55.36, 63.79, 65.77, 114.9, 130.32, 132.05, 163.4, 171.63, 190.85 ppm; HRMS-FAB (m/z): [M]+ calculated 315.02, found 315.0232.

- **Synthesis of benzaldehyde-polyMPC (17)**
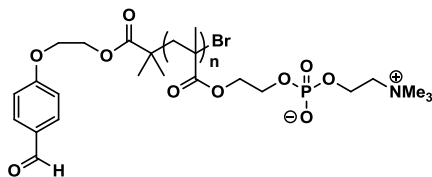
To a stirring solution of initiator **16** (18.8 mg, 0.060 mmol) in DMSO (2 mL) under nitrogen atmosphere was added Cu(I)Br (8.6 mg, 0.06 mmol) and bipyridine (18.7 mg, 0.120 mmol). The mixture was then subjected to two freeze-pump-thaw cycles. A solution of MPC (479.5 mg, 1.62 mmol) in MeOH (1 mL) was then added to the mixture using a degassed syringe. Three freeze-pump-thaw cycles were performed. The reaction mixture was brought to room temperature, and the reaction was stirred for 18 hours. ^{1}H NMR spectroscopy was used to monitor monomer conversion. To remove copper and DMSO, the mixture was purified by column chromatography over silica gel, eluting with methanol. Solvent was removed by rotary evaporation and dried overnight under vacuum yielding a white, crystalline solid (300 mg). ^{1}H NMR (300 MHz, D$_2$O): δ 0.6-1.1 (br), 1.6-2.1 (br), 3.12 (s), 3.57 (s), 3.97 (br), 4.1-4.3 (br), 7.15 (d), 7.91 (d), 9.77 (s) ppm. The polymer was also characterized by aqueous GPC against poly(ethylene oxide) calibration standards, eluting with 0.1 M aqueous NaNO$_3$ containing 0.2 weight percent NaN$_3$: Mn = 7,000, Mp =7,500, Mw = 8,000, PDI = 1.12.

- **Preparation of lysozyme-polyMPC conjugate (18)**
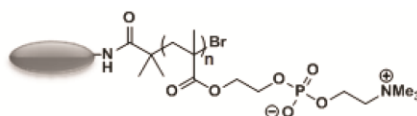
Lysozyme (1 mg, 3.3x10-5 mmol) and polymer **17** (2.5 mg, 3.5x10-4 mmol) was dissolved in 1.5 mL of pH 6 phosphate buffer. The reaction mixture was maintained at

ambient temperature, and gently shaken for 1 hour. NaCNBH$_3$ (20 mg, 0.32 mmol) was then added to the reaction. After 1 day, additional NaCNBH$_3$ (40 mg, 0.63 mmol) was added. The solution was incubated at room temperature with continuous, gentle shaking. The reaction was monitored with SEC-HPLC, using a Shodex KW-804 column and a UV detector set at 280 nm, and with SDS-PAGE.

- **Synthesis of pentafluorophenol ATRP initiator (20)**
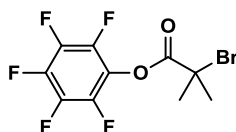
Pentafluorophenol (3.00 g, 16.3 mmol) was dissolved in tetrahydrofuran (30 mL, anhydrous) in a dry 2-neck round bottom flask. Triethylamine (2.50 g, 24.5 mmol) was added to the stirring solution slowly, and the reaction mixture was cooled to 0 °C. 2-Bromoisobutyryl bromide (5.60 g, 24.5 mmol) was added to the reaction mixture dropwise. The mixture was allowed to warm to room temperature, and stirred for 18 hours, then passed through Celite to remove TEA salt, and solvent was removed by rotary evaporation. The residue was redissolved in dichloromethane, and washed with 1M HCl (aq), saturated NaHCO$_3$ (aq), and brine. The organic layers were dried over MgSO$_4$, and filtered, and solvent was removed. The orange liquid obtained was purified by column chromatography over silica gel, eluting with ethyl acetate/hexanes mixture, to obtain the pure product as a colorless liquid (4.0 g, 76 %). ^{1}H NMR (300 MHz, CDCl$_3$): δ = 2.10 (s, 6H); ^{19}F NMR (282 MHz, CDCl$_3$): δ = -152.9 (2F), -157.2 (1F), -162.0 (2F); ^{13}C NMR (75 MHz, CDCl$_3$): δ = 30.5, 52.9, 124.8, 136.1, 138.1, 139.4, 141.4, 142.7, 168.1. HRMS-FAB (*m/z*): calculated: 331.9483, found: 331.9434.

- **Synthesis of PFP-polyMPC (21)**
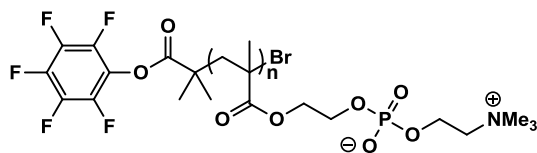
In a dry 2-neck round bottom flask, initiator **20** (8.0 mg, 0.025 mmol) and MPC monomer (500 mg, 1.7 mmol) were dissolved in 1:1 methanol/dimethylsulfoxide (3 mL), and the stirring solution was degassed with nitrogen. Cu(I)Br (4.0 mg, 0.025 mmol) and bipyridine (8.0 mg, 0.05 mmol) were added simultaneously as solids to the reaction flask. The mixture was degassed for 20 minutes by bubbling with dry nitrogen gas, then sealed and let stir at room temperature. Most reactions were run for 8-16 hours, then stopped by exposing the reaction to air to oxidize the catalyst. Polymers were generally purified by a short silica plug eluting with methanol, followed by precipitation into THF or acetone to isolate a white solid (350 mg, 70 % yield). ^{1}H NMR (300 MHz, MeOD): δ = 0.93-1.08 (3H, br), 1.85-2.1 (2H, br), 3.50 (2H, br), 4.04 (2H, br), 4.19 (2H, br), 4.29 (2H, br). ^{31}P NMR (122 MHz, MeOD): δ = 0.0. ^{19}F NMR (282 MHz, CDCl$_3$): δ = -152.8 (2F), -156.8 (1F), -161.6. (2F). Aqueous GPC (0.1 M NaNO$_3$ + 0.02 wt% of NaN$_3$): M_n, 11,700 g/mole; M_w, 15,000 g/mole; PDI, 1.3.

- **Synthesis of carboxylic acid 22**
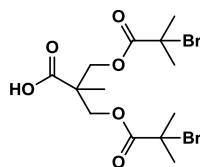
Bis-(MPA) (8.0 g, 60 mmol), pyridine (9 mL), and DMAP (732 mg, 6 mmol) were suspended in dry dichloromethane (30 mL). 2-Bromoisobutyryl bromide (54 g, 29 mL)

was added dropwise. A white solid precipitant was observed. The reaction mixture was stirred for 12 hours, then methanol (100 mL) and glacial acetic acid (2 mL) was added. The reaction mixture was filtered, and the solvent was collected and evaporated. The product was purified by column chromatography using ethyl acetate/hexanes/1 % acetic acid mixtures to afford a white solid (22 g, 38.3 %). ^{1}H NMR (300 MHz, CDCl$_3$): δ = 1.40 (s, 3H), 1.94 (s, 12H), 4.39 (q, 4H); ^{13}C NMR (75 MHz, CDCl$_3$): δ = 17.7, 30.6, 46.5, 55.2, 65.9, 170.9, 178.6. FAB-MS (*m/z*): calculated: 429.96, found: 429.97.

- **Synthesis of acid chloride 23**
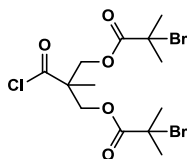
Compound **22** (1.0 g, 2.3 mmol) was dissolved in DCM (10 mL), then cooled to 0 °C with an ice bath. Oxalyl chloride (431 mg, 3.40 mmol) was added dropwise to the stirring solution, then several drops of DMF were added. The mixture was warmed to room temperature, then heated to reflux. After 3 hours, TLC indicated that the reaction was complete, and the solvent was removed under reduced pressure. The isolated product was dried under vacuum, yielding 700 mg of **23** as a colorless oil (70 %). ^{1}H NMR (300 MHz, CDCl$_3$): δ = 1.40 (s, 3H), 1.94 (s, 12H), 4.39 (q, 4H); ^{13}C NMR (700 MHz, CDCl$_3$): δ = 17.7, 30.6, 46.5, 55.2, 65.9, 170.9, 174.8.

- **Synthesis of compound 24**
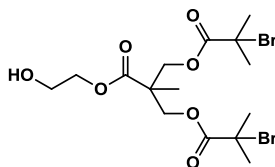
Ethylene glycol (930 mg, 15.0 mmol) was dissolved in anhydrous THF (5 mL) in a dry round bottom flask. Triethylamine (181 mg, 1.80 mmol) was added slowly, then the reaction flask was cooled over an ice bath. Using an addition funnel, a solution of compound **23** (1.13 g, 2.5 mmol, dissolved in 5 mL THF) was added to the stirring solution dropwise. The mixture was allowed to warm to room temperature, and let stir for several hours while monitoring by TLC. TEA salt was removed by filtration over a plug of Celite, and the product was isolated by column chromatography (silica gel, eluting with ethyl acetate/hexanes mixture). The solvent was removed by rotovap, and the product was dried under vacuum, yielding **24** as a colorless oil in 60 % yield (714 mg). ^{1}H NMR (300 MHz, CDCl$_3$): δ = 1.40 (s, 3H), 1.94 (s, 12H), 3.83 (t, 2H), 4.25 (t, 2H), 4.39 (q, 4H); ^{13}C NMR (75 MHz, CDCl$_3$): δ = 17.9, 30.6, 46.9, 55.3, 60.8, 66.3, 67.1, 171.1, 172.6.

- **Synthesis of pentafluorophenyl carbonate 25**
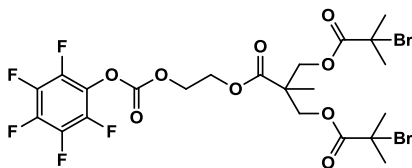
Compound **24** (2 g, 4.2 mmol) was dissolved in THF (5 mL) in a dry 100 mL round bottom flask. Triethylamine (505 mg, 5.00 mmol) was added slowly to the stirring solution. Bis(pentafluorophenyl) carbonate was dissolved in THF (2 mL), then added

dropwise to the reaction mixture at 0 °C. The mixture was stirred for 16 hours, then the solution was washed with water and saturated $NaHCO_3$ (aq). The organic layers were collected and dried over $MgSO_4$, filtered and concentrated by rotary evaporation. The residue was purified by column chromatography over silica gel, eluting with ethyl acetate/hexanes mixtures, to afford a pale yellow oil (1.9 g, 70 %). ^{1}H NMR (300 MHz, $CDCl_3$): δ = 1.40 (s, 3H), 1.94 (s, 12H), 4.39 (q, 4H), 4.49 (t, 2H), 4.59 (t, 2H); ^{13}C NMR (75 MHz): δ = 17.7, 30.5, 46.7, 55.3, 62.4, 66.1, 67.6, 124.8, 136.1, 138.1, 139.4, 141.4, 142.7, 151.2, 170.9, 172.1; ^{19}F NMR (282 MHz, $CDCl_3$): δ = -152.8 (2F), -156.8 (1F), -161.6. (2F). HRMS-FAB (*m/z*): calculated: 684.9730, found: 684.9697.

- **Synthesis of two-arm PFP-polyMPC (26)**
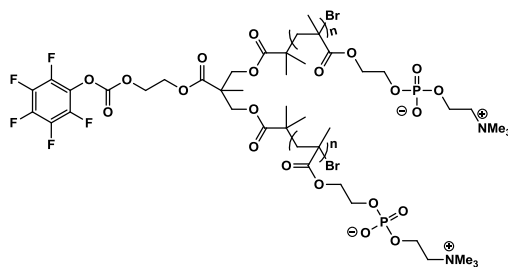
Two-arm polyMPC was prepared using ATRP, according to the same procedure used for polymer **21**.

- **Synthesis of 5-(phosphorylcholine) cyclooctene (27)**
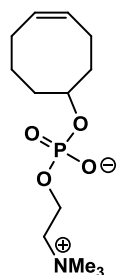
PC-COE was prepared by Dr. Katrina Kratz, according to literature procedures.[3]

- **Synthesis of 5-carboxylic acid cyclooctene (28)**
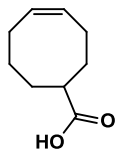
PC-COE was prepared by Dr. Katrina Kratz, according to literature procedures.[4]

- **Synthesis of 5-(pentafluorophenyl ester) cyclooctene (29)**
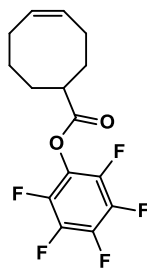
PC-COE was prepared by Dr. Katrina Kratz. Into a flame-dried two-neck flask equipped with a N_2 inlet and addition funnel, a solution of 5-carboxylic acid cycloocetene (0.032 mol, 5.0g) in THF (150 mL) was cooled to 0 °C. Thionyl chloride (0.034 mol, 2.5 mL) was added dropwise and the solution was warmed to room temperature and stirred for 1 hour. The reaction was cooled to 0 °C and triethylamine (0.064 mol, 9.0 mL) was added as a white precipitate formed. After 15 minutes, a solution of pentafluorophenol (0.035 mol, 6.5g) in THF (25mL) was added dropwise and the solution was stirred at room temperature for 12 hours. The white solid was removed by filtration through celite and the filtrate was concentrated. Product was purified by silica gel column chromatography with chloroform as an eluent (R_f value: 0.8). Product was isolated in 78 % yield (0.025 mol, 6.4 g). as a yellow oil. ^{1}H NMR (300 MHz, $CDCl_3$): δ = 5.66 (m, 2H), 3.85 (m, 1H), 2.50-2.00 (br, m, 6H), 1.80-2.0 (br m, 4H), ^{13}C NMR (75 MHz, $CDCl_3$): δ = 171.7, 142.6,

140.6, 139.9, 139.2, 138.1, 136.7, 125.3, 43.1, 31.2, 29.5, 27.8, 25.5, 23.4. ^{19}F NMR (282 MHz, CDCl$_3$): δ = -152.77 (2H), -158.66 (1F), -162.77 (2F). ESI-MS: calculated 320.250, found: 321.090 (M+H$^+$).

- **Synthesis of poly(PC-COE-co-PFP-COE) (30)**
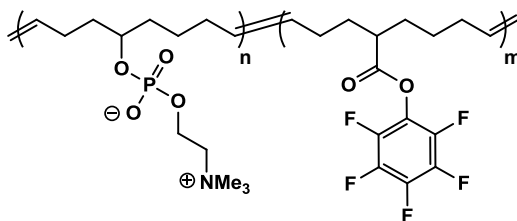
Poly(PC-COE-co-PFP-COE) was prepared by Dr. Katrina Kratz. PC-COE monomer **27** (3.40 mmol, 1.00 g) and PFP-COE monomer **29** (0.170 mmol, 0.042 g) were dissolved in 2 mL of dry 30 % trifluoroethanol in dichloromethane, and stirred under nitrogen. In a separate vial, the pyridine substituted ruthenium benzylidene methathesis catalyst[5] (0.024 mmol, 30 mg) was dissolved in dichloromethane (0.1 mL). The catalyst solution was injected rapidly into the monomer solution, and the mixture was stirred for 30 min. Ethyl vinyl ether (0.5 mL) was added to terminate the polymerization, and the solution was concentrated under vacuum. The crude product was dissolved in methanol (~0.1 mL) and poured into an excess of acetone. The resulting polymer was filtered, dried under vacuum, purified by dialysis in water (2,000 g/mol MWCO) and then lyophilized to afford 70 % of a white solid. ^{1}H-NMR (300 MHz, 25 % MeOD in CDCl$_3$): δ = 5.17 (m, 2H), 4.0 (m, 3H), 3.48 (t, 2H), 3.0 (s, 9H), 2.60 (br, 1H) 1.80-2.0 (br m, 4H), 1.5-1.7 (br m, 2H), 1.2-1.4 (br m, 4H). ^{13}C-NMR (75 MHz, 25% MeOD in CDCl$_3$): δ = 171.7, 142.6, 140.6, 139.9, 139.2, 138.1, 136.7, 135.0, 134.0, 70.0, 65.0, 58.2, 47.2, 43.1, 34.6,

34.0, 24.8, 24.1, 21,8. ^{31}P-NMR (122 MHz, 25% MeOD in CDCl$_3$): δ 0.0. ^{19}F-NMR (282 MHz, 25% MeOD in CDCl$_3$): δ = -152.77 (2H), -158.66 (1F), -162.77 (2F).

- **Preparation of Lysozyme-polyMPC Conjugates (32-34)**
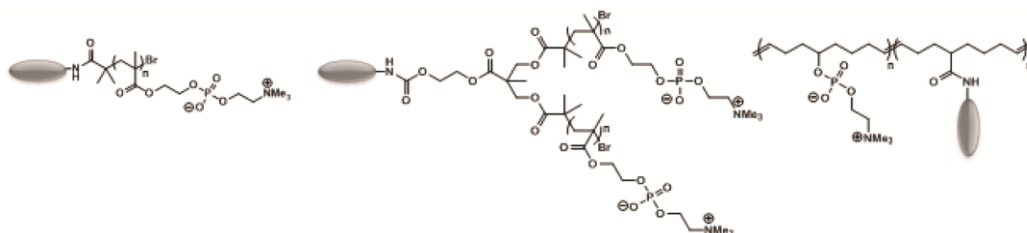
In general, lysozyme was dissolved in pH 9 borate buffer at a concentration of 10 mg/mL. The buffered protein solution was added to a vial containing an excess of the phosphorylcholine polymer (20 molar equivalents). The reaction mixture was gently shaken at room temperature, and conjugation progress was monitored by size exclusion high performance liquid chromatography (SEC-HPLC) eluting with 10 % ethanol/PBS at 1.0 mL/min. The conjugates were purified using fast protein liquid chromatography (FPLC) eluting with PBS at 0.5 mL/min, or dialysis (MWCO 20,000).

- **Preparation of AF647-labeled lysozyme-polyMPC conjugate (35)**
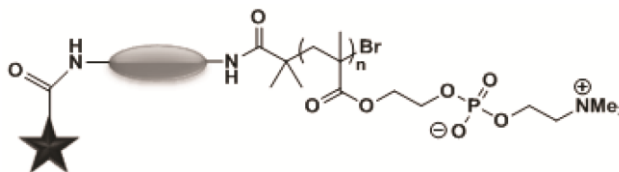
Lysozyme and lysozyme-polyMPC conjugates were labelled with Alexa Fluor 647 succinimidyl ester purchased from Invitrogen, according to the manufacturer's instructions. The labeled lysozyme and conjugates were purified by passage through a bio-gel P4 gel column with PBS as eluent. Fractions containing the labeled products were collected and combined. The labeled lysozyme and conjugates were concentrated with

Centricon YM-3 by filtering off the PBS. After measuring the UV/Vis absorbance at 280 and 650 nm, the concentration and degree of labeling were calculated based on the manufacturer's protocol. The purified conjugates were also characterized by fluorescence spectroscopy, and HPLC with a fluorescence detector..

- **Synthesis of 2-hydroxyethyl 2-bromoisobutyrate (38)**
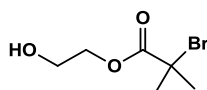
To a solution of ethylene glycol (2 g, 0.032 mol) in 10 mL of anhydrous tetrahydrofuran (THF), triethylamine (1.95 g, 0.019 mol) was added. The solution was cooled on ice while stirring. Using an addition funnel, 2-bromoisobutyryl bromide (3.6 g, 0.16 mol) in 5 mL THF was added dropwise to the solution. Gradually allowed to warm to room temperature, and continued to stir for 18 hours. The TEA salt was subsequently filtered off, and the remaining solution was concentrated by rotary evaporation. The residue was the purified by column chromatography on silica gel, eluting with 20:80 ethyl acetate/hexanes. The product was obtained as a colorless liquid (2 g, 59 %). ^{1}H NMR (300 MHz, CDCl$_3$): δ = 1.95 (s, 6H), 3.87 (t, 2H), 4.41 (t, 2H). HRMS-FAB (m/z): [M+H]+ calculated for C$_6$H$_{11}$BrO$_3$: 210.99, found: 210.9970.

- **Synthesis of t-boc-aminooxy ATRP initiator (39)**
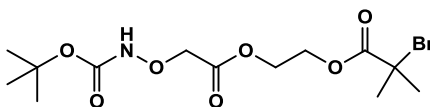
Compound **38** (1 g, 4.76 mmol) and t-boc aminooxy acetic (909 mg, 4.76 mmol) were dissolved in 50 mL of anhydrous dichloromethane. The flask was cooled to 0 °C on ice, and EDC and DMAP were added simultaneously to the reaction. Gradually let warm to

125

room temperature, and continued stirring for 18 hours. The solvent was then removed by rotary evaporation, and the residue was purified by column chromatography on silica gel, eluting with 80:20 ethyl acetate/hexanes, to afford to product as a colorless oil in (1.7 g, 94 %). 1H NMR (300 MHz, CDCl3): δ = 1.46 (s, 9H), 1.93 (s, 6H), 4.4 - 4.7 (m, 6H), 7.78 (s, 1H). 13C NMR (75 MHz, CDCl3): δ = 28.16, 30.60, 55.28, 62.35, 63.21, 72.50, 82.14, 156.24, 169.39, 171.52. FAB-MS (m/z): [M+H] calculated for C13H22BrNO7: 384.06, found: 384.07.

- **Synthesis of aminooxy-polyMPC (40)**
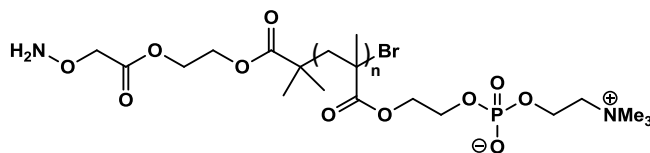
MPC monomer (2 g, 6.75 mmol) and initiator **39** (75 mg, 0.198 mmol) were added to a round bottom flask and dissolved in 3 mL of anhydrous methanol and 5 mL of anhydrous DMSO with stirring. The solution was purged with nitrogen for 10 minutes. Cu(I)Br (28 mg, 0.198 mmol) and bipyridine (62 mg, 0.397 mmol) were added as solids to the reaction mixture under a stream of nitrogen. The mixture was degassed with nitrogen for 10 minutes, then let stir overnight at room temperature. The polymerization was monitored using ^{1}H NMR, stopped by exposure to air, oxidizing the Cu catalyst. The mixture was precipitated into THF, redissolved, and passed over a plug of silica eluting with methanol. Solvent was removed to give the polymer product as a white solid (1.5 g, 72 %). Polymers were characterized by ^{1}H NMR and aqueous GPC for relative molecular weight determination. PolyMPC (1g) was dissolved in 10 mL of 10 % methanol in trifluoroacetic acid solution and stirred at room temperature to achieve chain-end deprotection. After 3 hours, solvent was removed by rotary evaporation. The

polymer residue was dissolved in water, and purified by dialysis (MWCO 1000). Lyophilization resulted in the desired polymers as white solids. GPC analysis confirmed that no polymer degradation was caused by the harsh acid treatment, and ^{1}H NMR was used to confirm the disappearance of the t-boc protecting group.

- **Synthesis of 4-hydroxybenzaldoxime-polyMPC (41)**
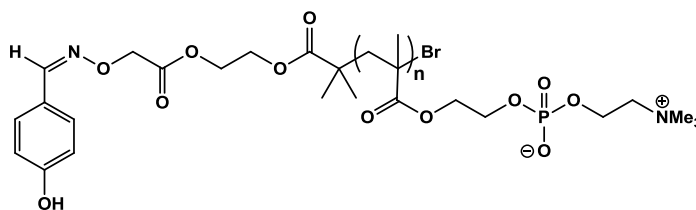
PolyMPC **40** (100 mg, 0.02 mmol) was added to a small reaction vessel, and dissolved in 300 uL of pH 9 borate buffer. 4-hydroxybenzaldehyde (3 mg, 0.024 mmol) was added, and the reaction was vortexed to dissolve, then gently shaken for 18 hours at room temperature. A 20 uL aliquot was removed and diluted to 1mL and injected onto aqueous GPC, monitoring with a UV detector set to 280 nm. Comparing the signal intensity obtained from polymer **40** and conjugate **41** indicated that oxime formation occurred, linking the UV-active benzaldehyde moiety to the polymer chain.

- **Synthesis of pentafluorophenyl levulinate (43)**
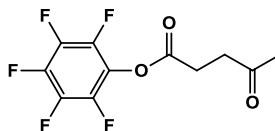
Levulinic acid (1 g, 0.0085 mol) and pentafluorophenol (1.4 g, 0.0075 mol) were added to a 100 mL round bottom flask, and dissolved in 30 mL of anhydrous dichloromethane. The reaction flask was cooled on ice, then EDC (1.7 g, 0.009 mol) and DMAP (92 mg, 0.00075 mol) were added together as solids. The reaction was allowed to gradually warm

to room temperature, and continued stirring for 18 hours. The desired product was purified by column chromatography on silica gel, eluting with 1-5 % methanol in DCM, to yield **43** as a white solid (2 g, 95 %). ^{1}H NMR (300 MHz, CDCl$_3$): δ = 2.22 (s, 3H), 2.88 - 2.95 (m, 4H). ^{19}F NMR (282 MHz, CDCl$_3$): δ = -152.5 (2F), -157.9 (1F), -162.3 (2F).

- **Synthesis of lysozyme-levinate (44)**
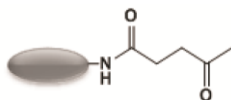
Lysozyme (250 mg, 0.0174 mmol) was dissolved in 10 mL of pH 9 sodium borate buffer. In a separate vial, **43** (50 mg, 0.174 mmol) was dissolved in 1 mL of DMSO, then added dropwise to the protein solution. After 2 hours, cation exchange FPLC indicated complete conversion from native lysozyme. The reaction mixture was transferred to a dialysis membrane and dialyzed against pure water. Lyophilization afforded a white solid. ESI-MS revealed a mixture of products.

- **Synthesis of lysozyme-polyMPC conjugate (45)**
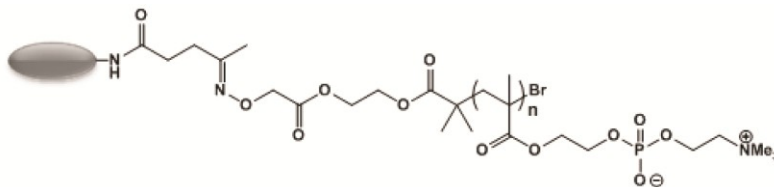
A 10 mg/mL solution of lysozyme in the desired buffer was prepared, and to it, 20 molar equivalents of aminooxy polyMPC was added. The reactions were kept at room temperature and gently agitated, and 50 uL aliquots were removed at predetermined time points and diluted to a final volume of 500 uL. 50uL was injected to SEC-HPLC to monitor conversion to conjugate.

- **Synthesis of TMS-propargyl methacrylate (47)**
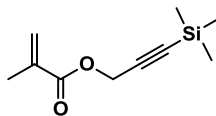
The TMS protected alkyne monomer was synthesized according to the literature.[6] 3-(Trimethylsilyl)propargyl alcohol (2 g, 15.6 mmol) and triethylamine (2 g, 20.3 mmol) in 20 mL of dry ethyl ether was cooled to -20 °C. A solution of methacryloyl chloride (2 g, 18.7 mmol) in 10 mL of dry ethyl ether was added dropwise over 30 min. The reaction mixture was stirred for 30 min at -20 °C, then overnight at room temperature. The precipitation was removed by filtration and the solvent was removed by rotary evaporation. The crude product was further purified on silica column chromatography eluted with hexane-ethyl ether (100:1) to give the pure TMS-PgMA monomer as clear oil (4.0 g, 58 % yield). IR: (cm^{-1}) 2961 (C-H), 1723 (C=O), 1638 (C=C). ^{1}H NMR (CDCl$_3$, 300 MHz): δ 6.16 (m, 1H), 5.61 (m, 1H), 4.75 (s, 2H), 1.95 (m, 3H), 0.18 (s, 9H). ^{13}C NMR (CDCl$_3$, 75 MHz): δ 166.6, 135.7, 126.4, 99.1, 91.9, 53.0, 18.3, 0.3. HRMS-FAB (m/z): [M]+ calculated for C$_{10}$H$_{16}$O$_2$Si: 196.0920, found: 196.0891.

- **Synthesis of CPT-azides (48)**
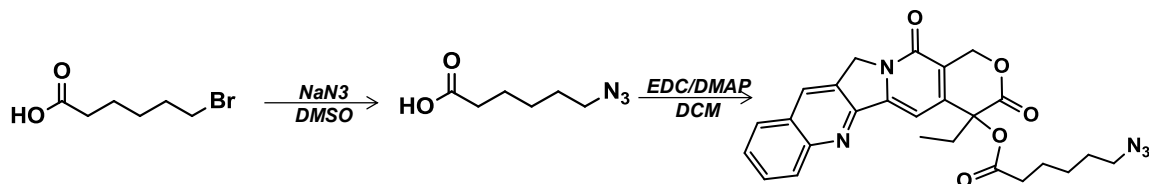
Several linkers were prepared for CPT. for example, an alkyl linker was synthesized according to the literature.[7] 6-bromohexanoic acid (5 g, 25.6 mmol) was reacted with sodium azide (8.4 g, 129 mmol) in 50 mL of DMSO at room temperature to generate 6-azidohexanoic acid, which then was reacted with CPT using EDC/DMAP as coupling agents in DCM to obtain compound **48**. IR: (cm^{-1}) 2094 (N=N=N). ^{1}H NMR (CDCl$_3$, 300

MHz): δ 8.43 (s, 1H), 8.24 (d, J = 8.3 Hz, 1H), 7.97 (d, J = 8.0 Hz, 1H), 7.87 (t, J = 7.0 Hz, 1H), 7.70 (t, J = 7.1 Hz, 1H), 7.23 (s, 1H), 5.71 (d, J = 17.6 Hz, 1H), 5.43 (d, J = 17.6 Hz, 1H), 5.31 (s, 2H), 3.25 (t, J = 6.8 Hz, 2H), 2.45-2.63 (m, 2H), 2.11-2.37 (m, 2H), 1.71 (qp, J = 7.6 Hz, 2H), 1.63 (m, 2H), 1.42 (m, 2H), 1.00 (t, J = 7.3 Hz, 3H).
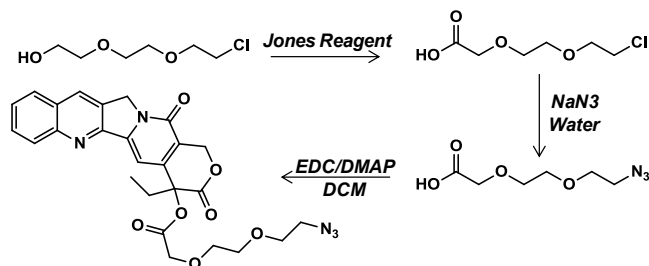
Alternatively, chromium trioxide (25 g, 164 mmol) was dissolved into 300 mL of 1.5 M H_2SO_4 and the solution was cooled to 0 °C. 2-[2-(2-chloroethoxy)ethoxy]ethanol (8.3 g, 49 mmol) in 150 mL acetone was added into the Jones reagent dropwise and the reaction mixture was stirred at room temperature for 6 h. The acetone was removed by evaporation under vacuum and the aqueous phase was extracted with DCM (3 × 100 mL). After the combined organic phase was dried over $MgSO_4$, 2-[2-(2-chloroethoxy)ethoxy]acetic acid (6.3 g, 70 % yield) was obtained by removing the solvent by rotary evaporation. IR: (cm-1) 1734 (C=O). ^{1}H NMR (CDCl$_3$, 300 MHz): δ 10.49 (b, 1H), 4.23 (s, 2H), 3.80 (t, J = 5.8 Hz, 4H), 3.74 (t, J = 5.7 Hz, 2H), 3.66 (t, J = 5.8 Hz, 2H). ^{13}C NMR (CDCl$_3$, 75 MHz): δ 174.4, 71.4, 71.1, 70.4, 68.5, 42.6. 2-[2-(2-chloroethoxy)ethoxy]acetic acid (6.3 g, 34.4 mmol) and NaN_3 (9 g, 138 mmol) were dissolved in 20 mL of water. The reaction mixture was refluxed at 80 °C for 48 h. After cooling to room temperature, the reaction mixture was acidified with HCl solution and extracted with DCM (4 × 50 mL). The combined organic phase was dried over $MgSO_4$ and then $MgSO_4$ was removed by filtration. Solvent was removed under reduced pressure

to obtain the linker as clear oil (5.0 g, 77 % yield). IR: (cm^{-1}) 2097 (N=N=N). ^{1}H NMR (CDCl$_3$, 300 MHz): δ 10.80 (b, 1H), 4.22 (s, 2H), 3.79 (t, J = 5.7 Hz, 2H), 3.69-3.74 (m, 4H), 3.43 (t, J = 5.3 Hz, 2H). ^{13}C NMR (CDCl$_3$, 75 MHz): δ 174.7, 71.2, 70.5, 70.1, 68.4, 50.6. HRMS-FAB (m/z): [M+H]+ calculated for C$_6$H$_{12}$O$_4$N$_3$: 190.0828, found: 190.0816. 2-[2-(2-azidoethoxy)ethoxy]acetic acid (327 mg, 1.72 mmol) and EDC hydrochloride (330 mg, 1.72 mmol) were dissolved in 20 mL DCM at 0 °C. CPT (300 mg, 0.86 mmol) and DMAP (210 mg, 1.72 mmol) were added. The reaction was stirred at room temperature till the suspension turned clear. After washing with 1 N HCl (50 mL × 3), 1 % NaHCO$_3$ (50 mL × 3), and brine (50 mL × 1), the organic phase was dried over MgSO$_4$. After filtration, the solvent was removed by evaporation to gave a yellow solid, which is recrystallized from MeOH/CH$_2$Cl$_2$ (95:5) to give CPT azide **48** (389 mg, 87 % yield) as light yellow solid. IR: (cm^{-1}) 2104 (N=N=N). ^{1}H NMR (CDCl$_3$, 300 MHz): δ 8.43 (s, 1H), 8.24 (d, J = 8.0 Hz, 1H), 7.97 (d, J = 8.0 Hz, 1H), 7.87 (t, J = 7.5 Hz, 1H), 7.70 (t, J = 7.5 Hz, 1H), 7.23 (s, 1H), 5.73 (d, J = 17.4 Hz, 1H), 5.44 (d, J = 17.4 Hz, 1H), 5.31 (s, 2H), 4.39 (d, J = 5.0 Hz, 2H), 3.77 (t, J = 5.5 Hz, 2H), 3.66-3.70 (m, 4H), 3.40 (t, J = 5.1 Hz, 2H), 2.13-2.39 (m, 2H), 1.00 (t, J = 7.4 Hz, 3H). ^{13}C NMR (CDCl$_3$, 75 MHz): δ 169.7, 167.3, 157.3, 152.2, 148.9, 146.4, 145.4, 131.2, 130.7, 129.6, 128.4, 128.2, 128.2, 128.1, 120.3, 95.9, 76.4, 71.1, 70.6, 70.0, 68.2, 67.2, 50.6, 50.0, 31.8, 7.6. HRMS-FAB (m/z): [M+H]+ calculated for C$_{26}$H$_{26}$O$_7$N$_5$: 520.1832, found: 520.1821.

- **Synthesis of poly(MPC-g-CPT) (49)**
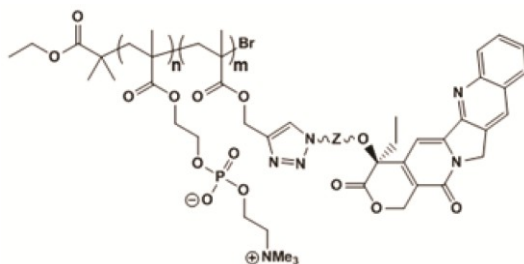
CPT azide compound was charged into a 10 mL two-neck round-bottom flask and three cycles of vacuum-nitrogen were employed. Nitrogen gas bubbled DMSO (2 mL) was injected with a syringe. After the CPT azide was completely dissolved, a solution of ethyl 2-bromoisobutyrate (11.7 mg. 0.06 mmol), MPC and alkyne monomer in 0.7 mL methanol was injected. CuBr (17 mg, 0.12 mmol) and bipyridine (37.4 mg, 0.24 mmol) were added quickly under nitrogen atmosphere. The reaction mixture was then subjected to four freeze-pump-thaw cycles. The reaction mixture was stirred at room temperature for 20 h and the polymerization conversion was monitored by ^{1}H NMR. The polymerization was stopped by precipitating the reaction mixture into THF (100 mL) and the crude product was isolated by filtration. The crude product was further purified on silica column with MeOH/CH$_2$Cl$_2$ (95:5) as eluent to give the polyMPC-g-CPT copolymers as light yellow solid. The polymers were characterized using NMR and aqueous GPC.

- **Synthesis of HEMA-LA monomer (51)**
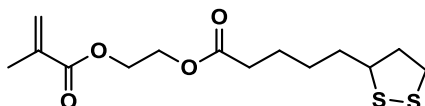
Lipoic acid (4.00 g, 19.4 mmol) and 2-hydroxyethyl methacrylate (2.50 g, 19.4 mmol) were dissolved in 60 mL of anhydrous CH$_2$Cl$_2$ in a dry roundbottom flask. The stirring

solution was cooled to 0 °C, and EDC (7.40 g, 38.8 mmol) and DMAP (2.40 g, 19.4 mmol) were added as solids. The reaction mixture was allowed to warm to room temperature, and stirred for 18 hours. The mixture was diluted with dichloromethane, and washed with 1 M HCl$_{(aq)}$, saturated NaHCO$_{3(aq)}$, and brine. The organic layer was dried over MgSO$_4$, filtered, and concentrated by rotary evaporation, to give monomer **51** as a yellow oil (4.9 g, 80 % yield). ^{1}H NMR (300 MHz, CDCl$_3$): δ = 6.06 (s, 1H), 5.36 (s, 1H), 4.26 (s, 4H), 3.5 (m, 1 H), 3.11 (m, 2H), 2.40 (m, 1H), 2.3 (t, 2H), 1.87 (s, 3H), 1.35-1.70 (m, 8H) ppm. ^{13}C NMR (75 MHz, CDCl$_3$): δ = 18.31, 24.60, 28.70, 33.87, 34.58, 38.49, 40.21, 56.29, 61.99, 62.43, 126.10, 135.89, 167.08, 173.22 ppm.

- **Synthesis of poly(MPC-*b*-DHLA) copolymer (55)**
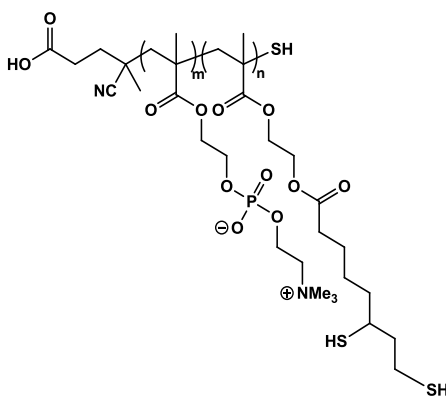
MPC (1.00 g, 3.37 mmol), 4-cyano-4-(phenylcarbonothioylthio)pentanoic acid (19 mg, 0.067 mmol), and 4,4'-azobis(4-cyanovaleric acid) (ACVA) (4.0 mg, 0.014 mmol) were added to a dry round bottom flask. Methanol (3 mL) and dimethylsulfoxide (DMSO) (2 mL) were added and the solution was degassed for 20 minutes by bubbling with dry nitrogen gas. The reaction mixture was placed in a preheated oil bath at 70 °C and stirred for 6 hours. In a separate vial, HEMA-LA **51** (212 mg, 0.67 mmol) was dissolved in DMSO (1 mL) and degassed for 30 minutes. The solution of **1** was added rapidly to the reaction flask by syringe, and stirring was continued for 12 hours. Propagation was

133

terminated by placing the solution in liquid nitrogen, then allowing the mixture to warm while open to air. The solution was then passed through a short plug of silica gel, eluting with methanol, then precipitated into THF to afford polymer **54** as a pink solid. This solid was dissolved in 20 mL of degassed water, and stirred at 0 °C. Sodium borohydride (102 mg, 2.68 mmol) was added under a stream of nitrogen. The reaction mixture was stirred at 0 °C for 1 hour, then at 25 °C for 1 hour. HCl$_{conc}$ was added to adjust the pH to ~3, and the polymer was purified by dialysis (MWCO 1,000) against methanol and water at 4 °C. Lyophilization afforded the desired block copolymer **55** in 80 % yield as white solids. ^{1}H NMR (300 MHz, MeOD/CDCl$_3$): δ = 4.32 (2H, br), 4.22 (2H, br), 4.07 (2H, br), 3.75 (2H, br), 2.95 (2H, br), 2.71 (2H, br), 2.45 (2H, br), 1.37-2.28 (H, br), 0.52, 1.23 (3H, br). ^{13}C NMR (175 MHz, MeOD/CDCl$_3$): δ = 16.91, 18.59, 21.81, 24.45, 26.31, 33.78, 38.43, 39.01, 42.70, 44.70, 45.10, 53.76, 59.09, 64.70, 66.09, 173.44, 176.79, 177.60, 177.87. GPC (TFE + 0.2 M Na trifluoroacetate, 1 eq DTT, PMMA standards): M$_n$, 26,900; PDI 1.24.

- **Synthesis of 3-(pyridyl disulfide) propionic acid linker (56)**
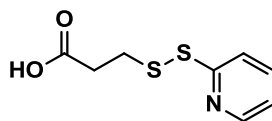
Comound **56** was synthesized according to literature procedure.[8] 2,2'-Dithiodipyridine (500 mg, 2.27 mmol) was dissolved in ethyl acetate (2.5 mL) with stirring in a roundbottom flask. Separately, 3-mercaptopropionic acid (160 mg, 1.51 mmol) was dissolved in ethyl acetate (1.5 mL), and added dropwise to the stirring solution, which gradually became yellow. One drop of boron trifluoride diethyl etherate was added. After 7 hours, the reaction mixture was concentrated by rotary evaporation and purified

by column chromatography on silica gel, eluting with methanol/dichloromethane mixtures to give the desired product as a yellow oil in 95 % yield (307 mg). ^{1}H NMR (300 MHz, CDCl$_3$): δ = 12.8 (s, 1H), 8.4 (br, 1H), 7.6 (br, 2H), 7.1 (br, 1H), 3.04 (tr, 2H), 2.8 (tr, 2H). ^{13}C NMR (75 MHz, CDCl$_3$): δ = 33.71, 34.01, 114.32, 121.19, 134.00, 138.06, 149.93, 176.16.

- **Synthesis of CPT-pyridyl disulfide (57)**
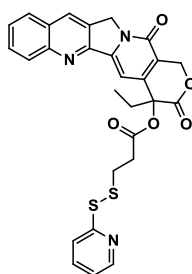
Camptothecin-pyridyl disulfide was prepared according to literature procedures.[9] Compound **56** (232 mg, 1.07 mmol) was dissolved in anhydrous dichloromethane (30 mL) in a roundbottom flask. Camptothecin (250 mg, 0.718 mmol) was added to form a pale yellow suspension. EDC (276 mg, 1.44 mmol) and DMAP (175 mg, 1.44 mmol) were added. The mixture was stirred for 24 hours, then diluted with dichloromethane, and washed with 1M HCl (aq), brine, and water. The organic layer was dried over MgSO$_4$, filtered, and concentrated by rotary evaporation. The residue was further purified by column chromatography on silica gel, eluting with methanol/dichloromethane to give the desired product as a yellow solid in 50 % yield (195 mg). ^{1}H NMR (300 MHz, DMSO): δ = 8.71 (s, 1H), 8.48 (d, 1H), 8.14 (m, 2H), 7.62-7.83 (m, 3H), 7.36 (d, 1H), 7.11-7.2 (m, 2H), 5.51 (s, 2H), 5.31 (s, 2H), 3.34 (m, 2H), 2.96 (m, 2H), 2.15 (m, 2H), 0.90 (tr, 3H). ^{13}C NMR (175 MHz, DMSO): δ = 171.01, 167.57, 157.61, 156.96, 153.82, 150.01, 148.33, 146.37, 145.73, 137.10, 132.00, 130.90, 130.25, 129.29, 129.00, 128.42, 128.14,

135

122.75, 120.40, 119.28, 95.66, 76.56, 66.72, 50.66, 34.25, 30.65, 29.36, 7.99. HRMS-FAB [M+H]: calculated: 546.115, found: 546.113 g/mole.

- **Synthesis of polyMPC-CPT loaded micelles (58)**
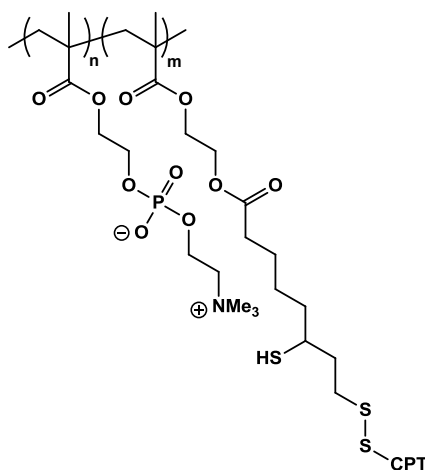
Polymer **55** (50 mg, 0.064 mmol DHLA) and camptothecin-pyridyl disulfide (16 mg, 0.029 mmol) were dissolved in methanol/DMSO (5 mL). The solution was stirred vigorously at 37 °C for 72 hours, then dialyzed against methanol to remove unconjugated camptothecin. The polymer solution was dialyzed against water to induce micelle formation, and bubbled with air to promote disulfide formation from residual thiols. Micelle solutions were passed through 0.45 μm filters to remove any free CPT, and lyophilized to produce off-white solids which were re-dissolved in water or methanol for characterization. CPT loading, as a weight percent, was determined using UV/Vis spectroscopy, comparing to a sample of known concentration.

- **Synthesis of 2-ethoxy-2-oxoethyl methacrylate (59)**
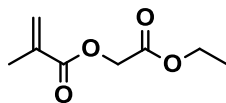
Monomer **59** was prepared by Dr. Xiangji Chen. Sodium methacrylate (9.7 g, 90 mmol) and 10.02 g of ethyl bromoacetate (60 mmol) were added into 55 mL of dry acetonitrile. To the suspension, 3.5 g of tetrabutylammonium bromide (TBAB) was added. The reaction mixture was heated to reflux overnight. The salt was removed by filtration and solvent was removed by evaporation under reduced pressure. The residue was redissolved in ethyl acetate and washed four times with water. The organic phase was dried over MgSO$_4$ and removal of the solvent gave the desired monomer as a pale yellow oil (9.8 g, 95 %). ^{1}H NMR (CDCl$_3$, 300 MHz): δ 6.21 (s, 1H), 5.64 (m, 1H), 4.66 (s, 2H), 4.22 (q, 2H), 1.97 (s, 3H), 1.27 (t, 3H). ^{13}C NMR (CDCl$_3$, 75 MHz): δ 167.9, 166.7, 135.4, 126.8, 61.4, 60.9, 18.2, 14.1.

- **Synthesis of polyMPC-*co*-EtOEMA (60)**
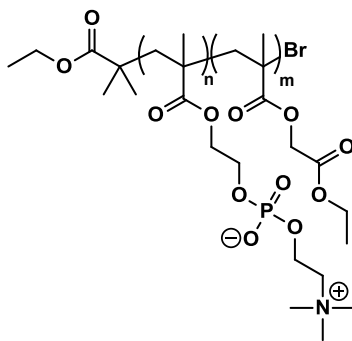
Initiator EBiB (5.9 mg, 0.03 mmol), MPC and EtOEMA were charged to a 10 mL two-neck round-bottom flask and three cycles of vacuum-nitrogen were employed. Nitrogen gas-bubbled DMSO and MeOH were injected with a degassed syringe. The reaction mixture was bubbled with nitrogen gas for 20 min. Cu(I)Br (8.6 mg, 0.06 mmol) and

bipyridine (18.7 mg, 0.12 mmol) were added as solids quickly under nitrogen atmosphere. The reaction mixture was then bubbled with nitrogen gas for another 20 min and left under nitrogen atmosphere. The reaction mixture was stirred at room temperature and the polymerization conversion was monitored by ^{1}H NMR. The polymerization was stopped by exposing to air. The crude product was purified by silica column eluting with methanol to give the poly(MPC-*co*-EtOEMA) random copolymer as a white solid. The monomer ratio in the copolymer was characterized by ^{1}H NMR spectroscopy, comparing the peak integration at 3.58 ppm (-CH_2-N in MPC) to peak integration at 1.27 ppm ((-CH_3) in EtOEMA).

- **Synthesis of polyMPC-*co*-Hydrazine (61)**
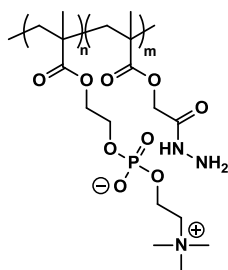
Poly(MPC-*co*-EtOEMA) **60** was dissolved in methanol at a concentration of 100-200 mg /mL. Hydrazine monohydrate was added to the polymer solution to a final concentration of 25 %. The reaction mixture was stirred at room temperature, monitoring by ^{1}H NMR spectroscopy. Upon completion, the reaction mixture was diluted with water and purified by dialysis against water with MWCO 1000 membrane for 2 days and filtered through a 0.45 μm filter. The copolymer was obtained as a white powder after lyophilization. The average yield was over 80 % and the loading of the hydrazine group was calculated by comparing the peak integration at 3.58 ppm (–CH_2-N in MPC) to peak integration at 4.64 ppm (-CH_2-CONHNH$_2$) on ^{1}H NMR spectrum. ^{1}H NMR (MeOD, 300 MHz): δ = 0.9-1.2

(br, 3H), 1.8-2.3 (br, 2H), 3.3 (s, 9H), 3.75 (br, 2H), 4.16 (br, 2H), 4.3 (br, 2H), 4.38 (br, 2H), 4.64 (br, 2H). ^{13}C NMR (MeOD, 100 MHz): δ = 16.8, 18.5, 44.7, 45.0, 53.4, 59.3, 62.2, 62.9, 64.8, 66.1, 167.1, 176.9, 178.1. GPC (0.1 M NaNO$_3$ + 0.02 wt % NaN$_3$, PEO standards): M$_n$, 25,000; PDI 1.4.

- **Synthesis of polyMPC-DOX (62)**
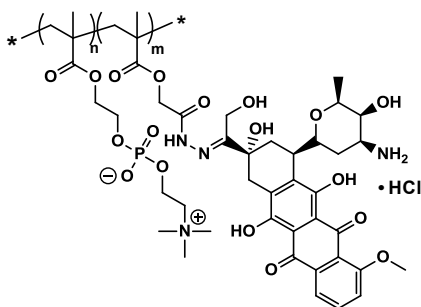
MPC copolymer **61** (200 mg, 0.165 mmol -NHNH$_2$) and DOX•HCl (58 mg, 0.1 mmol) were dissolved in anhydrous methanol (5 mL). To this solution, 60 µL of acetic acid and 200 mg of anhydrous magnesium sulfate were added. The reaction mixture was stirred in the dark at room temperature for 2 days. The resulting conjugate was purified first by passage over a Sephadex LH-20 column eluting with methanol. Fractions containing polymer-DOX conjugate were concentrated by rotary evaporation, redissolved in water, and further purified by Sephadex G-25 column eluting with pure water. PolyMPC-DOX conjugate **62** was obtained as a dark red powder after lyophilization (230 mg, 88 %).

- **Synthesis of GRGDS-methacrylamide (63)**
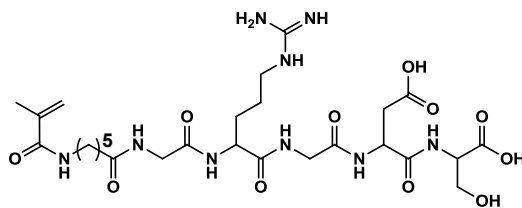
Standard solid phase peptide synthesis procedures were used, starting from a 2-chlorotrityl chloride resin containing 1.6 mmol/g active sites. Resin (3.0 g, 4.8 mmol) was added to the reaction vessel, and 30 mL of anhydrous dichloromethane was added. The suspension was agitated with dry nitrogen pressure for 30 minutes to swell the resin. Separately, Fmoc-Ser(But)-OH (3.7 g, 9.6 mmol) was dissolved in 30 mL of anhydrous dichloromethance. DIPEA (2.47 g, 19.2 mmol) was injected to the serine solution immediately prior to addition to the reaction vessel. The peptide-resin mixture was agitated with nitrogen pressure for one hour at room temperature. The reaction mixture was filtered. CH_2Cl_2:MeOH:DIPEA (80:15:5) (30 mL) was added, and agitated with nitrogen pressure for 10 minutes, to block any unreacted active sites. The solution was filtered, and 30 mL of fresh CH_2Cl_2/MeOH/DIPEA solution was added and agitated for 10 minutes. The resin was washed with 30 mL DMF (3 x 1 minute each). The amino acid was deprotected using a 25 % piperidine solution in DMF, agitating for three minutes, then exchanging for fresh solution and agitating for 20 minutes. The resin was washed with DMF (6x), CH_2Cl_2 (3x), isopropanol (3x), hexanes (6x), and once with dichloromethane, then dried under vacuum overnight. Serine loading was calculated to be 1.36 mmol/g. Aspartic acid (6.7 g, 16.32 mmol), HBTU (5.3 g, 16.3 mmol), and HOBt (2.20 g, 16.3 mmol) were dissolved in 40 mL anhydrous DMF. DIPEA (4.20 g, 32.6 mmol) was added, and the solution was quickly transferred to the reaction vessel containing the serine-loaded resin and agitated with nitrogen pressure for 1 hour. The solution was filtered, and washed with DMF (3x), then deprotected with 25 % piperidine in DMF. After filtering, the resin was washed with DMF (6x). This procedure was repeated for the additions of glycine, arginine, glycine, N-Fmoc-amidocaproic acid, and

methacrylic acid. After the addition of methacrylic acid, the resin was washed with dichloromethane (6x), and then agitated for 1 hour with a 95:2.5:2.5 trifluoroacetic acid:water:triisopropylsilane solution to cleave the peptide from the resin. The solution was filtered into a dry round bottom flask; the cleavage procedure was then repeated twice. The peptide solution was concentrated to a minimal volume using rotary evaporation and precipitated into 1 L diethyl ether. The GRGDS-methacrylamide monomer **63** was recovered as a white solid by filtration and dried under vacuum (1.9 g, 45 %). ^{1}H NMR (300 MHz, DMSO): δ = 7.9-8.5 (br, 8H), 5.61 (s, 1H), 5.28 (s, 1H), 4.55-4.75 (br, 3H), 4.2-4.4 (br, 2H), 3.6-3.85 (br, 6H), 3.15 (br, 4H), 3.0 (br, 1H), 2.85 (br, 1H), 2.7 (br, 1H), 2.55 (br, 2H), 2.12 (tr, 2H), 1.84 (s, 3H), 1.5 (br, 8H), 1.25 (br, 2H). ^{13}C NMR (75 MHz, DMSO): δ = 173.19, 172.27, 172.15, 171.97, 171.39, 171.11, 170.23, 169.78, 169.10, 167.85, 157.12, 140.53, 119.21, 67.08, 65.38, 55.28, 52.65, 51.06, 49.65, 42.42, 36.72, 35.53, 29.48, 29.30, 26.56, 25.38, 19.13. ESI-MS [M+H]: calculated, 672.3; found, 672.4.

- **Synthesis of polyMPC-*co*-DHLA-*co*-GRGDS (64)**
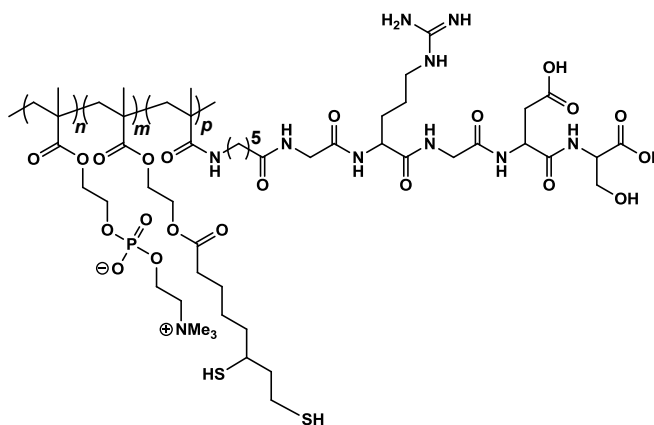
MPC (1.0 g, 3.4 mmol), HEMA-LA (218 mg, 0.69 mmol), and 2,2'-azobisisobutyrylnitrile (AIBN) (8 mg, 0.05 mmol) were added to a dry round bottom

flask. A 1:1 mixture of MeOH and DMSO (6 mL total volume) was added and the solution was purged with dry nitrogen gas. The reaction mixture was placed in a preheated oil bath at 70 °C and stirred for 4 hours. Propagation was terminated by placing the solution in liquid nitrogen, then allowing the mixture to warm while open to air. The solution was precipitated into THF to afford the polymer product as an off-white solid. This solid was dissolved in 20 mL of degassed water, and stirred at 0 °C. Sodium borohydride (104 mg, 2.74 mmol) was added under a stream of nitrogen. The reaction mixture was stirred at 0 °C for 1 hour, then at 25 °C for 1 hour. $HCl_{(conc)}$ was added to adjust the pH to ~3, and the polymer was purified by dialysis (MWCO 1,000) against methanol and water at 4 °C. Lyophilization afforded the desired copolymer **64** as a white solid. ^1H NMR (300 MHz, MeOD): $\delta =$ 4.4 (br, 2H), 4.3 (br, 2H), 4.1 (br, 2H), 3.75 (br, 2H), 3.0 (br, 2H), 2.75 (br, 2H), 2.5 (br, 2H), 1.5-2.1 (br, 5H), 0.8-1.1 (br, 3H). ^{13}C NMR (100 MHz, MeOD/CDCl$_3$): $\delta =$ 177.5, 66.1, 62.9, 59.3, 53.8, 45.0, 44.7, 42.7, 39.0, 38.4, 33.6, 26.4, 24.4, 21.8, 18.6, 16.7. Aqueous GPC (0.2 M NaNO$_3$ + 0.01 % NaN$_3$; PEO standards): M$_n$, 64,200 g/mole; PDI, 4.4. This general procedure was used for all of the GRGDS-containing polymers, adding the desired amount of oligopeptide comonomer at the outset of the polymerization.

- **Preparation of polyMPC hydrogel (65)**
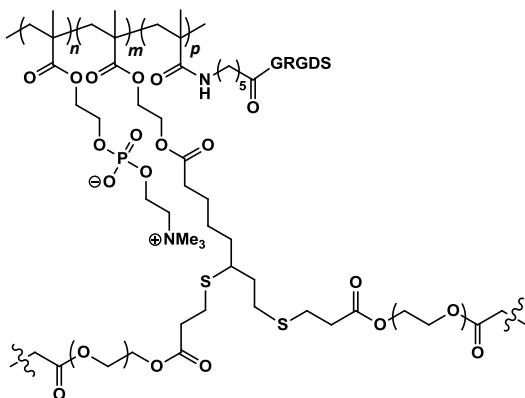
Stock solutions of poly(MPC-*co*-DHLA) (with and without the GRGDS peptide) were prepared at a concentration of 100 mg/mL in pH 9 sodium borate buffer. Separately, a stock solution of PEG$_{2000}$DA cross-linker was prepared at a concentration of 180 mg/mL in sodium borate buffer. The poly(MPC-*co*-DHLA) and PEGDA solutions were combined to give a [SH]:[acrylate] ratio of 1:1, then heated to 37 °C for 20 minutes. The resulting hydrogels were swelled in pure water or PBS, which was changed several times to remove any uncross-linked material. The equilibrium water content (EWC) was determined by comparing the weight of the gel after swelling in water for 3 days to the weight of the dry gel. Equation **1** was used to determine EWC (as a percent):

$$\text{EWC (\%)} = \left(1 - \left(\frac{W_d}{W_s}\right)\right) \times 100 \tag{1}$$

where W_s and W_d are the weights of the swollen and dried gels, respectively. Excess water was removed from the hydrogel by gently wicking with filter paper. Dynamic mechanical analysis was used to characterized the physical properties of the hydrogels. PolyMPC-*co*-DHLA hydrogels were prepared with PEG$_{700}$DA as the cross-linker, with a polyMPC-*co*-DHLA concentration of 50 mg/mL in pH 9 borate buffer. The hydrogel samples were swelled to equilibrium for 48 hours. Frequency response tests were conducted at room temperature, from 0 - 10 Hz, and the storage (G') and loss (G") moduli were recorded.

- **Determination of lysozyme activity**

The activity of lysozyme, and lysozyme – polymer conjugates, was measured using the EnzChek® Lysozyme Assay kit purchased from Invitrogen. The samples were diluted in the reaction buffer provided, generating samples of protein equivalent concentrations, and incubated at 37 °C for 1 hour with the substrate *Micrococcus lysodeikticus* fluorescently

labeled with fluorescein. The fluorescence intensity of the digestion product was measured using excitation/emission wavelengths of 485/535 nm, respectively. The activities of the conjugates were determined from the relative fluorescence intensities.

- **Pharmacokinetics of PC-polymer protein conjugates**

All procedures were performed in accordance with NIH guidelines for the ethical treatment of animals, and were approved by the Baystate Medical Center Institutional Animal Care and Use Committee. The AF647-labeled lysozyme and linear polyMPC conjugate were injected into the lateral tail vein of C57bl/6 mice (~20 g) intravenously, at a dose of 1.5 mg/kg (AF647 concentration) with 6 mice in each group. At specified time points, 40 uL of blood was withdrawn from the tail vein, followed by centrifugation at 1500 g for 15 minutes at 4 °C to sediment the blood cells. The samples were stored at -80 °C until analysis. 10 µL of the plasma sample was diluted with 20 µL of PBS in a HPLC vial, and 25 µL of each diluted sample was injected into the HPLC and analyzed using a fluorescence detector, with excitation at 650 nm and emission at 670 nm. The area under the curve (AUC) for the conjugate was recorded and converted to concentration of AF dye using a calibration curve constructed from samples of known concentrations.

- **Drug release from polyMPC-*g*-CPT conjugates**

The CPT containing polymers were dissolved into different media at concentration of 3 mg/mL. The mixtures were incubated at 37˚C and aliquots (100 µL) were taken out at different time points. Twenty µL of the sample from PBS and cell culture media were analyzed on SEC-HPLC. The sample taken from mouse serum and human plasma were mixed with 200 uL of PBS and filtered through 0.45 µm filter membrane; 60 µL of the

filtrate was analyzed on SEC-HPLC. The stability profile was generated by plotting the percentage of remaining CPT on the polymer over a time course. The percentage was calculated based on the peak area of UV absorbance at 370 nm. The sample was also analyzed on RP-HPLC and the integrity (lactone vs carboxylate) of the released CPT was based on the retention times.

- **Cell culture of polyMPC-*g*-CPT conjugates**

The COLO 205 and OVCAR 3 cancer cells were cultured in RPMI-1640 medium supplemented with 10 % fetal bovine serum (FBS) or 20 % FBS and 0.01 mg/ml bovine insulin, while MCF7 cells were cultured in MEM medium supplemented with 10 % FBS and 0.01 mg/ml bovine insulin. All cells were grown in 5 % CO2 incubators at 37 ˚C. For in vitro cytotoxicity assays cells were seeded into 96 well plates and after reaching about 40 % cell density were incubated for 72-96 hours with varying camptothecin equivalent concentrations of polymer drug conjugates as well as polymer control (i.e., without drug attachment). Cell viability post-treatment was measured using CellTiter-Glo luminescent cell viability assays (Promega) as per manufacturer's instructions on a FLUOstar OPTIMA plate reader (BMG LABTECH). The percentage camptothecin mediated toxicity was calculated with respect to untreated cells, and graphed to give dose response curves. IC50 values for each treatment were then calculated using the GraphPad Prism4 statistical analysis software.

- **Determination of critical micelle concentration (CMC) for poly(MPC-*b*-DHLA)**

CMC was determined using a pyrene fluorescence probe. Briefly, a stock solution of pyrene in acetone (1.2 x 10^{-4} M) was prepared. Polymers **55 A-C** were dissolved in PBS,

and diluted from 5 mg/ml to 1.25 μg/mL, with each solution having a total volume of 1 mL. 5 μL of pyrene solution was added to each for a final pyrene concentration of 6 x 10^{-7} M. The polymer solutions were kept at 18 °C for 18 hours. An excitation spectrum was recorded of each solution from 300-360 nm at a scan rate of 100 nm/s, with emission set to 394 nm. CMC was determined by plotting log(concentration) vs. the ratio of the intensities at 339 and 334 nm.

- **CPT release from cross-linked polyMPC-*b*-DHLA micelles**

Release of CPT from the polymer micelles was monitored by dialysis. Briefly, lyophilized polymer micelles containing CPT were dissolved in PBS (1 mL). The solution was transferred to a dialysis cassette (MWCO 3500) by syringe. The cassette was suspended in a sealed container with 300 mL of PB, or PBS containing 3 mM DTT. Containers were kept in a water bath at 37 °C, and at select time points 1 mL aliquots were removed from the external media and replaced with fresh buffer. The fluorescence intensity at 440 nm (λ_{ex}=370 nm) was monitored, and the experiments were carried out until a plateau was reached.

- **Cell culture of CPT-loaded polyMPC-*b*-DHLA micelles**

COLO205 cancer cells were cultured in RPMI-1640 medium supplemented with 10% fetal bovine serum (FBS), while MCF7 cells were cultured in MEM medium supplemented with 10% FBS and 0.01 mg/mL bovine insulin. All cells were grown in 5 % CO2 incubators at 37 °C. For in vitro cytotoxicity assays, cells were seeded in 96 well plates, and after reaching about 40 % cell density were incubated for 72 hours with varying camptothecin equivalent concentrations of prodrug micelles, as well as control samples, including polymer only and polymer micelles (physically entrapped CPT). Cell

viability post-treatment was measured using CellTiter-Glo luminescence cell viability assay (Promega) following the manufacturer instructions on a FLUOstar OPTIMA plate reader (BMG LABTECH). The CPT-mediated toxicity was calculated with respect to untreated cells, and graphed to give dose-response curves. IC_{50} values for each treatment were then calculated using GraphPad Prism4 statistical analysis software.

- **Pharmacokinetics of polyMPC-DOX**

All experiments were performed in accordance with protocols approved by the Baystate Institutional Animal Care and Use Committee. Four week old BALB/c female mice were injected subcutaneously into the right flank with 5 x 10^6 4T1 murine breast cancer cells suspended in 100 µL of Hank's Balanced Salt Solution (HBSS). Once tumors reached a size of 100-300 mm^3 (calculated by L x W^2 x π/6), mice were injected through the lateral tail vein with 100 µL HBSS, free doxorubicin (6 mg/kg), or polyMPC-DOX (6 mg/kg, DOX equivalent) (n=8/treatment). Blood samples (30-50 µL) were taken from the submandibular vein prior to injection, and then 30 minutes, 2 hours, 6 hours, 12 hours, 1 day, 2 days, 3 days, and 5 days post-injection. Blood samples were clotted on ice and centrifuged at 1500 x g for 15 minutes at 4 ˚C. Serum was collected and stored at -80 ˚C until HPLC analysis to determine doxorubicin concentration. On day 3 and day 5 post-injection, mice were euthanized from each treatment group. For HPLC analysis, 10 µL of each serum sample was diluted with 90 µL of HPLC mobile phase (40 % acetonitrile in water + 1 % trifluoroacetic acid), and incubated at room temperature for 2 hours, then overnight at 4 °C. Samples were centrifuged to sediment residual debris, and 25 µL was injected on the HPLC fitted with a reverse phase (C18) column, and monitoring with

fluorescence detection (480/580 nm, ex/em). DOX concentration was determined using a calibration curve, then plotted against post-injection time to generate the PK profile.

- **Immunogenicity of polyMPC-DOX**

Following completion of the PK study, blood from each mouse was collected by cardiac puncture (800 µL), and a complete blood count (CBC) was performed on 500 µl using the VetScan HM5. The remainder of the samples were allowed to clot on ice, centrifuged at 1500 x g for 15 minutes at 4 ˚C, serum was collected and stored at -80 ˚C for ELISA of cytokine responses.

- **Biodistribution of polyMPC-DOX**

Tumors, hearts, livers, lungs, kidneys, and spleens, were collected, weighed, and frozen in liquid nitrogen. Livers and spleens were divided and half of each tissue was additionally fixed in 10% buffered formalin overnight at 4 ˚C, transferred to 70 % EtOH at 4 ˚C, and paraffin embedded for histological analysis. Frozen tissues were homogenized at maximum speed in acidified isopropanol (90 % isopropanol containing 0.6 mL concentrated HCl). Samples were then centrifuged at 1500 x g for 15 minutes at 4 ˚C, and the upper aqueous phase was collected and stored at -80 ˚C until HPLC analysis of doxorubicin concentration. 50 µL of each tissue homogenate was transferred to a clean vial, and the IPA was evaporated under a stream of nitrogen, and redissolved in 50 µL of HPLC mobile phase (40 % acetonitrile in water + 1 % trifluoroacetic acid). Samples were centrifuged for 30 minutes at 12,000 rpm to sediment precipitated proteins and cell debris. 25 µL was injected in the HPLC equipped with a reverse phase (C18

column), monitoring with fluorescence detection. DOX concentration was calculated using a calibration curve, then normalized per gram of tissue.

- **Antitumor efficacy of polyMPC-DOX in 4T1 tumor-bearing mice**

Four week old BALB/c female mice were injected into lower right mammary fat pad with 5×10^6 4T1 murine breast cancer cells suspended in 100 µL of Hank's Balanced Salt Solution (HBSS). Once tumors reached a size of 42-132 mm^3 (calculated by L x W^2 x π/6), mice were injected through the lateral tail vein with free doxorubicin (3mg/kg), polyMPC-DOX (15mg/kg DOX equivalent), or HBSS (control) (n=15/treatment). A second injection of the same concentration was given on Day 7, and mice treated with polyMPC-DOX received a third dose on Day 17. Animals were monitored for signs of distress, and body weights and tumor measurements were collected every 2 days. Upon completion, tumors, hearts, livers, lungs, kidneys, and spleens, were collected, weighed, and fixed in 10 % buffered formalin overnight at 4 ˚C, transferred to 70 % EtOH at 4 ˚C, and paraffin embedded for histological analysis.

- **Cell culture, cell density, and proliferation studies for polyMPC hydrogels**

Mouse skeletal muscle myoblasts C2C12 cells were cultured in growth medium (Dulbecco's Modified Eagles Medium, DMEM), while human ovarian adenocarcinoma SKOV3 cells were cultured in growth medium (McCoy's 5A) supplemented with 10 % Fetal Bovine Serum (FBS) and Penicillin and Streptomycin, at 37 °C in a 5 % CO$_2$ incubator. Gels were prepared in a tissue culture 24-well plate, according to the general procedure described previously, with a final solution volume of 200 µL. The 24-well plate was incubated at 37 °C for 20 minutes. The gels were rinsed and swollen in PBS for 18 hours. The hydrogels were washed twice with sterile growth medium, and were

incubated with growth medium for 2 hours at 37 °C in 5 % CO_2 incubator. The medium was then replaced with 1 mL growth medium containing 10×10^4 proliferating C2C12 or SKOV3 cells and incubated at 37 °C for up to 24 hours. Cell spreading and proliferation were visualized by optical microscopy. Percent cell density was determined using the CellTiter-Glo reagent and a luminescence plate reader.

5.4 References

1.   Ishihara, K.; Ueda, T.; Nakabayashi, N. Preparation of phospholipid polymers and their properties as polymer hydrogel membranes. *Polymer Journal* **1990** *22*, 355-60.

2.   Nicolas, J.; Miguel, V. S.; Mantovani, G.; Haddleton, D. M. Fluorescently tagged polymer bioconjugates from protein derived macroinitiators. *Chemical Communications* **2006** 4697–9.

3.   Kratz, K.; Breitenkamp, K.; Hule, R.; Pochan, D.; Emrick, T. PC-Polyolefins: Synthesis and Assembly Behavior in Water. *Macromolecules* **2009**, *42*, 3227-9.

4.   Hillmyer, M. A.; Laredo, W. R.; Grubbs, R. H. Ring-Opening Metathesis Polymerization of Functionalized Cyclooctenes by a Ruthenium-Based Metathesis Catalyst. *Macromolecules* **1995**, *28*, 6311-16.

5.   Love, J.; Morgan, J.; Trnka, T.; Grubbs, R. A practical and highly active ruthenium-based catalyst that effects the cross metathesis of acrylonitrile. *Angewandte Chemie (International ed. in English)* **2002**, *41*, 4035–7.

6.   Ladmiral, V.; Mantovani, G.; Clarkson, G.; Cauet, S.; Irwin, J.; Haddleton, D. Synthesis of neoglycopolymers by a combination of "click chemistry" and living radical polymerization. *Journal of the American Chemical Society* **2006**, *128*, 4823–30.

7.   Parrish, B.; Emrick, T. Soluble camptothecin derivatives prepared by click cycloaddition chemistry on functional aliphatic polyesters. *Bioconjugate Chemistry* **2006**, *18*, 263–7.

8.   Digilio, G.; Menchise, V.; Gianolio, E.; Catanzaro, V.; Carrera, C.; Napolitano, R.; Fedeli, F.; Aime, S. Exofacial protein thiols as a route for the internalization of Gd(III)-based complexes for magnetic resonance imaging cell labeling. *Journal of Medicinal Chemistry* **2010**, *53*, 4877–90.

9.   Cabral, H.; Nakanishi, M.; Kumagai, M.; Jang, W.-D.; Nishiyama, N.; Kataoka, K. A photo-activated targeting chemotherapy using glutathione sensitive camptothecin-loaded polymeric micelles. *Pharmaceutical Research* **2008**, *26*, 82–92.

BIBLIOGRAPHY

Abuchowski, A.; Davis, F.F. Preparation and properties of polyethylene glycol-trypsin adducts. *Biochimica et Biophysica Acta* **1979**, *578*, 41-46.

Abuchowski, A.; Karp, D.; Davis, F.F. Reduction of plasma urate levels in the cockerel with polyethylene glycol-uricase. *Journal of Pharmacology and Experimental Therapeutics* **1981**, *219*, 352-354.

Abuchowski, A.; van Es, T.; Palczuk, N.C.; Davis, F.F. Alteration of immunological properties of bovine serum albumin by covalent attachment of polyethylene glycol. *Journal of Biological Chemistry* **1977**, *252*, 3578-3581.

Alakhov, V.; Klinski, E.; Li, S.; Pietrzynski, G.; Venne, A.; Batrakova, E.V.; Bronitch, T.; Kabanov, A.V. Block copolymer-based formulation of doxorubicin. From cell screen to clinical trials. *Colloids and Surfaces B: Biointerfaces* **1999**, *16*, 113-34.

Bae, Y.; Fukushima, S.; Harada, A.; Kataoka, K. Design of environment-sensitive supramolecular assemblies for intracellular drug delivery: polymeric micelles that are responsive to intracellular pH change. *Angewandte Chemie (International ed. in English)* **2003**, *42*, 4640–3.

Barckyz, M.; Carracedo, S.; Gullberg, D. Integrins. *Cell Tissue Research* **2010**, *339,* 269-280.

Berry, G.; Billingham, M.; Alderman, E.; Richardson, P.; Torti, F.; Lum, B.; Patek, A.; Martin, F. The use of cardiac biopsy to demonstrate reduced cardiotoxicity in AIDS Kaposi's sarcoma patients treated with pegylated liposomal doxorubicin. *Annals of Oncology* **1998**, *9*, 711–6.

Bhadra, D.; Bhadra, S.; Jain, S.; Jain, N.K. Pegnology: a review of PEG-ylated systems. *International Journal of Pharmaceutics* **2003**, *257*, 111-24.

Bhatt, R.; de Vries, P.; Tulinsky, J.; Bellamy, G.; Baker, B.; Singer, J.; Klein, P. Synthesis and in vivo antitumor activity of poly(l-glutamic acid) conjugates of 20S-camptothecin. *Journal of Medicinal Chemistry* **2003**, *46*, 190–3.

Bissett, D.; Cassidy, J.; Bono, J.S.; Muirhead, F.; Main, M.; Robson, L.; Fraier, D.; Magne, M.L.; Pellizzoni, C.; Porro, M.G.; Spinelli, R.; Speed, W.; Twelves, C. Phase I and pharmacokinetic (PK) study of MAG-CPT (PNU 166148): a polymeric derivative of camptothecin (CPT). *British Journal of Cancer* **2004**, *91*, 50-5.

Bontempo, D.; Li, R.C.; Ly, T.; Brubaker, C.E.; Maynard, H.D. One-step synthesis of low polydispersity, biotinylated poly(N-isopropylacrylamide) by ATRP *Chemical Communications* **2005**, *37*, 4702-4704.

152

Bontempo, D.; Maynard, H. Streptavidin as a macroinitiator for polymerization: in situ protein-polymer conjugate formation. *Journal of the American Chemical Society* **2005**, *127*, 6508–9.

Bridges, A.; García, A. Anti-inflammatory polymeric coatings for implantable biomaterials and devices. *Journal of Diabetes Science and Technology* **2008**, *2*, 984–94.

Bryant, S.; Cuy, J.; Hauch, K.; Ratner, B. Photo-patterning of porous hydrogels for tissue engineering. *Biomaterials* **2007**, *28*, 2978–86.

Bukowski, R.; Tendler, C.; Cutler, D.; Rose, E.; Laughlin, M.; Statkevich, P. Treating cancer with PEG Intron: pharmacokinetic profile and dosing guidelines for an improved interferon-alpha-2b formulation. *Cancer* **2002**, *95*, 389–96.

Burdick, J.; Anseth, K. Photoencapsulation of osteoblasts in injectable RGD-modified PEG hydrogels for bone tissue engineering. *Biomaterials* **2002**, *23*, 4315–23.

Cabral, H.; Nakanishi, M.; Kumagai, M.; Jang, W.-D.; Nishiyama, N.; Kataoka, K. A photo- activated targeting chemotherapy using glutathione sensitive camptothecin-loaded polymer micelles. *Pharmaceutical Research* **2008**, *26*, 82-92.

Caiolfa, V. R.; Zamai, M.; Fiorino, A.; Frigerio, E.; Pellizzoni, C.; d'Argy, R.; Ghiglieri, A.; Castelli, M. G.; Farao, M.; Pesenti, E.; Gigli, M.; Angelucci, F.; Suarato, A. *In 9th International Symposium on Recent Advances in Drug Delivery Systems*; Elsevier Science: Salt Lake City, Utah, **1999**, 105-19.

Caliceti, P.; Veronese, F. Pharmacokinetic and biodistribution properties of poly(ethylene glycol)-protein conjugates. *Advanced Drug Delivery Reviews* **2003**, *55*, 1261–77.

Carrico, I.S.; Carlson, B.L.; Bertozzi, C.R. Introducing genetically encoded aldehydes into proteins. *Nature Chemical Biology* **2007**, *3*, 321-322.

Cascone, M. G.; Laus, M.; Ricci, D.; Guerra, R. S. D. Evaluation of poly(vinyl alcohol) hydrogels as a component of hybrid artificial tissues. *Journal of Materials Science: Materials in Medicine* **1995**, *6*, 71-75.

Casey, R.; Skubitz, A. CD44 and beta1 integrins mediate ovarian carcinoma cell migration toward extracellular matrix proteins. *Clinical and Experimental Metastasis* **1999**, *18*, 67–75.

Charles, S.A.; (Oligasis Corporation, USA). US Patent Application Publication US 2010/0166700 A1, July 1, 2010.

Chen, M.; Briscoe, W.; Armes, S.; Klein, J. Lubrication at physiological pressures by polyzwitterionic brushes. *Science* **2009**, *323*, 1698–701.

Chen, X.; Lawrence, J.; Parelkar, S.; Emrick, T. Novel Zwitterionic Copolymers with Dihydrolipoic Acid: Synthesis and Preparation of Nonfouling Nanorods. *Macromolecules* **2012**, *46*, 119-27.

Chen, X.; McRae, S.; Parelkar, S.; Emrick, T. Polymeric phosphorylcholine-camptothecin conjugates prepared by controlled free radical polymerization and click chemistry. *Bioconjugate Chemistry* **2009**, *20*, 2331–41.

Chen, X.; McRae, S.; Samanta, D.; Emrick, T. Polymer−Protein Conjugation in Ionic Liquids. *Macromolecules* **2010**, *43*, 6261-3.

Chen, X.; Parelkar, S.; Henchey, E.; Schneider, S.; Emrick, T. PolyMPC-Doxorubicin Prodrugs. *Bioconjugate Chemistry* **2012**, *23*, 1753-63.

Cheng, J.; Khin, K.; Davis, M. Antitumor activity of beta-cyclodextrin polymer-camptothecin conjugates. *Molecular Pharmaceutics* **2003**, *1*, 183–93.

Cheng, J.; Khin, K.; Jensen, G.; Liu, A.; Davis, M. Synthesis of linear, beta-cyclodextrin-based polymers and their camptothecin conjugates. *Bioconjugate Chemistry* **2002**, *14*, 1007–17.

Cheng, R.; Feng, F.; Meng, F.; Deng, C.; Feijen, J.; Zhong, Z. Glutathione-responsive nano-vehicles as a promising platform for targeted intracellular drug and gene delivery. *Journal of Controlled Release* **2011**, *152*, 2-12.

Christian, D.A.; Cai, S.; Garbuzenko, O.B.; Harada, T.; Zajac, A.L.; Minko, T.; Discher, D.E. Flexible Filaments for in Vivo Imaging and Delivery: Persistent Circulation of Filomicelles Opens the Dosage Window for Sustained Tumor Shrinkage. *Molecular Pharmaceutics* **2009**, *6*, 1343-52.

Chu, H.; Liu, N.; Wang, X.; Jiao, Z.; Chen, Z. Morphology and in vitro release kinetics of drug-loaded micelles based on well-defined PMPC-b-PBMA copolymer. *International Journal of Pharmaceutics* **2009**, *371*, 190-6.

Convertine, A.J.; Diab, C.; Prieve, M.; Paschal, A.; Hoffman, A.S.; Johnson, P.H.; Stayton, P.S. pH-Responsive polymeric micelle carriers for siRNA drugs. *Biomacromolecules* **2010**, *11*, 2904-11.

Court, J.; Redman, R.; Wang, J.; Leppard, S.; Obyrne, V.; Small, S.; Lewis, A.; Jones, S.; Stratford, P. A novel phosphorylcholine-coated contact lens for extended wear use. *Biomaterials* **2001**, *22*, 3261–72.

Cruise, G.; Scharp, D.; Hubbell, J. Characterization of permeability and network structure of interfacially photopolymerized poly(ethylene glycol) diacrylate hydrogels. *Biomaterials* **1998**, *19*, 1287–94.

da Silva Freitas, D.; Abrahao-Neto, J. Biochemical and biophysical characterization of lysozyme modified by PEGylation. *International Journal of Pharmaceutics* **2010**, *392*, 111-117.

Davis, M.E.; Chen, Z.; Shin, D.M. Nanoparticle therapeutics: an emerging treatment modality for cancer. *Nature Reviews Drug Discovery* **2008**, *7*, 771-82.

Davis, S.; Abuchowski, A.; Park, Y.K.; Davis, F.F. Alteration of the circulating life and antigenic properties of bovine adenosine deaminase in mice by attachment of polyethylene glycol. *Clinical and Experimental Immunology* **1981**, *46*, 649-52.

Digilio, G.; Menchise, V.; Gianolo, E.; Catanzaro, V.; Carrera, C.; Napolitano, R.; Fedeli, F.; Aime, S. Exofacial protein thiols as a route for the internalization of Gd(III)-based complexes for magnetic resonance imaging cell labeling. *Journal of Medicinal Chemistry* **2010**, *53*, 4877-90.

Dirksen, A.; Dawson, P.E. Rapid oxime and hydrazone ligations with aromatic aldehydes for biomolecular labeling. *Bioconjugate Chemistry* **2008**, *19*, 2543-2548.

Duncan, R. Polymer conjugates as anticancer nanomedicines. *Nature Reviews Cancer* **2006**, *6*, 688-701.

Duncan, R. The dawning era of polymer therapeutics. *Nature Reviews Drug Discovery* **2003**, *2*, 347-60.

Duncan, R.; Ringsdorf, H.; Satchi-Fainaro, R. Polymer Therapeutics - Polymers as Drugs, Conjugates and Gene Delivery Systems: Past, present and future opportunities. *Advanced in Polymer Science* **2006**, *192*, 1-8.

Duong, H.T.T.; Nguyen, T.L.U.; Stenzel, M.H. Micelles with surface conjugated RGD peptide and crosslinked polyurea core via RAFT polymerization. *Polymer Chemistry* **2010**, *1*, 171-82.

Eberhardt, M.; Mruk, R.; Zentel, R.; Théato, P. Synthesis of pentafluorophenyl(meth)acrylate polymers: New precursor polymers for the synthesis of multifunctional materials. *European Polymer Journal* **2005**, *41*, 1569-1575.

Eberhardt, M.; Théato, P. RAFT Polymerization of Pentafluorophenyl Methacrylate: Preparation of Reactive Linear Diblock Copolymers. *Macromolecular Rapid Communications* **2005**, *26*, 1488-1493.

Ehrick, J.; Deo, S.; Browning, T.; Bachas, L.; Madou, M.; Daunert, S. Genetically engineered protein in hydrogels tailors stimuli-responsive characteristics. *Nature Materials* **2005**, *4*, 298–302.

Elbayoumi, T. A.; Torchilin, V. P. Tumor-specific antibody-mediated targeted delivery of Doxil® reduces the manifestation of auricular erythema side effect in mice. *International Journal of Pharmaceutics* **2008**, *357*, 272-279.

Ellman, G.L. Tissue Sulfhydryl groups. *Archives of Biochemistry and Biophysics* **1959**, *82*, 70-7.

Engin, K.; Leeper, D.B.; Cater, J.R.; Thistlethwaite, A.J.; Tupchong, L.; McFarlane, J.D. *International Journal of Hyperthermia* **1995**, *11*, 211-6.

Etrych, T.; Jelínková, M.; Ríhová, B.; Ulbrich, K. New HPMA copolymers containing doxorubicin bound via pH-sensitive linkage: synthesis and preliminary in vitro and in vivo biological properties. *Journal of Controlled Release* **2001**, *73*, 89–102.

Etrych, T.; Sirova, M.; Starovoytova, L.; Rihova, B.; Ulbrich, K. HPMA Copolymer Conjugates of Paclitaxel and Docetaxel with pH-Controlled Drug Release. *Molecular Pharmaceutics* **2010**, *7*, 1015-26.

Gao, H.; Matyjaszewski, K. Synthesis of Star Polymers by a Combination of ATRP and the "Click" Coupling Method. *Macromolecules* **2006**, *39*, 4960-5.

Gao, Z.-G.; Tian, L.; Park, I.-S.; Bae, Y.H. Prevention of metastasis in 4T1 murine breast cancer model by doxorubicin carried by folate conjugated pH sensitive polymeric micelles. *Journal of Controlled Release* **2011**, *152*, 84-9.

Gibson, M. I.; Fröhlich, E.; Klok, H.-A. Postpolymerization modification of poly(pentafluorophenyl methacrylate): Synthesis of a diverse water-soluble polymer library. *Journal of Polymer Science Part A: Polymer Chemistry* **2009**, *47*, 4332-4345.

Glenn, H.; Wang, Z.; Schwartz, L. Acheron, a Lupus antigen family member, regulates integrin expression, adhesion, and motility in differentiating myoblasts. *American Journal of Physiology. Cell Physiology* **2009**, *298*, C46–55.

Goda, T.; Furukawa, H.; Gong, J. P.; Ishihara, K. Relaxation modes in chemically cross-linked poly(2-methacryloyloxyethyl phosphorylcholine) hydrogels. *Soft Matter* **2013**, *9*, 2166-2171.

Gohy, J.- F. Block Copolymer Micelles. *Advances in Polymer Science* **2005**, *190,* 65-136.

Greenwald, R. B.; Pendri, A.; Conover, C. D.; Lee, C.; Choe, Y. H.; Gilbert, C.; Martinez, A.; Xia, J.; Wu, D. C.; Hsue, M. Camptothecin-20-PEG ester transport forms: the effect of spacer groups on antitumor activity. *Bioorganic and Medicinal Chemistry* **1998**, *6*, 551-62.

Greenwald, R.; Pendri, A.; Conover, C.; Gilbert, C.; Yang, R.; Xia, J. Drug delivery systems. 2. Camptothecin 20-O-poly(ethylene glycol) ester transport forms. *Journal of Medicinal Chemistry* **1996**, *39*, 1938–40.

Greenwald, R.B.; Choe, Y.H.; McGuire, J.; Conover, C.D. Effective drug delivery by PEGylated drug conjugates. *Advanced Drug Delivery Reviews* **2003**, *55*, 217-50.

Guillaudeu, S.; Fox, M.; Haidar, Y.; Dy, E.; Szoka, F.; Fréchet, J. PEGylated dendrimers with core functionality for biological applications. *Bioconjugate Chemistry* **2008**, *19*, 461–9.

Gupta, K.; Barnes, S.; Tangaro, R.; Roberts, M.; Owen, D.; Katz, D.; Kiser, P. Temperature and pH sensitive hydrogels: an approach towards smart semen-triggered vaginal microbicidal vehicles. *Journal of pharmaceutical sciences* **2007**, *96*, 670–81.

Hamilton, A.; Biganzoli, L.; Coleman, R.; Mauriac, L.; Hennebert, P.; Awada, A.; Nooij, M.; Beex, L.; Piccart, M.; Van Hoorebeeck, I.; Bruning, P.; de Valeriola, D. EORTC 10968: a phase I clinical and pharmacokinetic study of polyethylene glycol liposomal doxorubicin (Caelyx, Doxil) at a 6-week interval in patients with metastatic breast cancer. *Annals of Oncology* **2002**, *13*, 910–8.

Han, I.; Han, M.-H.; Kim, J.; Lew, S.; Lee, Y.; Horkay, F.; Magda, J. Constant-volume hydrogel osmometer: a new device concept for miniature biosensors. *Biomacromolecules* **2001**, *3*, 1271–5.

Henselwood, F.; Liu, G. Water-soluble nanospheres of poly(2-cinnamoylethyl methacrylate)-block-poly(acrylic acid). *Macromolecules* **1997**, *30*, 488-93.

Herben, V. M. M.; Huinink, W.; Beijnen, J. H. Clinical pharmacokinetics of topotecan. *Clinical Pharmacokinetics* **1996**, *31*, 85-102.

Heredia, K.; Bontempo, D.; Ly, T.; Byers, J.; Halstenberg, S.; Maynard, H. In situ preparation of protein-"smart" polymer conjugates with retention of bioactivity. *Journal of the American Chemical Society* **2005**, *127*, 16955–60.

Heredia, K.L.; Tolstyka, Z.P.; Maynard, H.D. Aminooxy end-functionalized polymers synthesized by ATRP for chemoselective conjugation to proteins. *Macromolecules* **2007**, *40*, 4772-4779.

Hermanson, G.T. *Bioconjugate Techniques* **1996**, *Academic Press, Inc.*, 139-140.

Herrick, W.; Nguyen, T.; Sleiman, M.; McRae, S.; Emrick, T.; Peyton, S. PEG-Phosphorylcholine Hydrogels As Tunable and Versatile Platforms for Mechanobiology. *Biomacromolecules* **2013**, *14*, 2294–304.

Hersel, U.; Dahmen, C.; Kessler, H. RGD modified polymers: biomaterials for stimulated cell adhesion and beyond. *Biomaterials* **2003**, *24*, 4385–415.

Hillmyer, M. A.; Laredo, W. R.; Grubbs, R. H. Ring-Opening Metathesis Polymerization of Functionalized Cyclooctenes by a Ruthenium-Based Metathesis Catalyst. *Macromolecules* **1995**, *28*, 6311-6.

Hilmer, S.N.; Cogger, V.C.; Muller, M.; Le Couteur, D.G. The hepatic pharmacokinetics of doxorubicin and liposomal doxorubicin. *Drug Metabolism and Disposition* **2004**, *32*, 794-9.

Hinds, K.; Kim, S. Effects of PEG conjugation on insulin properties. *Advanced Drug Delivery Reviews* **2002**, *54*, 505–30.

Hu, X.; Li, H.; Luo, S.; Liu, T.; Jiang, Y.; Liu, S. Thiol and pH dual-responsive dynamic covalent shell cross-linked micelles for triggered release of chemotherapeutic drugs. *Polymer Chemistry* **2013**, *4*, 695-706.

Iijima, M.; Nagasaki, Y.; Okada, T.; Kato, M.; Kataoka, K. Core-polymerized reactive micelles from heterotelechelic amphiphilic block copolymers. *Macromolecules* **1999**, *32*, 1140-6.

Ikada, Y. Surface modification of polymers for medical applications. *Biomaterials* **1994**, *15*, 725–36.

Ishihara, K. New polymeric biomaterials - phospholipid polymers with a biocompatible surface. *Frontiers of Medical and Biological Engineering* **2000**, *10*, 83-95.

Ishihara, K.; Iwasaki, Y. J. Reduced protein adsorption on novel phospholipid polymers. *Journal of Biomaterials Applications* **1998**, *13*, 111-127.

Ishihara, K.; Nomura, H.; Mihara, T.; Kurita, K.; Iwasaki, Y.; Nakabayashi, N. Why do phospholipid polymers reduce protein adsorption? *Journal of Biomedical Materials Research* **1998**, *39*, 323–30.

Ishihara, K.; Takai, M. Bioinspired interface for nanobiodevices based on phospholipid polymer chemistry. *Journal of the Royal Society Interface* **2009**, *6*, S279-S291.

Ishihara, K.; Ueda, T.; Nakabayashi, N. Preparation of phospholipid polymers and their properties as polymer hydrogel membranes. *Polymer Journal* **1990**, *22*, 355-360.

Ito, H.; Arimoto, K.; Sensul, H.; Hosomi, A. Direct alkynyl group transfer from silicon to copper: New preparation method of alkynylcopper (I) reagents. *Tetrahedron Letters* **1997**, *38*, 3977-80.

Iwasaki, Y.; Ishihara, K. Phosphorylcholine-containing polymers for biomedical applications. *Analytical and Bioanalytical Chemistry* **2005**, *381*, 534–46.

Jatzkewitz, H. Peptamin (glycyl-L-leucyl-mescaline) bound to blood plasma expander (polyvinylpyrrolidone) as a new depot form of a biologically active primary amine (mescaline). *Z. Naturforsch* **1955**, *10b*, 27-31.

Jevsevar, S.; Kunstelj, M.; Porekar, V. PEGylation of therapeutic proteins. *Biotechnology Journal* **2009**, *5*, 113–28.

Jones, M.-C.; Leroux, J.-C. Polymeric micelles-a new generation of colloidal drug carriers. *European Journal of Pharmaceutics and Biopharmaceutics* **1999**, *48*, 101-11.

Joralemon, M.J.; McRae, S.; Emrick, T. PEGylated Polymers for Medicine: From conjugation to self-assembled systems. *Chemical Communications*, **2010**, *46*, 1377-93.

Kabanov, A.; Batrakova, E.; Alakhov, V. Pluronic block copolymers as novel polymer therapeutics for drug and gene delivery. *Journal of Controlled Release* **2002**, *82*, 189–212.

Kakizawa, Y.; Harada, A.; Kataoka, K. Environment-sensitive stabilization of core-chell structured polyion complex micelle by reverible cross-linking of the core throughdisulfide bond. *Journal of the American Chemical Society* **1999**, *121*, 11247-8.

Katre, N.V. The conjugation of proteins with polyethylene glycol and other polymers. *Advanced Drug Delivery Reviews* **1993**, *10*, 91-114.

Kessler, D.; Roth, P.; Theato, P. Reactive surface coatings based on polysilsesquioxanes: controlled functionalization for specific protein immobilization. *Langmuir : the ACS journal of surfaces and colloids* **2009**, *25*, 10068–76.

Kiew, L.V.; Cheong, S.K.; Ramli, E.; Sidik, K.; Lim, T.M.; Chung, L.Y. Efficacy of Poly-L-Glutamic Acid-Gemcitabine Conjugate in Tumor-Bearing Mice. *Drug Developement Research* **2012**, *73*, 120-9.

Kimura, M.; Fukumoto, K.; Watanabe, J.; Takai, M.; Ishihara, K. Spontaneously forming hydrogel from water-soluble random- and block-type phospholipid polymers. *Biomaterials* **2005**, *26*, 6853–62.

Kiritoshi, Y.; Ishihara, K. Preparation of cross-linked biocompatible poly(2-methacryloyloxyethyl phosphorylcholine) gel and its strange swelling behavior in water/ethanol mixture. *Journal of Biomaterials Science. Polymer Edition* **2001**, *13*, 213–24.

Kiritoshi, Y.; Ishihara, K. Synthesis of hydrophilic cross-linker having phosphorylcholine-like linkage for improvement of hydrogel properties. *Polymer* **2004**, *45*, 7499-7504.

Kisfaludy, L.; Schon, I. Preparation and applications of pentafluorophenyl esters of 9-fluorenylmethyloxycarbonyl amino acids for peptide synthesis. *Synthesis* **1983**, *4*, 325-327.

Kochendoerfer, G.G.; Chen, S.-Y.; Mao, F.; Cressman, S.; Traviglia, S.; Shao, H.; Hunter, C.L.; Low, D.W.; Cagle, E.N.; Carnevali, M.; Gueriguian, V.; Keogh, P.J.; Porter, H.; Stratton, S.M.; Wiedeke, M.C.; Wilken, J.; Tang, J.; Levy, J.J.; Miranda, L.P.; Crnogorac, M.M.; Kalbag, S.; Botti, P.; Schindler-Horvat, J.; Savatski, L.; Adamson, J.W.; Kung, A.; Kent, S.B.H.; Bradburne, J.A. Design and chemical synthesis of a homogenous polymer-modified erythropoiesis protein. *Science* **2003**, *299*, 884-887.

Konna, T.; Watanabe, J.; Ishihara, K. Enhanced solubility of paclitaxel using water-soluble and biocompatible 2-methacryloyloxyethyl phosphorylcholine polymers. *Journal of Biomedical Materials Research Part A* **2002**, *65*, 209-14.

Kopecek, J.; Kopeckova, P.; Minko, T.; Lu, Z. HPMA copolymer-anticancer drug conjugates: design, activity, and mechanism of action. *European Journal of Pharmaceutics and Biopharmaceutics* **2006**, *50*, 61-81.

Kratz, F.; Azab, S.; Zeisig, R.; Fichtner, I.; Warnecke, A. Evaluation of combination therapy schedules of doxorubicin and an acid-sensitive albumin-binding prodrug of doxorubicin in the MIA PaCa-2 pancreatic xenograft model. *International Journal of Pharmaceutics* **2013**, *441*, 499-506.

Kratz, K.; Breitenkamp, K.; Hule, R.; Pochan, D.; Emrick, T. PC-Polyolefins: Synthesis and Assembly Behavior in Water. *Macromolecules* **2009**, *42*, 3227-9.

Ladmiral, V.; Mantovani, G.; Clarkson, G.; Cauet, S.; Irwin, J.; Haddleton, D. Synthesis of neoglycopolymers by a combination of "click chemistry" and living radical polymerization. *Journal of the American Chemical Society* **2006**, *128*, 4823–30.

Lee, C.; Gillies, E.; Fox, M.; Guillaudeu, S.; Fréchet, J.; Dy, E.; Szoka, F. A single dose of doxorubicin-functionalized bow-tie dendrimer cures mice bearing C-26 colon carcinomas. *Proceedings of the National Academy of Sciences of the United States of America* **2006**, *103*, 16649–54.

Lee, K.; Mooney, D. Hydrogels for tissue engineering. *Chemical Reviews* **2001**, *101*, 1869–79.

Lee, W.-C.; Li, Y.-C.; Chu, I.-M. Amphiphilic poly(D,L-lactic acid)/poly(ethylene glycol)/poly(D,L-lactic acid) nanogels for controlled release of hydrophobic drugs. *Macromolecular Bioscience* **2006**, *6*, 846-54.

Lewis, A. L. Phosphorylcholine-based polymers and their use in the prevention of biofouling. *Colloids and surfaces. B, Biointerfaces* **2000**, *18*, 261–75.

Lewis, A.; Tang, Y.; Brocchini, S.; Choi, J.; Godwin, A. Poly(2-methacryloyloxyethyl phosphorylcholine) for protein conjugation. *Bioconjugate Chemistry* **2008**, *19*, 2144-55.

Li, L.; Wang, J.-H.; Xin, Z. Synthesis and biocompatibility of a novel silicone hydrogel containing phosphorylcholine. *European Polymer Journal* **2011**, *47*, 1795-1803.

Li, Y.T.; Lokitz, B.S.; McCormick, C.L. RAFT synthesis of a thermally responsive ABC triblock copolymer incorporating N-acryloxysuccinimide for facile in situ formation of shell cross-linked micelles in aqueous media. *Macromolecules* **2006**, *39*, 81-9.

Licciardi, M.; Tang, Y.; Billingham, N.; Armes, S.; Lewis, A. Synthesis of novel folic acid-functionalized biocompatible block copolymers by atom transfer radical polymerization for gene delivery and encapsulation of hydrophobic drugs. *Biomacromolecules* **2004**, *6*, 1085–96.

Lin, C.-C.; Anseth, K. PEG hydrogels for the controlled release of biomolecules in regenerative medicine. *Pharmaceutical Research* **2009**, *26*, 631–43.

Liu, Z.; Chen, K.; Davis, C.; Sherlock, S.; Cao, Q.; Chen, X.; Dai, H. Drug delivery with carbon nanotubes for in vivo cancer treatment. *Cancer Research* **2008**, *68*, 6652-60.

Lobb, E.; Ma, I.; Billingham, N.; Armes, S.; Lewis, A. Facile synthesis of well-defined, biocompatible phosphorylcholine-based methacrylate copolymers via atom transfer radical polymerization at 20 degrees C. *Journal of the American Chemical Society* **2001**, *123*, 7913–4.

Lotem, M.; Hubert, A.; Lyass, O.; Goldenhersh, M.A.; Ingber, A.; Peretz, T.; Gabizon, A. Skin toxic effects of polyethylene glycol-coated liposomal doxorubicin. *Archives of Dermatology* **2000**, *11*, 1029-33.

Love, J.; Morgan, J.; Trnka, T.; Grubbs, R. A practical and highly active ruthenium-based catalyst that effects the cross metathesis of acrylonitrile. *Angewandte Chemie (International ed. in English)* **2002**, *41*, 4035–7.

Lowe, A. B.; Hoyle, C. E.; Bowman, C. N. Thiol-yne click chemistry: A powerful and versatile methodology for materials synthesis. *Journal of Materials Chemistry* **2010**, *20*, 4745-4750.

Lowe, A.B.; McCormick, C.L. Synthesis and solution properties of zwitterionic polymers. *Chemical Reviews* **2002**, *102*, 4177-89.

Lu, Z.; Kopecková, P.; Wu, Z.; Kopecek, J. Functionalized semitelechelic poly[N-(2-hydroxypropyl)methacrylamide] for protein modification. *Bioconjugate Chemistry* **1998**, *9*, 793–804

Lutolf, M.; Hubbell, J. Synthetic biomaterials as instructive extracellular microenvironments for morphogenesis in tissue engineering. *Nature Biotechnology* **2004**, *23*, 47–55.

Ma, I. Y.; Lobb, E. J.; Billingham, N. C.; Armes, S. P.; Lewis, A. L.; Lloyd, A. W.; Salvage, J. Synthesis of Biocompatible Polymers. 1. Homopolymerization of 2-Methacryloyloxyethyl Phosphorylcholine via ATRP in Protic Solvents: An Optimization Study. *Macromolecules* **2002**, *35*, 9306-9314.

Ma, Y.; Tang, Y.; Billingham, N. C.; Armes, S. P.; Lewis, A. L.; Lloyd, A. W.; Salvage, J. P. Well-Defined Biocompatible Block Copolymers via Atom Transfer Radical Polymerization of 2-Methacryloyloxyethyl Phosphorylcholine in Protic Media. *Macromolecules* **2003**, *36*, 3475-3484.

Maeda, H.; Greish, K.; Fang, J. The EPR effect and polymeric drugs: a paradigm shift for cancer chemotherapy in the 21st century. *Advances in Polymer Science* **2006**, *193*, 103–121.

Maeda, H.; Wu, J.; Sawa, T.; Matsumura, Y.; Hori, K. Tumor vascular permeability and the EPR effect in macromolecular therapeutics: a review. *Journal of Controlled Release* **2000**, *65*, 271-84.

Malkoch, M.; Vestberg, R.; Gupta, N.; Mespouille, L.; Dubois, P.; Mason, A.; Hedrick, J.; Liao, Q.; Frank, C.; Kingsbury, K.; Hawker, C. Synthesis of well-defined hydrogel networks using click chemistry. *Chemical Communications* **2006**, *26*, 2774–6.

Mathijssen, R.; van Alphen, R.; Verweij, J.; Loos, W.; Nooter, K.; Stoter, G.; Sparreboom, A. Clinical pharmacokinetics and metabolism of irinotecan (CPT-11). *Clinical Cancer Research* **2001**, *7*, 2182–94.

Matsumura,Y.; Maeda, H. A new concept for macromolecular therapeutics in cancer chemotherapy: mechanism of tumoritropic accumulation of proteins and the antitumor agent smancs. *Cancer Research* **1986,** *46,* 6387-92.

Matsushima, A.; Nishimura, H.; Ashihara, Y.; Yokota, Y.; Inada, Y. Modification of E.Coli Aspariginase with 2,4-Bis(methoxypolyethyleneglycol)-6-chloro-s-triazine (activated PEG2); Disappearance of Binding Ability Towards Anti-Serum and Retention of Enzymatic Activity. *Chemistry Letters* **1980**, *9*, 773-776.

McRae, S.; Chen, X.; Kratz, K.; Samanta, D.; Henchey, E.; Schneider, S.; Emrick, T. Pentafluorophenyl ester-functionalized phosphorylcholine polymers: preparation of linear, two-arm, and grafted polymer-protein conjugates. *Biomacromolecules* **2012**, *13*, 2099–109.

Mellman, I.; Fuchs, R.; Helenius, A. Acidification of the endocytic and exocytic pathways. *Annual Review of Biochemistry* **1986**, *55*, 663-700.

Meng, F.; Hennink, W.E.; Zhong, Z. Reduction-sensitive polymers and bioconjugates for biomedical applications. *Biomaterials* **2009**, *30*, 2180-98.

Metters, A.; Anseth, K.S.; Bowman, C.N. Fundamental studies of a novel, biodegradable PEG-b-PLA hydrogel. *Polymer* **2000**, *41*, 3993-4004.

Miron, T.; Wilchek, M. A spectrophotometric assay for soluble and immobilized N-hydroxysuccinimide esters. *Analytical Biochemistry* **1982**, *126*, 433-435.

Miyamoto, D.; Watanabe, J.; Ishihara, K. Effect of water-soluble phospholipid polymers conjugated with papain on the enzymatic stability. *Biomaterials* **2003**, *25*, 71–6.

Moad, G.; Chiefari, J.; Chong, (Bill) Y.; Krstina, J.; Mayadunne, R. T.; Postma, A.; Rizzardo, E.; Thang, S. H. Living free radical polymerization with reversible addition - fragmentation chain transfer (the life of RAFT). *Polymer International* **2000**, *49*, 993-1001.

Mrkvan, T.; Sirova, M.; Etrych, T.; Chytil, P.; Strohalm, J.; Plocova, D.; Ulbrich, K.; Rihova, B. Chemotherapy based on HPMA copolymer conjugates with pH-controlled release of doxorubicin triggers anti-tumor immunity. *Journal of Controlled Release* **2005**, *110*, 119–29.

Muggia, F. M.; Dimery, I.; Arbuck, S. G. *In Conference on the Camptothecins - From Discovery to the Patient*; Pantazis, P., Giovanella, B. C., Rothenberg, M. L., Eds.; New York Acad Sciences: Bethesda, Md, **1996**, 213-23.

Nakabayashi, N.; Williams, D. Preparation of non-thrombogenic materials using 2-methacryloyloxyethyl phosphorylcholine. *Biomaterials* **2003**, *24*, 2431–5.

Nakanishi, T.; Fukushima, S.; Okamoto, K.; Suzuki, M.; Matsumura, Y.; Yokoyama, M.; Okano, T.; Sakurai, Y.; Kataoka, K. Development of the polymer micelle carrier system for doxorubicin *Journal of Controlled. Release* **2001**, *74*, 295-302

Nicolas, J.; Miguel, V. S.; Mantovani, G.; Haddleton, D. M. Fluorescently tagged polymer bioconjugates from protein derived macroinitiators. *Chemical Communications* **2006**, 4697-9.

Numbenjapon, T.; Wang, J.Y.; Colcher, D.; Schluep, T.; Davis, M.E.; Duringer, J.; Kretzner, L.; Yen, Y.; Forman, S.J.; Raubitschek, A. Preclinical results of camptothecin- polymer conjugate (IT-101) in multiple human lymphoma xenograft models. *Clinical Cancer Research* **2009**, *15*, 4365-73.

Nuttelman, C. R.; Mortisen, D. J.; Henry, S. M.; Anseth, K. S. Attachment of fibronectin to poly(vinyl alcohol) hydrogels promotes NIH3T3 cell adhesion, proliferation, and migration. *Journal of Biomedical Materials Research* **2001**, *57*, 217-223.

Opanasopit, P.; Yokoyama, M.; Watanabe, M.; Kawano, K.; Maitani, Y.; Okano, T. Block copolymer design for camptothecin incorporation into polymeric micelles for passive tumor targeting. *Pharmaceutical Research* **2004**, *21*, 2001–8.

O'Reilly, R.K.; Hawker, C.J.; Wooley, K.L. Cross-linked block copolymer micelles: functional nanostructures of great potential and versatility. *Chemical Society Reviews* **2006**, *35*, 1068-83.

Ossipov, D. A.; Hilborn, J. Poly(vinyl alcohol)-Based Hydrogels Formed by "Click Chemistry." *Macromolecules* **2006**, *39*, 1709-1718.

Page, S.M.; Henchey, E.; Chen, X.; Schneider, S.; Emrick T. Efficacy of polyMPC-DOX prodrugs in 4T1 tumor-bearing mice. *Molecular Pharmaceutics* **2014**, Accepted.

Page, S.M.; Martorella, M.; Parelkar, S., Kosif, I.; Emrick, T. Disulfide Cross-Linked Phosphorylcholine Micelles for Triggered Release of Camptothecin. *Molecular Pharmaceutics* **2013**, *10*, 2684-92.

Page, S.M.; Parelkar, S.; Gerasimenko, A.; Shin, D.Y.; Peyton, S.; Emrick, T. Promoting Cell Adhesion on Slippery Phosphorylcholine Hydrogel Surfaces. *Journal of Materials Chemistry B* **2014**, *2*, 620-624.

Paraskar, A.; Soni, S.; Basu, S.; Amarasiriwardena, C.J.; Lupoli, N.; Srivats, S.; Roy, R.S.; Sengupta, S. Rationally engineered polymeric cisplatin nanoparticles for improved antitumor efficacy. *Nanotechnology* **2011**, *22*, 265101.

Paraskar, A.S.; Soni, S.; Chin, K.T.; Chaudhuri, P.; Muto, K.W.; Berkowitz, J.; Handlogten, M.W.; Alves, N.J.; Bilgicer, B.; Dinulescu, D.M.; Mashelkar, R.A.; Sengupta, S. Harnessing structure-activity relationship to engineer a cisplatin nanoparticle for enhanced antitumor efficacy. *Proceedings of the National Academy of Sciences USA* **2010**, *107*, 12435-40.

Parrish, B.; Emrick, T. Soluble camptothecin derivatives prepared by click cycloaddition chemistry on functional aliphatic polyesters. *Bioconjugate Chemistry* **2006**, *18*, 263–7.

Pasut, G.; Veronese, F.M.; PEG conjugates in clinical development or use as anticancer agents: An overview. *Advanced Drug Delivery Reviews* **2009**, *61*, 1177-88.

Peer, D.; Karp, J.M.; Hong, S.; Farokhzad, O.C.; Margalit, R.; Langer, R. Nanocarriers as an emerging platform for cancer therapy. *Nature Nanotechnology* **2007**, *2*, 751-60.

Peyton, S.; Raub, C.; Keschrumrus, V.; Putnam, A. The use of poly(ethylene glycol) hydrogels to investigate the impact of ECM chemistry and mechanics on smooth muscle cells. *Biomaterials* **2006**, *27*, 4881–93.

Pulaski, B.A.; Ostrand-Rosenberg, S. Mouse 4T1 Breast Tumor Model. *Current Protocols in Immunology* **2001**, *39*, 20.2.1-20.2.16.

Rajan, R.; Li, T.; Aras, M.; Sloey, C.; Sutherland, W.; Arai, H.; Briddell, R.; Kinstler, O.; Lueras, A.; Zhang, Y.; Yeghnazar, H.; Treuheit, M.; Brems, D. Modulation of protein aggregation by polyethylene glycol conjugation: GCSF as a case study. *Protein science : a publication of the Protein Society* **2006**, *15*, 1063–75.

Rhee, W.; Carlino, J.; Chu, S.; Higley, H. *Poly(ethylene glycol) Chemistry: Biotechnical and Biomedical Applications* **1992**, *Platinum Press, New York*, 183-198.

Ringsdorf, H. Structure and properties of pharmacologically active polymers. *Journal of Polymer Science: Symposium* **1975**, *51*, 135-53.

Roberts, M.; Harris, J. Attachment of degradable poly(ethylene glycol) to proteins has the potential to increase therapeutic efficacy. *Journal of Pharmaceutical Sciences* **1998**, *87*, 1440–5.

Rodrigues, P.; Beyer, U.; Schumacher, P.; Roth, T.; Fiebig, H.; Unger, C.; Messori, L.; Orioli, P.; Paper, D.; Mülhaupt, R.; Kratz, F. Acid-sensitive polyethylene glycol conjugates of doxorubicin: preparation, in vitro efficacy and intracellular distribution. *Bioorganic and Medicinal Chemistry* **1999**, *7*, 2517–24.

Roth, P. J.; Wiss, K. T.; Zentel, R.; Theato, P. Synthesis of Reactive Telechelic Polymers Based on Pentafluorophenyl Esters. *Macromolecules* **2008**, *41*, 8513-8519.

Roth, P.J.; Jochum, F.D; Zentel, R.; Theato, P. Synthesis of Hetero-Telechelic α,ω Bio-Functionalized Polymers. *Biomacromolecules* **2010**, *11*, 238-240.

Rowinsky, E.K.; Rizzo, J.; Ochoa, L.; Takimoto, C.H.; Forouzesh, B.; Schwartz, G.; Hammond, L.A.; Patnaik, A.; Kwiatek, J.; Goetz, A.; Denis, L.; McGuire, J.; Tolcher, A. A phase I and pharmacokinetic study of PEGylated camptothecin as a 1-hour infusion every 3 weeks in patients with advanced solid malignancies. *Journal of Clinical Oncology* **2003**, *21*, 148-157.

Rubina, A.; Pan'kov, S.; Dementieva, E.; Pen'kov, D.; Butygin, A.; Vasiliskov, V.; Chudinov, A.; Mikheikin, A.; Mikhailovich, V.; Mirzabekov, A. Hydrogel drop microchips with immobilized DNA: properties and methods for large-scale production. *Analytical Biochemistry* **2004**, *325*, 92–106.

Safra, T.; Jeffers, S.; Tsao-Wei, D.D.; Groshen, S.; Lyass, O.; Henderson, R.; Berry, G.; Gabizon, A. Pegylated liposomal doxorubicin (doxil): Reduced clinical cardiotoxicity in patients reaching or exceeding cumulative doses of 500 mg/m2. *Annals of Oncology* **2000**, *11*, 1029-33.

Saito, K.; Ingalls, L.R.; Lee, J.; Warner, J.C. Core-bound polymeric micellar system based on photocrosslinking of thymine. *Chemical Communications* **2007**, *24*, 2503-5.

Salmaso, S.; Semenzato, A.; Bersani, S.; Matricardi, P.; Rossi, F.; Caliceti, P. Cyclodextrin/PEG based hydrogels for multi-drug delivery. *International Journal of Pharmaceutics* **2007**, *345*, 42–50.

Samanta, D.; McRae, S.; Cooper, B.; Hu, Y.; Emrick, T.; Pratt, J.; Charles, S. End-functionalized phosphorylcholine methacrylates and their use in protein conjugation. *Biomacromolecules* **2008**, *9*, 2891–7.

Satchi-Fainaro, R.; Duncan, R.; Barnes, C. M. Polymer therapeutics for cancer: current status and future challenges. *Advances in Polymer Science* **2006**, *193*, 1–65.

Schafer, F.Q.; Buettner, G.R. Redox environment of the cell as viewed through the redox state of the glutathione disulfide/glutathione couple. *Free Radical Biology and Medicine* **2011**, *30*, 1191-1212.

Schluep, T.; Cheng, J.; Khin, K.; Davis, M. Pharmacokinetics and biodistribution of the camptothecin-polymer conjugate IT-101 in rats and tumor-bearing mice. *Cancer chemotherapy and pharmacology* **2006**, *57*, 654–62.

Schluep, T.; Hwang, J.; Cheng, J.J.; Heidel, J.D.; Bartlett, D.W.; Hollister, B.; Davis, M.E. Preclinical efficacy of the camptothecin-polymer conjugate IT-101 in multiple cancer models. *Clinical Cancer Research* **2006**, *12*, 1606-14.

Seo, J.; Matsuno, R.; Lee, Y.; Takai, M.; Ishihara, K. Conformation recovery and preservation of protein nature from heat-induced denaturation by water-soluble phospholipid polymer conjugation. *Biomaterials* **2009**, *30*, 4859-4867.

Seymour, L.W.; Ferry, D.R.; Kerr, D.J.; Rea, D.; Whitlock, M.; Poyner, R.; Boivin, C.; Hesslewood, S.; Twelves, C.; Blackie, R.; Schatzlein, A.; Jodrell, D.; Bissett, D.; Calvert, H.; Lind, M.; Robbins, A.; Burtles, S.; Duncan, R.; Cassidy, J. Phase II studies of polymer-doxorubicin (PK1, FCE 28068) in the treatment of breast, lung, and colorectal cancer. *International Journal of Oncology* **2009**, *34*, 1629-36.

Shao, H.; Crnogorac, M.M.; Kong, T.; Chen, S.Y.; Williams, J.M.; Tack, J.M.; Gueriguian, V.; Cagle, E.N.; Carnevali, M.; Tumelty, D.; Paliard, X.; Miranda, L.P.; Bradburne, J.A.; Kochendoerfer, G.G. Site-specific polymer attachment to a CCL-5 (RANTES) analogue by oxime exchange. *Journal of the American Chemical Society* **2005**, *127*, 1350-1351.

Shimizu, T.; Goda, T.; Minoura, N.; Takai, M.; Ishihara, K. Super-hydrophilic silicone hydrogels with interpenetrating poly(2-methacryloyloxyethyl phosphorylcholine) networks. *Biomaterials* **2010**, *31*, 3274–80.

Singer, J. W.; Bhatt, R.; Tulinsky, J.; Buhler, K. R.; Heasley, E.; Klein, P.; de Vries, P. *In International Symposium on Tumor Targeted Delivery Systems*; Elsevier Science: Bethesda, Maryland, **2000**, 243-7.

Slichenmyer, W.J.; Rowinsky, E.K.; Donehower, R.C.; Kaufman, S.H. The current status of camptothecin analogues as antitumor agents. *Journal of the National Cancer Institute* **1993**, *85*, 271-91.

Stile, R. A.; Burghardt, W. R.; Healy, K. E. Synthesis and Characterization of Injectable Poly(N -isopropylacrylamide)-Based Hydrogels That Support Tissue Formation in Vitro. *Macromolecules* **1999**, *32*, 7370-7379.

Sure, V.; Etrych, T.; Ulbrich, K.; Hirano, T.; Kondo, T.; Todoroki, T.; Jelinkova, M.; Rihova, B. Synthesis and Properties of Poly[N-(2-Hydroxypropyl) Methacrylamide] Conjugates of Superoxide Dismutase. *Journal of Bioactive and Compatible Polymers* **2002**, *17*, 105-122.

Tanaka, H.; Satake-Ishikawa, R.; Ishikawa, M.; Matsuki, S. Pharmacokinetics of recombinant human granulocyte colony-stimulating factor conjugated to polyethylene glycol in rats. *Cancer Research* **1991**, *51*, 3710-3714.

Tannock, I. F.; Rotin, D. Acid pH in tumors and its potential for therapeutic exploitation. *Cancer Research* **1989**, *49*, 4373–84.

Tao, K.; Fang, M.; Alroy, J.; Sahagian, G.G. Imagable 4T1 model for the study of late stage breast cancer. *BMC Cancer* **2008**, *8*, 228-46.

Tao, L.; Liu, J.; Davis, T. Branched polymer-protein conjugates made from mid-chain-functional P(HPMA). *Biomacromolecules* **2009**, *10*, 2847–51.

Tao, L.; Mantovani, G.; Lecolley, F.; Haddleton, D. M. α-Aldehyde terminally functional methacrylic polymers from living radical polymerization: application in protein conjugation "Pegylation". *Journal of the American Chemical Society* **2004**, *126*, 13220-13221.

Thomson, A.H.; Vasey, P.A.; Murray, L.S.; Cassidy, J.; Fraier, D.; Frigerio, E.; Twelves, C. Population pharmacokinetics in phase I drug development: a phase I study of PK1 in patients with solid tumours. *British Journal of Cancer* **1999**, *81*, 99-107.

Tillman, H.; Kuhn, B.; Kranzlin, B.; Sadick, M.; Gross, J.; Gretz, N.; Pill, J. Efficacy and immunogenicity of novel erythropoietic agents and conventional rhEPO in rats with renal insufficiency. *Kidney International* **2006**, *69*, 60-67.

Trappmann, B.; Gautrot, J.; Connelly, J.; Strange, D.; Li, Y.; Oyen, M.; Cohen Stuart, M.; Boehm, H.; Li, B.; Vogel, V.; Spatz, J.; Watt, F.; Huck, W. Extracellular-matrix tethering regulates stem-cell fate. *Nature Materials* **2012**, *11*, 642–9.

Tumelty, D.; Carnevali, M.; Miranda, L.P. A new approach to the chemical synthesis of keto-proteins. *Journal of the American Chemical Society* **2003**, *125*, 14238-39.

Ulbrich, K.; Etrych, T.; Chytil, P.; Jelínková, M.; Ríhová, B. HPMA copolymers with pH-controlled release of doxorubicin: in vitro cytotoxicity and in vivo antitumor activity. *Journal of Controlled Release 2003*, *87*, 33–47.

Ulbrich, K.; Strolhalm, J.; Plocova, D.; Oupicky, D.; Subr, V.; Soucek, J.; Pouckova, P.; Matousek, J. Poly [N-(2-Hydroypropyl) Methacrylamide] Conjugates of Bovine Seminal Ribonuclease. Synthesis, Physicochemical, and Preliminary Biological Evaluation. *Journal of Bioactive and Compatible Polymers* **2000**, *15*, 4-26.

Uziely, B.; Jeffers, S.; Isacson, R.; Kutsch, K.; Wei-Tsao, D.; Yehoshua, Z.; Libson, E.; Muggia, F.; Gabizon, A. Liposomal doxorubicin: antitumor activity and unique toxicities during two complementary phase I studies. *Journal of Clinical Oncology* **1995**, *13*, 1777–85.

Van De Wetering, P.; Metters, A.; Schoenmakers, R.; Hubbell, J. Poly(ethylene glycol) hydrogels formed by conjugate addition with controllable swelling, degradation, and release of pharmaceutically active proteins. *Journal of Controlled Release* **2005**, *102*, 619–27.

Van Der Poll, D.; Kieler-Ferguson, H.; Floyd, W.; Guillaudeu, S.; Jerger, K.; Szoka, F.; Fréchet, J. Design, synthesis, and biological evaluation of a robust, biodegradable dendrimer. *Bioconjugate Chemistry* **2010**, *21*, 764–73.

Van Nostrum, C.F. Covalently cross-linked amphiphilic block copolymer micelles. *Soft Matter* **2011**, *7*, 3246-59.

Vasquez-Dorbatt, V.; Tolstyka, Z.P.; Maynard, H.D. Synthesis of aminooxy end-functionalized pNIPAAM by RAFT polymerization for protein and polysaccharide conjugation. *Macromolecules* **2009**, *42*, 7650-7656.

Vaz, R.; Martins, G.; Thorsteinsdóttir, S.; Rodrigues, G. Fibronectin promotes migration, alignment and fusion in an in vitro myoblast cell model. *Cell and Tissue Research* **2012**, *348*, 569–78.

Veronese, F. M.; Monfardini, C.; Caliceti, P.; Schiavon, O.; Scrawen, M. D.; Beer, D. Improvement of pharmacokinetic, immunological and stability properties of asparaginase by conjugation to linear and branched monomethoxy poly(ethylene glycol). *Journal of Controlled Release* **1996**, *40*, 199-209.

Vetvicka, D.; Hruby, M.; Hovorka, O.; Etrych, T.; Vetrik, M.; Kovar, L.; Kovar, M.; Ulbrich, K.; Rihova, B. Biological evaluation of polymeric micelles with covalently bound doxorubicin. *Bioconjugate Chemistry* **2009**, *20*, 2090–7.

Vogel, N.; Théato, P. Controlled Synthesis of Reactive Polymeric Architectures Using 5-Norbornene-2-carboxylic Acid Pentafluorophenyl Ester. *Macromolecular Symposia* **2007**, 249-250.

Wachiralarpphaithoon, C.; Iwasaki, Y.; Akiyoshi, K. Enzyme-degradable phosphorylcholine porous hydrogels cross-linked with polyphosphoesters for cell matrices. *Biomaterials* **2007**, *28*, 984–93.

Wall, M. E.; Wani, M. C.; Cook, C. E.; Palmer, K. H.; McPhail, A. T.; Sim, G. A. Plant Antitumor Agents. I. The Isolation and Structure of Camptothecin, a Novel Alkaloidal Leukemia and Tumor Inhibitor from Camptotheca acuminata 1,2. *Journal of the American Chemical Society* **1966**, *88*, 3888-90.

Wang, J.-S.; Matyjaszewski, K. Controlled/"Living" Radical Polymerization. Halogen Atom Transfer Radical Polymerization Promoted by a Cu(I)/Cu(II) Redox Process. *Macromolecules* **1995**, *28*, 7901-7910.

Wang, Y.-S.; Youngster, S.; Grace, M.; Bausch, J.; Bordens, R.; Wyss, D. Structural and biological characterization of pegylated recombinant interferon alpha-2b and its therapeutic implications. *Advanced Drug Delivery Reviews* **2002**, *54*, 547–70.

Wei, R.; Cheng, L.; Zheng, M.; Cheng, R.; Meng, F.; Deng, C.; Zhong, Z. Reduction-responsive disassemblable core-cross-linked micelles based on poly(ethylene glycol)-b-poly(N-2-hydroxypropyl methacrylamide)-lipoic acid conjugates for triggered intracellular anticancer drug release. *Biomacromolecules* **2012**, *13*, 2429-38.

Wichterle, O.; Lím, D. Hydrophilic Gels for Biological Use. *Nature* **1960**, *185*, 117-118.

Wiss, K. T.; Krishna, O. D.; Roth, P. J.; Kiick, K. L.; Theato, P. A Versatile Grafting-to Approach for the Bioconjugation of Polymers to Collagen-like Peptides Using an Activated Ester Chain Transfer Agent. *Macromolecules* **2009**, *42*, 3860-3863.

Xu, Y.; Jang, K.; Konno, T.; Ishihara, K.; Mawatari, K.; Kitamori, T. The biological performance of cell-containing phospholipid polymer hydrogels in bulk and microscale form. *Biomaterials* **2010**, *31*, 8839–46.

Xu, Y.; Meng, F.; Cheng, R.; Zhong, Z. Reduction-sensitive reversible crosslinked biodgradable micelles for triggered release of doxorubicin. *Macromolecular Bioscience* **2009**, *9*, 1254-61.

Yamasaki, M.; Okabe, M.; Suzawa, T.; Yokoo, Y. New PEG2 type polyethylene glycol derivatives for protein modification. *Biotechnology Techniques* **1998**, *12*, 751-754.

Yang, T.; Long, H.; Malkoch, M.; Gamstedt, E. K.; Berglund, L.; Hult, A. Characterization of well-defined poly(ethylene glycol) hydrogels prepared by thiol-ene chemistry. *Journal of Polymer Science Part A: Polymer Chemistry* **2011**, *49*, 4044-4054.

Yigit, S.; Sanyal, R.; Sanyal, A. Fabrication and functionalization of hydrogels through "click" chemistry. *Chemistry, an Asian Journal* **2011**, *6*, 2648–59.

Yoshinaga, K.; Shafer, S.G.; Harris, J.M. Effects of Polyethylene Glycol Substitution on Enzyme Activity. *Journal of Bioactive and Compatible Polymers* **1987**, *2*, 49-56.

Yu, B.; Lowe, A.; Ishihara, K. RAFT synthesis and stimulus-induced self-assembly in water of copolymers based on the biocompatible monomer 2-(methacryloyloxy)ethyl phosphorylcholine. *Biomacromolecules* **2009**, *10*, 950–8.

Yusa, S.-I.; Fukuda, K.; Yamamoto, T.; Ishihara, K.; Morishima, Y. Synthesis of well-defined amphiphilic block copolymers having phospholipid polymer sequences as a novel biocompatible polymer micelle reagent. *Biomacromolecules* **2004**, *6*, 663–70.

Zamai, M.; VandeVen, M.; Farao, M.; Gratton, E.; Ghiglieri, A.; Castelli, M.; Fontana, E.; D'Argy, R.; Fiorino, A.; Pesenti, E.; Suarato, A.; Caiolfa, V. Camptothecin poly[n-(2-hydroxypropyl) methacrylamide] copolymers in antitopoisomerase-I tumor therapy: intratumor release and antitumor efficacy. *Molecular Cancer Therapeutics* **2002**, *2*, 29–40.

Zhang, J.; Gong, M.; Yang, S.; Gong, Y.-K. Crosslinked biomimetic random copolymer micelles as potential anti-cancer drug delivery vehicle. *Journal of Controlled Release* **2011**, *152*, e1-e132.

Zhang, Y.; Wang, G.; Huang, J. A new strategy for synthesis of "umbrella-like" poly(ethylene glycol) with monofunctional end group for bioconjugation. *Journal of Polymer Science Part A: Polymer Chemistry* **2010**, *48*, 5974-5981.

Zhao, H.; Lee, C.; Sai, P.; Choe, Y.; Boro, M.; Pendri, A.; Guan, S.; Greenwald, R. 20-O-acylcamptothecin derivatives: evidence for lactone stabilization. *The Journal of Organic Chemistry* **2000**, *65*, 4601–6.

Zhao, H.; Rubio, B.; Sapra, P.; Wu, D.; Reddy, P.; Sai, P.; Martinez, A.; Gao, Y.; Lozanguiez, Y.; Longley, C.; Greenberger, L.; Horak, I. Novel prodrugs of SN38 using multiarm poly(ethylene glycol) linkers. *Bioconjugate Chemistry* **2008**, *19*, 849–59.

Zhao, X.; Harris, J. Novel degradable poly(ethylene glycol) hydrogels for controlled release of protein. *Journal of pharmaceutical sciences* **1998**, *87*, 1450–8.

Zhou, L.; Cheng, R.; Tao, H.; Ma, S.; Guo, W.; Meng, F.; Liu, H.; Liu, Z.; Zhong, Z. Endosomal pH-Activatable Poly(ethylene oxide)-graft-Doxorubicin Prodrugs: Synthesis Drug Release, and Biodistribution in Tumor-Bearing Mice. *Biomacromolecules* **2011**, *12*, 1460-7.

Zhu, J. Bioactive modification of poly(ethylene glycol) hydrogels for tissue engineering. *Biomaterials* **2010**, *31*, 4639–56.

Zou, Y. Y.; Wu, Q. P.; Tansey, W.; Chow, D.; Hung, M. C.; Vej, C. C.; Wallace, S.; Li, C. Effectiveness of water soluble poly(L-glutamic acid)-camptothecin conjugate against resistant human lung cancer xenografted in nude mice. *International Journal of Oncology* **2001**, *18*, 331-6.